University of Alberta

A mutation in APOA4 confers susceptibility to a Mendelian form of IBD

by

Brooke Ashley Johannes

A thesis submitted to the Faculty of Graduate Studies and Research
in partial fulfillment of the requirements for the degree of

Master of Science
in
Medical Sciences – Medical Genetics

Edmonton, Alberta
Fall 2008

Your file Votre référence
ISBN: 978-0-494-47272-9
Our file Notre référence
ISBN: 978-0-494-47272-9

DEDICATION

To the Mennonite family that made this research possible.

ABSTRACT

Familial enteropathy with villous edema (FEVE; OMIM 600351) is an autosomal dominant disorder with variable penetrance that typically manifests in childhood as a recurrent acute, life-threatening secretory diarrhea associated with distinctive jejunal histologic changes. A genome-wide microsatellite screen and subsequent linkage analysis on the affected Mennonite kindred refined the FEVE critical region to 11q23.3 between D11S4142 and D11S1364. Ten positional candidate genes were sequenced before identifying a 198 bp in-frame duplication in APOA4 (c.552_749dup). This mutation was present in all known affected individuals, and absent in all ethnicity-matched and general population controls. It is hypothesized that the duplication is a dominant negative mutation that reduces wildtype apoA-IV expression or its half-life. Future investigations are warranted into the potential role of apoA-IV in other gastrointestinal disorders, such as inflammatory bowel disease, as well as its anti-inflammatory function in the gastrointestinal system.

ACKNOWLEDGEMENTS

First and foremost, I would like to thank my supervisor, Dr. Martin Somerville, who provided me with the opportunity to work on this very interesting research project. I am extremely grateful for his continuous support and guidance throughout my time here in the Department of Medical Genetics at the University of Alberta. His kindness and patience has made my graduate student experience a wonderful one. I would also like to thank him for taking a chance by having me as the first graduate student in the Molecular Diagnostic Laboratory.

Many thanks are due to all of the other wonderful members of the Molecular Diagnostic Laboratory who have been so kind and helpful to me over the past three years: Dr. Stacey Bléoo, Basil Elyas, Shelagh Haase, Mark Hicks, Lynn Podemski, Kathy Sprysak, Leanne Vicen, and Christine Walker. They have provided me with invaluable technical support, moral support, and friendships. Their company within the laboratory, and even on the sport fields/ice/courts, has enriched my graduate student experience. In particular, I would like to thank Basil, who has been the most involved in this research project during my time here. By far, Basil has spent the most time teaching me laboratory techniques and helping with various aspects of this project. He always made time for me, even though he had his own work to do, and I am incredibly grateful for all that he has done.

I would like to express my gratitude to my committee members, Dr. Henry Pabst, Dr. Michael Walter, and Dr. Karen Madsen, for taking the time to be on my committee and providing me with valuable input and advice. I also truly appreciate the genuine interest that they have all shown in this research project. Additionally, Dr. Henry Pabst has been exceptional at teaching me about both the family and the disease that were the focus of my research. His involvement ensured that the human aspect of this project was never lost.

Thanks also to Dr. Rachel Wevrick for providing me with some very useful advice which ended up being fundamental to the major discovery in this project, and for allowing me to run numerous western blots in her laboratory. I would also like to thank Jason Bush for teaching me how to do those western blots. Dr. Charlotte Foulston, from the Department of Pediatrics, at the University of Calgary, is thanked for helping in the acquisition of specimens for this research.

Finally, my most sincere thanks goes to my family. Without my parents' unconditional love, support, and encouragement, I would not be where I am today.

TABLE OF CONTENTS

LIST OF TABLES

LIST OF FIGURES

LIST OF ABBREVIATIONS

aa	Amino Acid
apoA-IV	Apolipoprotein A-IV (protein)
APOA4	Apolipoprotein A4 (gene)
bp	Base Pair
CD	Crohn's Disease
CDS	Coding Sequence
DNA	Deoxyribonucleic Acid
dNTPs	Deoxyribonucleotide Triphosphate
DTR	Dye Terminator Removal
EDTA	Ethylenediamine Tetraacetic Acid
EtBr	Ethidium Bromide
EtOH	Ethanol
FEVE	Familial Enteropathy with Villous Edema
gDNA	Genomic DNA
IBD	Inflammatory Bowel Disease
kDa	KiloDalton
Mb	Megabase
PCR	Polymerase Chain Reaction
RCF	Relative Centrifugal Force
RNA	Ribonucleic Acid
RT-PCR	Reverse Transcriptase Polymerase Chain Reaction
SDS	Sodium Dodecyl Sulfate

SDS-PAGE	Sodium Dodecyl Sulfate Polyacrylamide Gel Electrophoresis
SNP	Single Nucleotide Polymorphism
ssDNA	Single Stranded DNA
TBE	Tris/Borate/EDTA buffer
UC	Ulcerative Colitis
UTR	Untranslated Region
v/v	Volume per Volume
w/v	Weight (g) per Volume (mL)

CHAPTER 1: INTRODUCTION

Genetic components play an underlying or exclusive role in the development and severity of many human diseases (KUMAR *et al.* 2003c). With 20,000 to 25,000 protein-encoding genes in the human genome (INTERNATIONAL HUMAN GENOME CONSORTIUM 2004), the task of finding disease-causing mutations is not a trivial matter. However, mapping the genetic locus of a disease is much easier when there is a defined pattern of inheritance (as in monogenic disorders), as opposed to when there are more complex factors involved (as in multifactorial or polygenic disorders). Research into the cause of monogenic diseases can lead to an improved understanding of the affected molecular mechanisms, thereby contributing to the basic knowledge of human genetics. Such findings are also valuable for understanding related complex common diseases and identifying the corresponding susceptibility alleles. In fact, knowledge of the molecular mechanisms involved in common diseases is largely based on what has been learned from rare monogenic diseases (PELTONEN *et al.* 2006). So despite the commercial attractiveness of studying common diseases, the value of studying rare monogenic diseases can not be overlooked (ANTONARAKIS and BECKMANN 2006). This thesis describes the work involved in identifying the mutation responsible for a rare monogenic gastrointestinal disorder that could give insight into inflammatory bowel disease.

1.1) Identifying Disease Genes

There are various strategies for identifying the genetic locus of a disease. These methods can be dependent on, or independent of, the chromosomal position of the candidate gene, or rely on a combination of positional and nonpositional information (STRACHAN and READ 1999). The latter method describes the positional candidate approach used in this

thesis, and therefore is described in this section. Linkage mapping can identify the approximate chromosomal position of a disease locus by determining which loci are exclusively present in all of the affected individuals. Subsequent analysis of the functions and expression patterns of positional candidate genes helps to rank the genes for further investigative purposes.

1.1.1) Recombination & Linkage

Recombination is the reciprocal exchange of genetic material between homologous maternal and paternal chromosomes during meiosis. The recombination fraction (Θ) represents the fraction of meiotic events that result in a recombination event between two loci. The further apart the loci are, the more likely it is that they will be separated by recombination. Conversely, loci that are adjacent to each other will rarely be separated by recombination, and thus are usually inherited together. Therefore a low recombination fraction indicates that the loci have a greater tendency be inherited together due to their proximal distance. This phenomenon of loci tending to be inherited together is referred to as linkage. Together the multiple linked loci are referred to as a haplotype.

1.1.2) Genetic Markers

Polymorphic loci (genetic markers) are used to trace the segregation of DNA segments through generations. To be informative, a marker's chromosomal position must be known, and the marker must show whether or not a recombination event took place during meiosis. Therefore these markers are most informative when there is a high proportion of people heterozygous for the given loci in the population. Single nucleotide

polymorphisms (SNPs) and microsatellites (tandem repeats of 2 to 6 nucleotides) are commonly used as genetic markers. SNPs are abundant throughout the genome, but usually only vary between two bases, thus having limited heterozygosity. Microsatellites are not as abundant as SNPs, but have a high degree of heterozygosity with mutation rates as high as 10^{-2} per generation (LAI and SUN 2003).

1.1.3) Linkage Analysis

Linkage analysis identifies the genetic markers that associate with the disease in question. Since proximal loci are linked to each other (see section 1.1.1), the markers that are close to the disease locus will be inherited with the disease more frequently than expected if random segregation were occurring. In two-point mapping, each marker is individually assessed for its odds of linkage to the disease. This odds ratio (O.R.) is calculated with the numerator representing the likelihood that the disease and marker locus are linked (Θ = 0.00 to 0.49), and the denominator representing the likelihood that the disease and marker locus are unlinked ($\Theta = 0.50$):

$$O.R. = \frac{(\Theta)^R (1-\Theta)^N}{(0.5)^{R+N}}$$

Where N = the number of non-recombinants, R = the number of recombinants, and Θ is the recombination fraction between the two loci. When relevant, incomplete penetrance should also be factored into the odds ratio (BRIDGE 1997). This results in a much more complicated calculation that accounts for the possibility of individuals with the predisposing genotype not necessarily having the affected phenotype (TERWILLIGER and OTT 1994). The base 10 logarithm of the O.R. yields the LOD score (z), which can be used to evaluate the evidence of linkage:

$z(\Theta) \geq 3.0$ Significant evidence for linkage

$z(\Theta) \leq -2.0$ Significant evidence for non-linkage

$-2.0 < z(\Theta) < 3.0$ Inconclusive

The highest LOD score is obtained with the best estimate of the recombination fraction.

Once a marker is identified as having strong linkage to the disease, additional markers are employed to investigate the surrounding region at a higher resolution. The disease haplotype consists of the markers that segregate with the disease. Recombination events in affected and/or unaffected individuals define the boundaries of the disease haplotype, and thus candidate region.

1.1.4) Selection of Positional Candidate Genes

When the candidate gene (or critical) region has been reduced as much as possible, genes within that region must be investigated individually. Positional candidate genes can be prioritized for investigation by consideration of their expression patterns and functions. The expression pattern of a good candidate gene is consistent with the disease phenotype. This does not mean that the expression has to be limited to the affected tissue(s), but the gene should be expressed when and where the pathology is seen. Candidate genes should also have a function that corresponds with the pathology of the disease, or have a close functional relationship to a gene involved in a related disease. Therefore, candidate gene ranking is based largely on speculative insights into the role of gene function and expression in the pathological processes of the disease in question.

1.1.5) Mutation Screening

Candidate genes can be screened for mutations by direct sequencing. Sequence variants that are exclusive to affected individuals (i.e. not present in controls or reference databases) may be disease-causing mutations. However, variants must be thoroughly investigated on a case-by-case basis in order to make this determination. In addition to mutation screening, genes can be confirmed as a disease locus by: 1) demonstrating that a mutant phenotype can be reversed by complementing the genetic deficiency and/or 2) producing a knockout animal model for the corresponding gene that results in similar pathology to the human disease (STRACHAN and READ 1999).

1.2) The Gastrointestinal Immune System

The gastrointestinal immune system functions to maintain homeostasis, but its aberrant immune responses can lead to pathological inflammation resulting in gastrointestinal disorders. Physical barriers, such as epithelial layers and mucous membranes, as well as the innate and adaptive immune systems provide the immunological defense that is necessary to protect organisms from pathogens present in their external environment. Mucosal surfaces are particularly susceptible to pathogen entry (NAGLER-ANDERSON 2001). This potential for invasion is counteracted by the presence of mucosa-associated lymphoid tissue (MALT), which consists of scattered concentrations of lymphoid tissues along the mucosal linings. The gut-associated lymphoid tissue (GALT) is the category of MALT responsible for immune surveillance of the gastrointestinal mucosa. Since the lumen of the gastrointestinal tract receives its contents from the external environment, the gastrointestinal mucosa is exposed to a variety of potentially harmful antigens. However,

the digestive nature of the gastrointestinal tract requires that in addition to mounting immune responses to pathogens, the innate immune system and GALT must remain tolerant of both food antigens and normal intestinal flora (SPAHN and KUCHARZIK 2004). This fine balance between tolerance and active immunity is the key to maintaining intestinal homeostasis.

Peyer's patches are specialized lymph nodes of the GALT that are distributed throughout the small intestinal subepithelial wall (VAN KRUININGEN *et al.* 2002). Instead of filtering pathogens from lymph fluid like a typical lymph node, Peyer's patches acquire luminal antigens through microfold cells (M cells) or dendritic cells (MACDONALD 2003). M cells are specialized epithelial cells situated on the apical side of Peyer's patches, that endocytose and transfer luminal antigens to the underlying Peyer's patch (MÜLLER *et al.* 2005). Dendritic cells that are located in Peyer's patches also obtain antigens from the gut lumen, but they do so by extending pseudopods through the epithelial tight junctions (RESCIGNO *et al.* 2001). After reaching the Peyer's patch, foreign antigens are presented to $CD4^+$ helper T (T_H) cells by antigen presenting cells (i.e. dendritic cells and macrophages), which initiates a humoral response (IIJIMA *et al.* 2001). B cells proliferate in the germinal center of the Peyer's patch and differentiate into antibody secreting plasma cells (NAGLER-ANDERSON 2001). Most plasma cells of the gastrointestinal tract secrete immunoglobulin A, which is then transported to the mucous membrane of the intestinal lumen to prevent the attachment and invasion of microbial pathogens (FAGARASAN and HONJO 2003; MORA *et al.* 2006; SATO *et al.* 2003). Although there are only about 200 Peyer's patches in the small intestine of an average adult, there are tens of thousands of smaller subepithelial GALT aggregates, called

isolated lymphoid follicles, which have essentially the same function as Peyer's patches (HAMADA *et al.* 2002; MACDONALD and MONTELEONE 2005).

Various other immunological structures exist in the extensive space between Peyer's patches. Within the lumen itself, commensal flora interfere with the invasion of microbial pathogens by producing bacteriocins and competing for nutrients and host-cell binding sites (BROOK 1999; REID *et al.* 2001). Surrounding the lumen, the monolayer of intestinal epithelial cells (IECs) creates a physical barrier to potential pathogens through the formation of intercellular tight junctions (PURVES *et al.* 2001). These junctions prevent molecules from passing between the epithelial cells (MADARA 1998; TURNER *et al.* 1997), thereby preventing unmonitored entry of luminal contents into the internal milieu. IECs can also thwart invasive attempts by secreting chemoattractants and proinflammatory cytokines in response to pathogenic penetration of the intestinal barrier (ECKMANN *et al.* 1995). Additionally, these IECs express human leukocyte antigen class II molecules which process and present foreign antigens to T_H cells to initiate an immune response (HERSHBERG *et al.* 1997). IECs even have a role in suppressing inflammatory responses and promoting immunological tolerance, as has been illustrated by their effect on resident mucosal dendritic cells (ILIEV *et al.* 2007). The foundation of all of these IEC immunologic mechanisms is the expression of pattern recognition receptors by IECs. These receptors enable IECs to differentiate between commensal flora and pathogens based on the evolutionary conserved structures of bacteria and viruses (MACDONALD and MONTELEONE 2005), thereby enabling IECs to respond with appropriate pro- or anti-inflammatory signals. Further immunological defense, at the epithelial cell layer, is provided by both goblet and Paneth cells. Goblet cells are dispersed throughout the

crypts and villi of the intestinal mucosa (MOE 1953), whereas Paneth cells are found clustered at the bottom of intestinal crypts (PEETERS and VANTRAPPEN 1975). Mucin containing mucus is synthesized and secreted by goblet cells in response to both physiological and pathological stimuli (LAMONT 1992). The mucus forms a 400 μm thick semipermeable protective layer over the intestinal mucosa, in which mucins capture pathogens and subsequently expel them via peristalsis (ACHESON and LUCCIOLI 2004; LAMONT 1992). Microbicidal peptides such as lysozyme, α-defensins (HD-5 and HD-6), and type II phospholipidase A_2, are stored in Paneth cell granules and secreted in response to the presence of bacteria, bacterial antigens, or cholinergic agonists (AYABE *et al.* 2000; BEIL *et al.* 1995; MALLOW *et al.* 1996; PEETERS and VANTRAPPEN 1975; QU *et al.* 1996). Lysozyme lyses bacteria by cleaving the backbone of peptidoglycan, which is a major component of bacterial cell walls (MASSCHALCK and MICHIELS 2003). Similarly, Type II phospholipidase A_2 exerts its microbicidal effect by hydrolyzing a major bacterial phospholipid, phosphatidylglycerol (HARWIG *et al.* 1995). Defensins are thought to exert an antibacterial function by permeabilizing bacterial membranes (GANZ 2003), but they are also capable of upregulating various host inflammatory defenses (YANG *et al.* 2002). In addition to microbicidal peptides, Paneth cells also secrete a proinflammatory cytokine, tumor necrosis factor-α (BEIL *et al.* 1995). Therefore, goblet cells, Paneth cells, and IECs along with their tight junctions contribute to the immunological defense at the intestinal epithelial layer, with IECs and Paneth cells signaling further immune responses by secreting chemoattractants, proinflammatory mediators and defensins.

Dendritic cells, granulocytes, monocytes/macrophages, and mast cells can be recruited in response to the aforementioned epithelial cell signals as part of the innate

defense system (NIYONSABA *et al.* 2002; OPPENHEIM *et al.* 1991; SALAZAR-GONZALEZ *et al.* 2006; VASSALLI 1992; YANG *et al.* 1999). IEC expression of adhesion molecules, such as selectins, aids the transepithelial migration of such immune response cells (JAYE and PARKOS 2000; MICHAIL *et al.* 2005). Intraepithelial lymphocytes, and lymphocytes of the lamina propria can also respond to those signals to elicit an adaptive immune response at the site of infection (CHERTOV *et al.* 1996; OPPENHEIM *et al.* 1991; SHIBAHARA *et al.* 2001; YANG *et al.* 1999). Furthermore, lymphocytes circulating in the vascular lumen can be trafficked to sites of infection by chemokines and endothelial cell expression of adhesion molecules (KUMAR *et al.* 2003b; KUNKEL and BUTCHER 2002). If an antigen were to cross the epithelial barrier, then the large presence of macrophages, dendritic cells, and T cells in the lamina propria would likely identify it and mount an appropriate immune response (MACDONALD 2003). Furthermore, mesenteric lymph nodes of the GALT provide yet another level of immune surveillance by inspecting the lymph that drains from the Peyer's patches, lamina propria and villi (SPAHN and KUCHARZIK 2004). Yet, the cumulative force of these gastrointestinal defense mechanisms is not always enough to keep disease at bay.

1.3) Gastrointestinal Disorders

Familial enteropathy with villous edema (FEVE) is the intestinal disorder that is the focus of this thesis. FEVE bears some resemblance to other intestinal disorders, including Crohn's disease, ulcerative colitis, and cholera. As such, all of these disorders and their recognized etiologies are summarized below.

1.3.1) Inflammatory Bowel Disease (IBD)

The term inflammatory bowel disease (IBD) describes a group of chronic relapsing disorders characterized primarily by inflammation of the gastrointestinal tract. The two main types of IBD are Crohn's disease (CD) and ulcerative colitis (UC), which have a combined prevalence of approximately 490/100,000 in Canada (BERNSTEIN *et al.* 2006).

1.3.1.1) Crohn's Disease

Crohn's disease (CD) can affect any part of the alimentary tract from mouth to anus, but most commonly affects the terminal ileum (KUMAR *et al.* 2003a; XAVIER and PODOLSKY 2007). Diseased segments present as skip lesions, and exhibit mucosal damage with deep transmural ulcers that often penetrate through to the serosa (KUMAR *et al.* 2003a). Microscopically, lymphoid aggregates are found throughout the tissue layers, with neutrophil infiltrates in the epithelial layer and crypts (KUMAR *et al.* 2003a). Macrophage aggregates form noncaseating granulomas in 40% to 60% of affected individuals (KUMAR *et al.* 2003a; XAVIER and PODOLSKY 2007). Clinically, patients present with diarrhea, cramping abdominal pain, vomiting, fever, and potentially mild to severe melena (BEATTIE *et al.* 2006; KUMAR *et al.* 2003a). Most patients experience years of active disease that alternate with years of remission (KUMAR *et al.* 2003a). Although CD can first appear at any age, it has a peak incidence during the third decade of life (BERNSTEIN *et al.* 2006; LOFTUS and SANDBORN 2002).

1.3.1.2) Ulcerative Colitis

Ulcerative colitis (UC) is characterized by mucosal and submucosal inflammation that starts in the rectum and may extend in a continuous manner through part or all of the colon (KUMAR *et al.* 2003a). Typically the epithelial layer is infiltrated by neutrophils, and the lamina propria is infiltrated with monocytes, lymphocytes, and other mononucleic cells (KUMAR *et al.* 2003a). The inflammatory mucosal destruction results in bloody diarrhea, accompanied by abdominal pain and tenesmus (BEATTIE *et al.* 2006; KUMAR *et al.* 2003a). Patients usually experience days to months of active disease with intervening periods of remission for months to years (KUMAR *et al.* 2003a). Longer durations and greater extents of inflammation are associated with an increased risk for colon cancer (KUMAR *et al.* 2003a). UC can manifest at any age, but its peak incidence is during the fourth decade of life (BERNSTEIN *et al.* 2006; LOFTUS and SANDBORN 2002).

1.3.1.3) IBD Etiology and Genetic Susceptibility

Although the precise causes of IBD remain unknown (GOYETTE *et al.* 2007), it is generally accepted that there is a disruption in the balance between gastrointestinal immune tolerance and immune response (MÜLLER *et al.* 2005). Furthermore, IBD is considered to be a multifactorial disease, because no environmental or host factor can explain the complex phenotype on its own (ZHENG *et al.* 2003). Environmental factors that either increase risk or exert protective effects for IBD include microbial agents, diet, and smoking (FIOCCHI 1998). Host factors include intestinal barrier function along with the innate and adaptive immune systems, all of which can be affected by genetic factors (XAVIER and PODOLSKY 2007). Mounting evidence favours the hypothesis that

commensal flora trigger a maladaptive immune response due to host factors that have an underlying genetic susceptibility (BOUMA and STROBER 2003).

IBD is not a simple Mendelian disorder (ZHENG *et al.* 2003), but the underlying genetic susceptibility of IBD is evident from the results of ethnic, familial, twin, and linkage studies. Differences in IBD family history, disease location and extraintestinal manifestations have been noted between the Caucasian, Hispanic, and African American races (NGUYEN *et al.* 2006). Additionally, the life time risk for developing IBD is higher in Jewish individuals compared to their non-Jewish counterparts (LYNCH *et al.* 2004). Genetic anticipation has even been observed in a Jewish population (HERESBACH *et al.* 1998), however this phenomenon may not be present in the general population of IBD patients (HAMPE *et al.* 2000). Familial studies have illustrated that the greatest individual risk factor for developing IBD is having an affected relative (RUSSELL and SATSANGI 2004). First and second degree relatives of those with IBD are at greater risk of developing the same type of IBD as their affected relative compared to people without affected relatives (ORHOLM *et al.* 1991; PEETERS *et al.* 1996). Additionally, parent-child pairs and sibling pairs exhibit >63% and >76% concordance, respectively, with regards to their disease type, disease extent, and extraintestinal manifestations (SATSANGI *et al.* 1996). Twin studies have shown probandwise concordance rates[1] for monozygotic twins in the range of 6.3%-18.2% for UC and at 58.3% for CD (ORHOLM *et al.* 2000; TYSK *et al.* 1988). The concordance rates for dizygotic twins were significantly lower than their

---

[1] Probandwise concordance rate = $\frac{2C_1 + C_2}{2C_1 + C_2 + D}$

Where C_1 is the number of concordant pairs discovered independently as index cases, C_2 is the number of concordant pairs discovered secondarily to interview with one of the twins, and D is the number of discordant twin pairs. Therefore, unlike pair concordance which simply shows the proportion of concordant twins, this calculation takes into consideration how the concordance was discovered (TYSK *et al.* 1988).

monozygotic counterparts (ORHOLM *et al.* 2000; THOMPSON *et al.* 1996). Furthermore, these twin studies have illustrated a greater genetic contribution to the development of CD than UC (ORHOLM *et al.* 2000; THOMPSON *et al.* 1996; TYSK *et al.* 1988).

Seven loci (known as IBD1-7) that confer susceptibility to CD, UC or both have been identified by genome-wide scans (WEERSMA *et al.* 2007). Subsequent fine mapping and candidate gene studies have associated various genes with IBD susceptibility (WEERSMA *et al.* 2007). The most well established IBD association is with nucleotide-binding oligomerization domain 2 (*NOD2*; also known as *CARD15*) which maps to the IBD1 locus and has three independent susceptibility variants: R702W, G908R and L1007fsinsC (AHMAD *et al.* 2002; CUTHBERT *et al.* 2002; HAMPE *et al.* 2001; HUGOT *et al.* 2001; OGURA *et al.* 2001). Each of these variants are significant risk factors for CD, but not UC (ECONOMOU *et al.* 2004; OOSTENBRUG *et al.* 2006). Furthermore, the *NOD2* variants are associated with ileal disease location in CD patients (AHMAD *et al.* 2002; ECONOMOU *et al.* 2004). NOD2 normally detects the muramyl dipeptide (MDP) component of bacterial cell walls, which in turn activates nuclear factor κB (NF-κB) (GIRARDIN *et al.* 2003; INOHARA *et al.* 2003; KOBAYASHI *et al.* 2005). However, the aforementioned variants decrease NF-Kb activation by MDP (BONEN *et al.* 2003; GIRARDIN *et al.* 2003; OGURA *et al.* 2001), suggesting that these NOD2 variants are unable to recognize and/or properly respond to luminal bacteria (OGURA *et al.* 2003). Additionally, Paneth cells, which abundantly express *NOD2* (LALA *et al.* 2003; OGURA *et al.* 2003), have decreased α-defensin expression in the ileum of CD patients, and this decrease is even more pronounced in those with *NOD2* variants (WEHKAMP *et al.* 2004; WEHKAMP *et al.* 2005). Since Paneth cells are highly concentrated in the ileum, their

decreased expression of α-defensins, which have an antibacterial role, may partly explain the ileal disease location in patients with *NOD2* variants (LALA *et al.* 2003). The above findings indicate that *NOD2* variants may increase CD susceptibility through impaired responses to luminal bacteria (OGURA *et al.* 2003; WEHKAMP *et al.* 2005). Other genes associated with IBD susceptibility include *IL23R* (on IBD7), *TLR4*, *OCTN1* (on IBD5), *TNFSF15*, *DLG5*, and *ATG16L*, amongst many others (DUERR *et al.* 2006; HAMPE *et al.* 2007; OOSTENBRUG *et al.* 2005; PELTEKOVA *et al.* 2004; STOLL *et al.* 2004; YAMAZAKI *et al.* 2005). However, the reported odds ratios for these genes are much lower than the odds ratio for *NOD2* (Table 1.1). Yet, despite having the most notable contribution to IBD of any genetic loci, the penetrance for homozygotes/compound heterozygotes of *NOD2* variants is only 4.9% (BRANT *et al.* 2007).

Table 1-1 Reported odds ratios (O.R.) for IBD susceptibility genes. Although this is not a comprehensive list of IBD susceptibility genes, it does illustrate the vast difference in IBD susceptibility associated with *NOD2* versus any other implicated genes.

Susceptibility Gene	Function	Disease Association	O.R.
NOD2/CARD15	Muramyl dipeptide recognition	CD	40.0*
IL23R	Subunit of proinflammatory cytokine receptor	CD and UC	2.46†
TLR4	Lipopolysaccharide recognition	CD and UC	2.45‡
OCTN1	Organic cation transporter	CD	2.19§
TNFSF15	Tumor necrosis factor cytokine	CD	2.17**
DLG5	Epithelial cell maintenance	CD and UC	1.74††
ATG16L	Role in autophagosome pathway	CD	1.45‡‡

* BRANT *et al.* (2007); † GLAS *et al.* (2007); ‡ FRANCHIMONT *et al.* (2004); § LEUNG *et al.* (2006); ** YAMAZAKI *et al.* (2005); †† STOLL *et al.* (2004); ‡‡ CUMMINGS *et al.* (2007)

1.3.2) Cholera

Cholera is an acute diarrheal disease caused by infection with the *Vibrio cholerae* bacterium, which is contracted through fecal-oral contamination or ingestion of contaminated food or water (WORLD HEALTH ORGANIZATION 2007). *Vibrio cholerae* efficiently produces the cholera toxin (CT) which has a high binding affinity and specificity for GM1 cell membrane receptors (SÁNCHEZ and HOLMGREN 2008). Upon binding, CT is endocytosed by the corresponding enterocyte and then travels to the endoplasmic recticulum where it enhances adenylate cyclase activity (SÁNCHEZ and HOLMGREN 2008). In turn, adenylate cyclase increases the intracellular cyclic adenosine monophosphate concentration which affects the function of the cystic fibrosis trans-membrane conductance regulator (SÁNCHEZ and HOLMGREN 2008). The resultant decrease in sodium uptake reduces the water intake by enterocytes, and the increase in anion (i.e. chloride) extrusion results in greater water output (SÁNCHEZ and HOLMGREN 2008). CT also increases the permeability of the intestinal mucosa by altering the structure of intercellular tight junctions (FASANO *et al.* 1991). The combined effect of decreased water absorption, increased water secretion, and enhanced mucosal permeability results in the characteristic copious, watery diarrhea observed in 20% of infected individuals (FASANO *et al.* 1991; FIELD 2003; SÁNCHEZ and HOLMGREN 2008; WORLD HEALTH ORGANIZATION 2007). Cholera patients are typically treated by oral administration of a salt and glucose solution which helps restore electrolyte balance and hydration (FIELD 2003; WORLD HEALTH ORGANIZATION 2007).

1.3.3) Familial Enteropathy with Villous Edema (FEVE)

Familial enteropathy with villous edema (FEVE; OMIM 600351) is a life-threatening gastrointestinal disorder that was identified in a large Mennonite kindred (Figure 1-1) (SMITH *et al.* 1994). Most members of this kindred are located in southern Alberta, Canada, but a number of affected individuals have been found in the northern United States (Oregon, Idaho, Montana, Wyoming, Maryland, Virginia, and Pennsylvania) (SMITH *et al.* 1994). Affected individuals experience recurrent episodes that are characterized by a sudden onset of fever and occasional abdominal pain, that progresses to intense nausea, persistent vomiting, and very profuse watery diarrhea within 5 to 6 hours (SMITH *et al.* 1994). Laboratory results indicate hyponatremia, hypokalemia, moderate metabolic acidosis, hypoalbuminemia, neutropenia, and severe hypogammaglobulinemia during the acute phase of illness (SMITH *et al.* 1994). These patients are treated with large volumes of replacement fluids and oral administration of immune globulin, after which the diarrhea begins to abate within 2 to 5 hours (SMITH *et al.* 1994). Malabsorption screens showed that affected individuals had no characteristic defects in absorption (SMITH *et al.* 1994). Small-bowel bacterial overgrowth was identified in some affected individuals via lactulose breath tests, but this phenomenon was also observed in unaffected individuals (SMITH *et al.* 1994). On gross inspection, jejunal biopsy specimens taken from affected individuals during remission showed a white, edematous mucosa, with microscopically visible club-like deformity of the villi resulting from massive edema of the lamina propria (Figure 1-2). Patchy acute enteritis was associated with a mainly interstitial neutrophil infiltrate along with edematous intracellular vacuoles in the most severely affected areas (SMITH *et al.* 1994). Epithelial

tight junctions were well preserved, but there was a loss of basement membrane integrity in some areas (SMITH *et al.* 1994). Biopsy specimens were obtained during clinical remission, sometimes years after the last FEVE episode, illustrating that these pathologic features persist throughout the lifespan of affected individuals (SMITH *et al.* 1994). The clinical manifestations are usually restricted to early childhood (SMITH *et al.* 1994), however adults have also been hospitalized for the condition. To date, more than 8 family members have died from hypovolemic shock during an acute episode of this form of IBD at ages ranging from 11 months to 22 years. All affected survivors grow and develop normally (SMITH *et al.* 1994). The precipitating factor of these episodes remains unknown despite extensive microbiological investigation (SMITH *et al.* 1994).

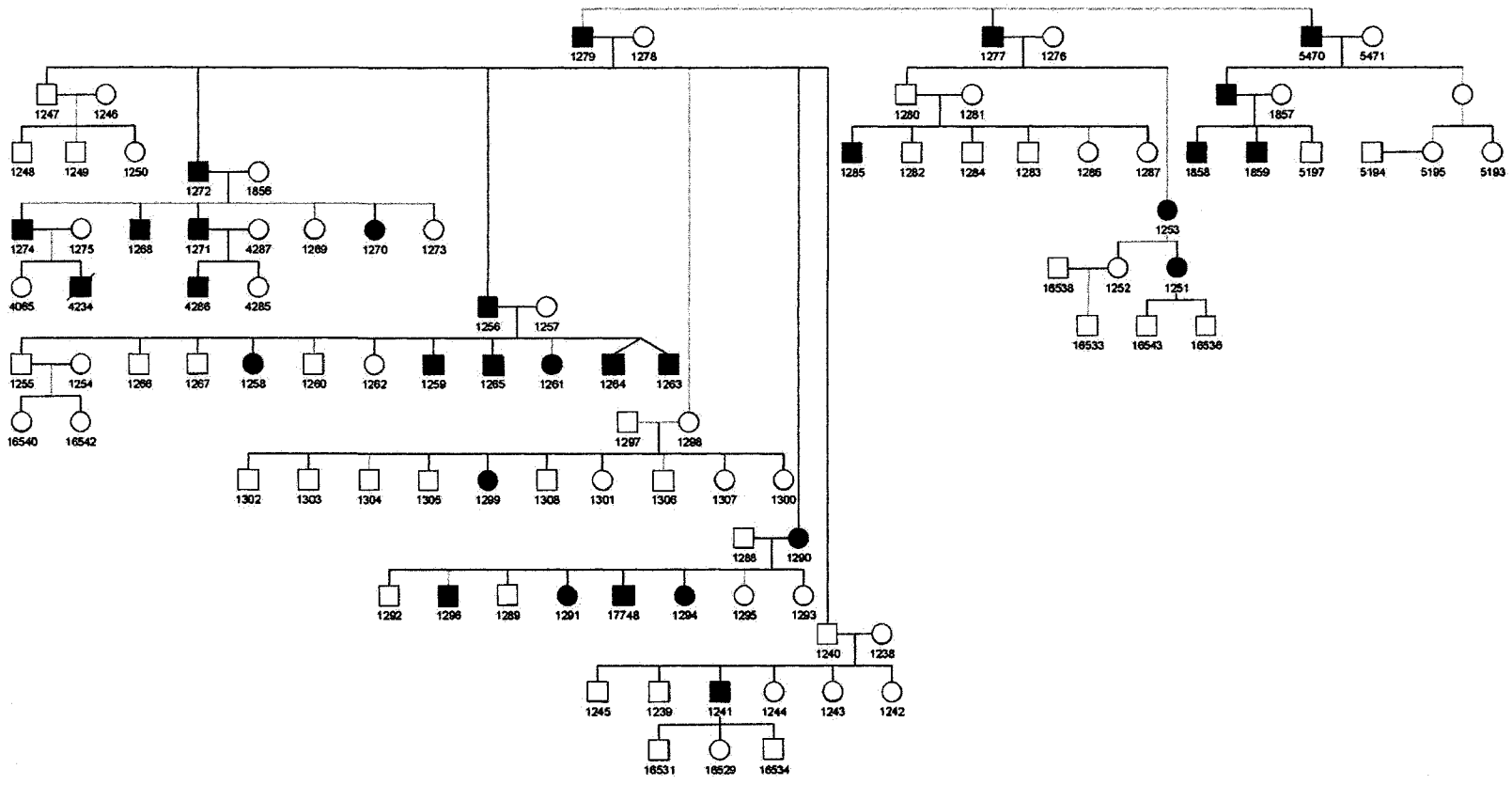

Figure 1-1 Pedigree of FEVE-affected kindred based on family reports of clinical history. Ninety-eight individuals from the Mennonite kindred are shown. Sample accession numbers are included for reference. Penetrance of the disorder is 0.91, based on the 30 clinically affected individuals (black circles/squares) and the 3 obligate carriers (1240, 1280, and 1298).

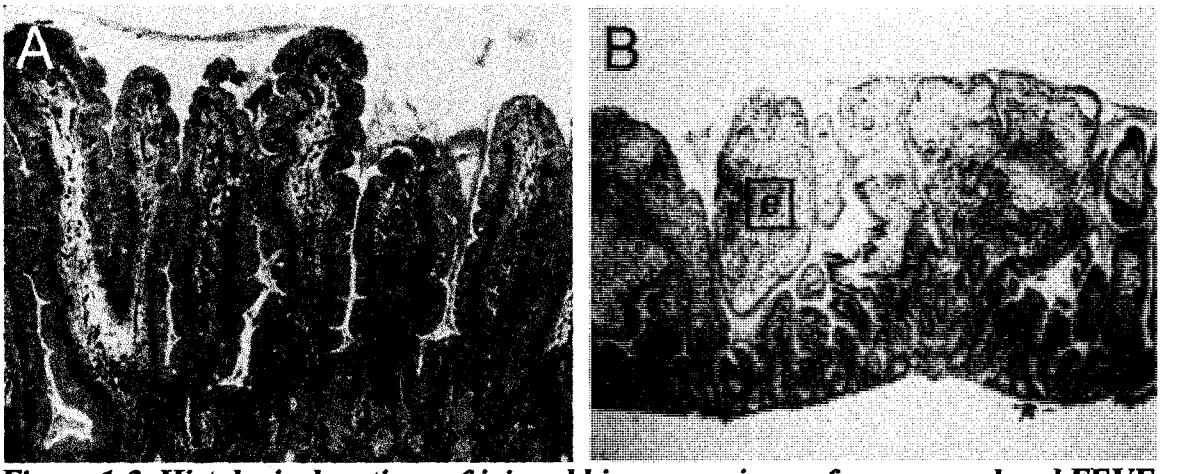

Figure 1-2 Histological sections of jejunal biopsy specimens from normal and FEVE affected individuals. **a)** Normal biopsy specimen. **b)** Affected biopsy specimen. Although the basic villous architecture is well preserved, there is a club-like deformity of the villi resulting from massive edema of the lamina propria (e). Figure image 'b' reprinted from SMITH *et al.* (1994) with permission from Elsevier.

1.3.3.1) Preliminary FEVE Research

An autosomal dominant mode of inheritance was established by compiling family history data in an extended pedigree (Figure 1-1). Variable penetrance and expressivity were indicated by obligate carriers who experienced intermittent mild diarrhea throughout life, without the characteristic FEVE symptoms, or were completely asymptomatic. Based on clinical history, the penetrance of FEVE is approximately 0.91 (Figure 1-1). Since the characteristic FEVE histology is present in obligate carriers (SMITH *et al.* 1994), biopsy specimens of the small bowel at the ligament of Treitz were the gold standard for diagnosing the disorder. Linkage analysis was carried out on 14 biopsy-confirmed positive and 4 biopsy-confirmed negative family members, enabling the assumption of 100% penetrance. Two-point LOD scores were calculated to determine linkage between the disease phenotype and markers. FEVE was linked to marker D11S908 on chromosome 11q23 with a maximum LOD score of 6.2 with a recombination fraction of 0. Thirty-three additional markers surrounding D11S908, and flanked by genome-wide microsatellites D11S898 and D11S925, were genotyped in 66 family members. This identified two key recombinants, and established a minimum candidate interval of 2.0 Mb on chromosome 11q23.3, between markers D11S4142 and D11S1364. Two positional candidate genes, *CD3D* and *IL10RA*, were sequenced and ruled out as candidates for FEVE based on the absence of mutations in affected individuals.

1.3.3.2) Summary of FEVE Thesis Research

This thesis describes the work I put forth to identify the genetic mutation responsible for the characteristic FEVE phenotype. Following refinement of the informative crossover positions, the open reading frames of 8 positional candidate genes were sequenced. A 198 bp in-frame intragenic duplication (c.552_749dup) was found in the APOA4 gene in all known affected individuals that was not seen in 32 ethnicity-matched control chromosomes, or in 400 normal chromosomes from the general population. This mutation, which adds 66 amino acids within the central portion of the 396 aa apoA-IV protein (p.184_250dup), is predicted to have a profound effect on normal protein structure, resulting in disruption of function. It is hypothesized that the duplication is a dominant negative mutation that reduces wildtype apoA-IV expression or its half-life. Furthermore, this mutant form of apoA-IV may be unable to suppress the endothelial expression of P-selectin, thereby allowing venular leukocyte adhesion and its resultant inflammation. Additionally, apoA-IV interactions with α-catenin and α_1-antichymotrypsin may exert an anti-inflammatory effect that is disrupted by the mutant protein.

FEVE is a unique gastrointestinal disorder, but it bears resemblance to the patchy histology of CD, the mucosal inflammatory response of UC, and the profuse watery diarrhea of cholera. Future investigations are warranted into the potential role of apoA-IV in other gastrointestinal disorders, such as CD and UC, as well as its anti-inflammatory function in the gastrointestinal system.

CHAPTER 2: MATERIALS & METHODS

2.1) Cases & Controls

Specimens from 96 FEVE kindred members, including 16 ethnicity-matched controls (married-in family members), were obtained following informed consent. Clinical status was assigned on the basis of clinical history and was previously verified for 20 individuals through biopsy specimens of the small bowel at the ligament of Treitz. These biopsies were taken from children and adults who had a history of acute attacks of FEVE (presumably affected) while they were asymptomatic, or from ones who had never had an attack (controls). Unrelated controls were selected from banked DNA (15μg/mL). This study was approved by the Faculty of Medicine Research Ethics Board at the University of Alberta.

2.2) Specimens

2.2.1) Blood

Three to 5 mL of peripheral venous blood was collected in EDTA-containing vacutainer tubes (BD, Franklin Lakes, NJ) and, in some cases, PAXgene tubes (PreAnalytiX, Oakville, ON) while individuals were clinically well.

2.2.2) Buccal

Sterile nylon bristle cytology brushes (Puritan, Guilford, ME) were used to scrape the inside cheek with a 360° rotation. After sampling, each brush was put in a labeled 1.7 mL microcentrifuge tube and the plastic straw was clipped off. Two samples (one per cheek) were collected from each person to obtain an adequate quantity of DNA.

2.2.3) Skin Punch Biopsy

Skin punch biopsy specimens were collected in tubes containing Hank's balanced salt solution (Invitrogen, Carlsbad, CA) by Dr. Charlotte Foulston of Medicine Hat, Alberta. Cells were cultured from these biopsy specimens in AmnioMAX^{TM}-C100 medium (Invitrogen, Carlsbad, CA) by the Stollery Children's Hospital Cytogenetics Laboratory (Edmonton, AB). RNA extractions were performed once cells reached confluence.

2.3) Nucleic Acid Extractions

2.3.1) DNA from Blood

Unless stated otherwise, DNA extractions from blood were performed by Leanne Vicen in the Stollery Children's Hospital Molecular Diagnostic Laboratory (Edmonton, AB). Based on when venous blood samples were received, they underwent one of the following three DNA extraction protocols:

2.3.1.1) Phenol/Chloroform

Most phenol/chloroform extractions were performed by Troy Johnson in Dr. Fiona Bamforth's laboratory at the University of Alberta Hospital (Edmonton, AB). Whole blood samples > 5 mL were spun at 3,000 RCF for 25 minutes, and the resulting buffy coat layer was added to a 50 mL conical tube containing 20 mL of RBC lysis buffer (2M HN_4Cl; 1 M $KHCO_3$; 0.5 M EDTA, pH 8.0; pH 7.4). If the blood sample was < 5 mL, then the initial centrifugation was omitted and RBC lysis buffer was added directly to the whole blood. Tube contents were mixed, and placed on ice for 20 minutes, followed by centrifugation at 3,000

RCF for 10 minutes. After decanting the supernatant, the remaining buffy coat pellet was broken up by flicking the bottom of the tube. Following the addition of 10 mL of RBC lysis buffer, the tube was placed on ice for another 10 minutes and then centrifuged at 3,000 RCF for 10 minutes. The supernatant was decanted, and 1.5 mL of sodium chloride-Tris-EDTA, 2 mL of cell lysis buffer (Applied Biosystems, Foster City, CA), and 50 μL Proteinase K (20 mg/mL, Applied Biosystems, Foster City, CA) were added to the broken pellet before incubating for 12 hours at 50°C. An equal volume of equilibrated phenol (approximately 5 mL; Sigma-Aldrich, St. Louis, MO) was added to each sample before mixing on a rotary shaker for 20 to 30 minutes. After centrifuging the sample at 3,000 RCF for 10 minutes, the aqueous layer was transferred to a new tube. Four mL of High TE (2 M Tris-Cl, pH 8.0; 0.5 M EDTA, pH 8.0), 1 mL of 5 M NaCl, and an equal volume of phenol / chloroform / isoamyl alcohol (25:24:1) were added to the aqueous solution. The sample was mixed on a Nutating Mixer (VWR, Chester, PA) or with a Hematology/Chemistry Mixer (Fischer Scientific, Pittsburgh, PA) for 20 minutes prior to be centrifuged at 3,000 RCF for 10 minutes. After isolating the aqueous phase, another equal volume of phenol / chloroform / isoamyl alcohol (25:24:1) was added, mixed, and centrifuged as stated previously. The aqueous phase was then extracted twice using an equal volume of chloroform / isoamyl alcohol (24:1), and mixed and centrifuged again as described previously. Two volumes of 99% EtOH were added and mixed well, prior to placing the sample on ice to precipitate the DNA. Spooled strands of high molecular weight DNA were pulled out using a glass rod, and washed in a 1.5 mL tube containing 1 mL of 70% EtOH. The DNA was removed from the EtOH and briefly air dried before being dissolved in 200 μL to 500 μL of low TE (2 M Tris-Cl, pH 8.0; 0.5 M EDTA, pH 8.0).

2.3.1.2) QIAamp® DNA Blood Mini Kit

This DNA extraction method involved the use of the QIAamp® DNA Blood Mini Kit (QIAGEN, Germany). This kit delivers purified DNA that is free of protein, nucleases, and other contaminants or inhibitors. Whole blood samples > 3 mL were spun at 3,000 RCF for 15 to 30 minutes, and the resulting buffy coat layer was added to a 50 mL conical tube containing 30 mL of RBC lysis buffer (2M HN_4Cl; 1 M $KHCO_3$; 0.5 M EDTA, pH 8.0; pH 7.4). If the blood sample was < 3 mL, then the initial centrifugation was omitted and RBC lysis buffer was added directly to the whole blood. Tube contents were mixed, placed on ice for 20 minutes, centrifuged at 1,920 RCF for 10 minutes, and the supernatant was decanted. If the remaining buffy coat pellet was excessively bloody or if the extraction was being done on whole blood, then 10 mL of RBC lysis buffer was added, the sample was put on ice for 10 minutes, centrifuged at 1,920 RCF for 10 minutes, and the supernatant was decanted. The buffy coat pellet was resuspended in 400 μL of PBS and mixed well. Exactly 200 μL of this solution was transferred to a 1.7 mL tube, and 40 μL of QIAGEN Protease (QIAGEN, Germany) was added and mixed well. While ensuring the previously added solution remained evenly suspended, 200 μL of AL Lysis Buffer (QIAGEN, Germany) was aliquoted. After mixing the sample, it was vortexed and incubated for 12 hours in a 56°C water bath. A white precipitate was formed by adding 220 μL of 100% EtOH to the lysed sample. The entire sample was loaded onto a QIAamp spin column in a 2 mL collection tube and centrifuged at 18,300 RCF for 1 minute. The column was transferred to a new 2 mL tube and the collection tube containing the filtrate was discarded. After adding 500 μL of AW1 Buffer to the column, the sample was centrifuged at 6,000 RCF for 1 minute. The filtrate was

discarded and the column was placed in a new 2 mL tube. Following the addition of 500 μL of AW2 Buffer to the column, the tube was centrifuged at 18,300 RCF for 3 minutes. The filtrate was discarded, and the column was transferred to a new 2 mL tube which was centrifuged at 18,300 RCF for 1 minute. After transferring the column to a new 1.7 mL tube, 100 μL of AE Buffer was added, and the tube was placed in a 65°C water bath for 5 minutes. The DNA was eluted by centrifugation at 6,000 RCF for 1 minute, and then reloaded onto the column for another centrifugation at 6,000 RCF for 1 minute. The final elute was transferred to a 2 mL screw top tube and stored at 4°C.

2.3.1.3) Puregene® DNA Purification Kit

This DNA extraction method involved the use of the Puregene® DNA Purification Kit (Gentra, Minneapolis, MN), which delivers purified DNA free of enzyme inhibitors and other contaminants. Three mL of whole blood was added to a 15 mL centrifuge tube containing 9 mL of Puregene® RBC Lysis Solution (Gentra, Minneapolis, MN). The sample was mixed by inversion, incubated at room temperature for 10 minutes, and inverted at least once during the incubation period. Following centrifugation at 2,000 RCF for ten minutes, the supernatant was removed leaving behind the buffy coat pellet and approximately 100 μL of the residual liquid. The remaining buffy coat pellet was resuspended in the residual liquid by flicking the tube, and 3 mL of Puregene® Cell Lysis Solution (Gentra, Minneapolis, MN) was added. If cell clumps were visible, the solution was incubated at 37°C until homogeneous. After adding 15 μL of Proteinase K (20 mg/mL), the sample was incubated at 56°C for 1 to 12 hours. The cell lysate was mixed by 25 inversions with 15 μL of Puregene® RNase A Solution (4 mg/mL) and incubated at 37°C for 30 minutes. Once cooled to room

temperature, 1 mL of Puregene® Protein Precipitation Solution was added to the sample, followed by 20 seconds of vortexing at high speed. Centrifugation at 2,000 RCF for 10 minutes formed a tight dark brown pellet of precipitated proteins. If this pellet was not firmly packed at the bottom of the tube, the sample was vortexed at high speed for 20 seconds, incubated on ice for 5 minutes, and then centrifuged again at 2,000 RCF for 10 minutes. The DNA-containing supernatant was poured into a clean 15 mL centrifuge tube containing 3 mL of HPLC grade 100 % Isopropanol. Following 50 gentle inversions, the white threads of DNA formed a visible clump. DNA was pelleted by centrifuging the sample at 2,000 RCF for 3 minutes. The supernatant was decanted and the tube was briefly drained on a Kim-Wipe. After adding 3 mL of 70% EtOH, the tube was inverted several times to wash the DNA pellet, which was released from the bottom of the tube by flicking or vortexing as needed. The ethanol was carefully poured off following a final centrifugation at 2,000 RCF for 1 minute. The tube was inverted and drained on a Kim-Wipe for 10 to 15 minutes, prior to resuspension of the pellet in 250 μL of Puregene® DNA Hydration Solution (Gentra, Minneapolis, MN). Following an incubation at 55°C for 1 hour or at room temperature for 12 hours, the hydrated DNA was stored at 4°C.

2.3.2) DNA from Buccal Cells

DNA was extracted from buccal cells using the Puregene® DNA Purification Kit (Gentra, Minneapolis, MN), which delivers purified DNA free of enzyme inhibitors and other contaminants. The cytology brush was dipped up and down 10 times in a 1.7 mL centrifuge tube containing 300 μL of Puregene® Cell Lysis Solution (Gentra/QIAGEN, Germany). Following the addition of 1.5 mL of Proteinase K Solution (20 mg/mL), the cell lysate was

incubated at 55°C for 1 to 12 hours and then cooled to room temperature. After adding 100 μL of Puregene® Protein Precipitation Solution (Gentra/QIAGEN, Germany) the sample was subjected to 20 seconds of vigorous vortexing and a 5 minute ice bath. A protein pellet was formed by centrifugation of the sample at 13,000-16,000 RCF for 3 minutes. The supernatant containing the DNA was transferred to a clean 1.7 mL tube containing 300 uL of HPLC grade 100% Isopropanol (2-propanol). The sample was gently mixed by 50 inversions and kept at room temperature for 5 minutes. Precipitated DNA was separated from solution by centrifugation of the sample at 13,000-16,000 RCF for 5 minutes. The resultant supernatant was discarded and the tube was drained on a clean Kim-Wipe. The DNA pellet was washed by inverting the tube several times with 300 μL of 70% EtOH. After centrifugation at 13,000-16,000 RCF for 3 minutes, the ethanol was poured off carefully. The tube was drained on a clean Kim-Wipe and left to air dry for 10-15 minutes. Resuspension of the DNA pellet in 20 μL of Puregene® DNA Hydration Solution (Gentra/QIAGEN, Germany) was followed by incubation for 1 hour at 55°C or 12 hours at room temperature. The sample was stored at 4°C until further use.

2.3.3) RNA from Blood

Intracellular RNA was isolated using the PAXgene Blood RNA Kit (PreAnalytiX, Oakville, ON). This kit stabilizes and purifies RNA by degrading proteins, homogenizing cell lysate, and removing both cellular debris and DNA. Whole blood was collected in PAXgene Blood RNA Tubes and stored at room temperature for 2 to 72 hours to facilitate cell lysis. Total RNA was subsequently purified according to the manufacturer's directions and stored at -80°C until further use.

2.3.4) RNA from Cultured Cells

RNA was purified from cultured fibroblast cells using the RNeasy® Plus Mini Kit (QIAGEN, Germay) according to the manufacturer's instructions. This method lysed cells and denatured proteins in a guanidine-isothiocyanate-containing buffer. Samples were then homogenized using a QIAshredder spin column which sheared high molecular weight cellular components including DNA. Genomic DNA was removed from the sample by passing the lysate through a gDNA Eliminator spin column. Seventy percent ethanol was added to the flow-through and the resulting mixture was transferred to an RNeasy® spin column. After potential column contaminants had been washed away Buffers RW1 and RPE, the bound RNA was eluted from the column in RNase-free water and stored at -80°C until further use.

2.4) Nucleic Acid Quantification

Genomic DNA was dissolved in low TE buffer (10 mM Tris-chloride, pH 8.0; 1 mM EDTA, pH 8.0) at room temperature for at least 24 hours, prior to diluting samples in H_2O for spectrometry. Samples were quantified by measuring absorbance at 260 nm (A_{260}) using a SpectraMax® Plus^{384} spectrometer (Molecular Devices, Sunnyvale, CA) with SoftMax Pro software (Molecular Devices, Sunnyvale, CA) according to the manufacturer's directions. DNA concentration was calculated based on a the conversion factor $A_{260}(1.0) = 50$ μg/mL DNA, taking into account the dilution factor of the original stock (i.e. 10μL of DNA resuspended in 190μL of H2O has a dilution factor of 20):

$$\text{DNA concentration } (\mu g/mL) = A_{260} \times (\text{dilution factor}) \times (50\ \mu g/mL)$$

DNA sample purity was assessed using the 260 nm / 280 nm absorbance ratio with the acceptable range being 1.7 to 1.9 for blood extractions, 1.7 to 2.0 for cell cultures, and 1.5 to 1.9 for buccals. Each sample was diluted to a final concentration of 150 μg/mL.

RNA was quantified by spectrometry as described in Appendix B of the Sensiscript Reverse Transcription Handbook (QIAGEN, Germany). RNA concentration was calculated based on a the conversion factor $A_{260}(1.0) = 40$ μg/mL RNA, taking into account the dilution factor of the original stock:

$$\text{RNA concentration } (\mu g/mL) = A_{260} \times (\text{dilution factor}) \times (40\ \mu g/mL)$$

Sample purity was assessed using the 260 nm / 280 nm absorbance ratio, for which pure RNA has a value between 1.9 and 2.1 in Tris buffer.

2.5) Linkage Analysis

2.5.1) Microsatellite Markers

Marker primer pairs were designed to flank dinucleotide microsatellite repeats between markers D11S4142 and D11S4092, as well as D11S1341 and D11S1364 (Table 2-1). These primers were designed using Primer Express® software v2.0 (Applied Biosystems, Foster City, CA) and nucleotide sequence specificity was checked using the Basic Local Alignment Search Tool (BLAST; http://ncbi.nlm.nih.gov/blast; ALTSCHUL *et al.* 1990) . Each forward primer was bound to a 6-FAM, HEX or TET fluorophore label (Table 2-1). Primers were synthesized by Integrated DNA Technologies, Inc. (Coralville, IA) and resuspended in 250 μL of low TE buffer (10 mM Tris-chloride, pH 8.0; 1 mM EDTA, pH 8.0) upon arrival. Concentrations were calculated based on the information provided in the oligonucleotide

specification sheets. Microsatellite marker aliquots were diluted to 100 μg/mL and stored at -20°C.

2.5.2) Amplification

Microsatellites were amplified in 25 μL reactions consisting of 150 ng of gDNA, 4 μL of dNTPs (4x 1.25 mM; Invitrogen, Carlsbad, CA), 2.5 μL of 10x Platinum® *Taq* buffer (Invitrogen, Carlsbad, CA), 1.25 μL or 1.5 μL of Sigma® $MgCl_2$ (25 mM; Sigma-Aldrich, St. Louis, MO), 0.25 μL of Platinum® *Taq* DNA polymerase (5U / μL; Invitrogen, Carlsbad, CA), and 0.5 μL each of 100 μg/mL forward and reverse microsatellite primers (Table 2-1). Amplifications were conducted in PerkinElmer 9600 thermal cyclers (PerkinElmer, Waltham, MA). After an initial denaturation step at 94°C for two minutes, the DNA was amplified with thirty 3-step cycles that varied with each microsatellite marker set (Table 2-1). This was followed by a final extension step at 72°C for ten minutes and then held at 4°C or 15°C. Samples were subsequently stored at 4°C.

2.5.3) Gel Electrophoresis

The specificity of Microsatellite marker products was verified by running 5μL of each product combined with 2 μL of Ficoll-based 10x loading buffer on a 1.5% (w/v) agarose/TBE gel at 80V for 1 hour or 120V for 40 minutes and visualizing the gel by EtBr staining.

2.5.4) Fragment Analysis

Microsatellite PCR products were pooled 1:1:1 for 6FAM:HEX:TET. 1 μL of the pooled mixture was mixed with 0.3 μL of GS500Rox size standard (Applied Biosystems, Foster City, CA), and 8.7 μL of Hi-Di™ formamide (Applied Biosystems, Foster City, CA) for a total reaction volume of 10μL. Samples were denatured at 95°C for 5 minutes, cooled on wet ice for 2 minutes, and then run on a 3130 Genetic Analyzer (Applied Biosystems, Foster City, CA) according to the manufacturer's instructions. Fragments were analyzed using GeneMapper® software v4.0 (Applied Biosystems, Foster City, CA).

2.6) Mutation Detection

2.6.1) Selection Criteria for Candidate Genes

Positional candidate genes were identified using the UCSC Human Genome Browser (http://genome.ucsc.edu). A subset of those genes were selected for sequencing based on having an expression profile and/or function that was consistent with the disease phenotype. Intestinal expression was assessed using the SymAtlas *Mus musculus* gene expression database (http://symatlas.gnf.org/SymAtlas; Su *et al.* 2002) and/or by literature review. Gene functions were assessed by literature review.

2.6.2) Primers

Oligonucleotides were designed to amplify the entire coding sequence of each gene. Exons approximately 500 bp or larger were amplified in smaller overlapping fragments (Figure 1-1). Each oligonucleotide was designed using Primer Express® software v2.0 (Applied

Biosystems, Foster City, CA) and nucleotide sequence specificity was checked using the Basic Local Alignment Search Tool (BLAST; http://ncbi.nlm.nih.gov/blast; ALTSCHUL *et al.* 1990). Primers were synthesized by Integrated DNA Technologies, Inc. (Coralville, IA) and resuspended in 250 μL of low TE buffer (10 mM Tris-chloride, pH 8.0; 1 mM EDTA, pH 8.0) upon arrival. Concentrations were calculated based on the information provided in the oligonucleotide specification sheets. Primer aliquots were diluted to either 100 μg/mL for PCR amplification reactions or 3.2 μM for sequencing reactions and stored at -20°C. Primers used for candidate gene amplification are listed in Table 2-2.

2.6.3) DNA Amplification

DNA was amplified in 25 μL to 50 μL reactions consisting of 15 ng to 150 ng of gDNA, 5 nmol of each of the four dNTPs (Invitrogen, Carlsbad, CA), 10% of final reaction volume of 10x Platinum® *Taq* buffer (Invitrogen, Carlsbad, CA), 1.25 mM to 1.75 mM of Sigma® $MgCl_2$ (25 mM, Sigma-Aldrich, St. Louis, MO), 1.25 U of Platinum® *Taq* DNA polymerase (Invitrogen, Carlsbad, CA), and 50 nmol each of forward and reverse primers (Table 2-2). Amplifications were conducted in PerkinElmer 9600 thermal cyclers (PerkinElmer, Waltham, MA) or Applied Biosystems 9800 fast thermal cyclers (Applied Biosystems, Foster City, CA). After an initial denaturation step at 94°C for two minutes, the DNA was amplified with thirty 3-step cycles that varied with each primer set (Table 2-2). This was followed by a final extension step at 72°C for ten minutes and then held at 4°C or 15°C. Samples were subsequently stored at 4°C.

2.6.4) PCR Fragment Purification

One of the following three methods was used for fragment purification.

2.6.4.1) QuickStep™*2* PCR Purification Kit

Amplification efficiency and specificity of PCR products was checked by running 5μL of each product combined with 2 μL of Ficoll-based 10x loading buffer on a 1.5% (w/v) agarose/TBE gel at 80V for 1 hour or 120V for 40 minutes and visualizing the gel by EtBr staining. Suitable PCR products were purified with QuickStep™*2* PCR Purification Kit (Edge Biosystems, Gaithersburg, MD) according to the manufacturer's instructions. This kit purifies DNA by removing proteins, primers, ssDNA, dNTPs, salts, buffers, and other small molecules. Purified samples were quantified spectrophotometrically by measuring the absorbances at 260 and 280 nm with a Spectramax SpectraMax Plus[384] spectrometer (Molecular Devices, Sunnyvale, CA).

2.6.4.2) ExoSAP-IT®

PCR products were purified with ExoSAP-IT® (USB Corporation, Cleveland, OH) according to the manufacturer's protocol. This PCR clean-up product utilizes Exonuclease I to degrade primers and ssDNA, and Shrimp Alkaline Phosphatase to hydrolyze residual dNTPs. Purified samples were quantified by running 5 μL of each product combined with 2 μL of Ficoll-based 10x loading buffer alongside 3 lanes containing 2 μL, 4 μL, and 8 μL respectively of a Low DNA Mass Ladder (Invitrogen, Carlsbad, CA) on a 1.5% (w/v) agarose/TBE gel at 80 V for 1 hour or 120 V for 40 minutes and visualizing the gel by EtBr staining. PCR product mass was estimated by a visual comparison to the mass ladder band

intensities (see Low DNA Mass Ladder manual, Invitrogen, Carlsbad, CA). Sample concentration was calculated by dividing the estimated mass by the 5 μL loading amount. The electrophoretic gel also served to ensure that the PCR products had amplified specifically and efficiently.

2.6.4.3) Extraction of DNA from Agarose Gels

Following DNA amplification using primer sets APOA4_Ex3c:F / APOA4_Ex3b:R and APOA4_Ex3dup:F / APOA4_Ex3dup:R (Table 2-2), 5 μL of each PCR product was combined with 2 μL of Ficoll-based 10x loading buffer and loaded onto a 1.5% (w/v) agarose/TBE gel. PCR products were separated at 120 V for 1 hour. Bands of interest were cut out of the gel over an ultraviolet Transilluminator FBTIV-816 (Fischer Scientific, Pittsburgh, PA) and extracted using the QIAquick® Gel Extraction Kit (QIAGEN, Germany) according to the manufacturer's spin protocol. This kit causes DNA to adsorb to the silica membrane of the QIAquick® column (QIAGEN, Germany) in the presence of a high concentration of salts, while contaminants, such as agarose and ethidium bromide, pass through the column. For the final step, DNA was eluted in 30 μL of Tris elution buffer.

2.6.5) Cycle Sequencing Reaction

Sequencing reactions were performed in strip tubes or 96-well plates with reagents from the BigDye® Terminator v3.1 Cycle Sequencing Kit (Applied Biosystems, Foster City, CA). Each 20 μL reaction contained 20 ng to 50 ng of purified PCR product, 3.2 pmol of the appropriate forward or reverse primer (Table 2-2), and either 4 μL and 1 μL or 1 μL and 3.5

μL of Ready Reaction Premix and BigDye® Sequencing Buffer (5x) respectively. Thermal cycling was performed according to the manufacturer's instructions.

2.6.6) Cycle Sequencing Reaction Clean-Up

One of the following two methods was used for cycle sequencing reaction clean-up.

2.6.6.1) Performa® DTR Gel Filtration Cartridges

Cycle sequencing products were purified using Performa® DTR Gel Filtration Cartridges (Edge Biosystems, Gaithersburg, MD) which remove dye terminators, dNTPs, primers, and other low molecular weight material. Each Performa® DTR Gel Filtration Cartridge was centrifuged at 770 RCF for 2 minutes and then transferred to a new 1.5 mL tube. The 20 μL sequencing reaction product was loaded onto the gel of the packed column, followed by centrifugation at 770 RCF for 2 minutes. After removing the cartridge, samples were dried down in a Savant Vacuum concentrator (Thermo Savant, Waltham, MA) for 20 to 30 minutes or until all of the liquid had evaporated. Dried sequencing samples were stored at 4°C until further use.

2.6.6.2) Ethanol Precipitation

The purification of cycle sequencing products began with the addition of 5 μL of 125 mM EDTA and 80 μL of cold precipitation solution (38mL of 95% EtOH, 250 μL of 3% (w/v) dextran blue solution, 1750 μL H_2O). After mixing contents by inversion, samples sat at room temperature for 3 minutes in strip tubes or 10 minutes in a 96-well plate. Mixtures were centrifuged in strip tubes for 10 minutes or in a 96-well plate at 2,000 RCF for 12

minutes. Supernatant was removed from strip tubes by pipetting, whereas 96-well plates were inverted to drain the supernatant and then spun inverted at 290 RCF for 30 seconds. 150 μL of cold 70% EtOH was added to each sample. Strip tubes were spun for 3 minutes and the supernatant was pipetted off. 96-well plates were spun at 2,000 RCF for 5 minutes, and then spun inverted at 290 RCF for 1 minute to remove the supernatant. After air drying for 10 minutes, samples were stored at 4°C.

2.6.7) Automated Sequencing

Dried samples were resuspended in 20 μL Hi-Di™ formamide (Applied Biosystems, Foster City, CA) and transferred to a 96-well plate. After sealing the plate with a 96-well septa (Applied Biosystems, Foster City, CA), samples were denatured at 95°C for 5 minutes, and then placed on wet ice for 2 minutes. Plates were run on the 3130 Genetic Analyzer (Applied Biosystems, Foster City, CA) according to the manufacturer's instructions using POP6 polymer, GenericSeqPOP6 or SeqPOP6v3.1SHORT instrument protocol, and GenericSequencing or GenericSeq_v3.1_POP6 analysis protocol.

2.6.8) Sequence Analysis

Sequence analysis was performed on both forward and reverse DNA strands using Sequencing Analysis software v5.2 (Applied Biosystems, Foster City, CA) and Mutation Surveyor™ v3.00 demo software (Softgenetics, Pennsylvania, USA). Reference sequences were retrieved from the GenBank® database (http://www.ncbi.nlm.nih.gov/Genbank). Sequence variants in affected individuals were excluded as possible causative mutations based on their absence in another affected individual, or their presence in an ethnicity-

matched control, population control, the GenBank® reference sequence, and/or having been previously reported in the Single Nucleotide Polymorphism database (dbSNP; http://www.ncbi.nih.gov/SNP). Sequence variants were described using the nomenclature recommendations put forth by the Human Genome Variation Society (http://www.hgvs.org; DEN DUNNEN and ANTONARAKIS 2000).

2.7) RNA Expression Analysis

2.7.1) RT-PCR

Prior to RT-PCR, RNA quality was assessed by running 5 μL of RNA combined with 3 μL of 10x Ficoll-based loading buffer on a 1% (w/v) agarose/TBE gel at 100V for 1 hour and visualizing the gel by EtBr staining.

RT-PCR was conducted using the Sensiscript® RT Kit (QIAGEN, Germany) which is designed for highly sensitive reverse transcription with less than 50 ng RNA. The 7 μL master mix for each reaction consisted of 2 μL of 5 mM dNTP Mix (QIAGEN, Germany), 2 μL of 10x Buffer RT (QIAGEN, Germany), 2 μL of 40U/μL RNasin® RNase Inhibitor (Promega, Madison, WI) and 1 μL of Sensiscript® Reverse Transcriptase (QIAGEN, Germany). RNase-free water (QIAGEN, Germany) was added to approximately 40 ng of total RNA for a sample volume of 11 μL. RNA was denatured at 65°C for 5 minutes, and then held at 4°C in Applied Biosystems 9800 fast thermal cyclers (Applied Biosystems, Foster City, CA). After aliquoting 2 μL of 250ng/mL Oligo-dT primer to the sample, primers were annealed at 25°C for 10 minutes. Addition of a 7 μL aliquot of the master mix was followed by 37°C for 60 minutes.

2.7.2) Verification of Successful RT-PCR

Following RT-PCR, the presence of cDNA was verified using a previously optimized PCR amplification with primers MLH1:16-2F and MLH1:18-1R (Table 2-3). These primers anneal to *MLH1* exons 16 and 18 respectively, thereby including two introns and an additional 1,127 nucleotides in possible DNA products. Electrophoretic separation of the amplified products enables the identification of cDNA versus DNA due to their differential size. cDNA was amplified in 25 μL reactions consisting of 4 μL of the RT-PCR product, 4 μL of dNTPs (4x 1.25 mM; Invitrogen, Carlsbad, CA), 2.5 μL of 10x Platinum® *Taq* buffer (Invitrogen, Carlsbad, CA), 1.5 μL of Sigma® $MgCl_2$ (25 mM; Sigma-Aldrich, St. Louis, MO), 0.5 μL of Platinum® *Taq* DNA polymerase (5U / μL; Invitrogen, Carlsbad, CA), and 1 μL of each primer (6.25 μM). Amplifications were conducted in Applied Biosystems 9800 fast thermal cyclers (Applied Biosystems, Foster City, CA). After an initial denaturation step at 94°C for two minutes, the cDNA was amplified by five 3-step touchdown PCR cycles, with each cycle consisting of 94°C for thirty seconds, 60°C, 59°C, 58°C, 57°C, or 56°C for thirty seconds, and 72°C for 1 minute. The reaction continued with 25 more cycles of 94°C for thirty seconds, 55°C for thirty seconds, and 72°C for 1 minute. The short 30 second amplification time was used to favour small cDNA products, as opposed to the possible larger DNA products. After the final extension step of 72°C for ten minutes, samples were held at 15°C. The presence of amplified cDNA products was verified by running 5μL of each product mixed with 2.5 μL of Ficoll-based 10x loading buffer alongside 1 Kb Plus DNA Ladder (Invitrogen, Carlsbad, CA) on a 1.5% (w/v) agarose/TBE gel at 100V for 1 hour and visualizing the gel by EtBr staining.

2.7.3) PCR I of RT Products

cDNA was amplified in 25 μL reactions containing 2 μL of the RT product, 4 μL of dNTPs (4x 1.25mM; Invitrogen, Carlsbad, CA), 2.5 μL of 10x Platinum® *Taq* buffer (Invitrogen, Carlsbad, CA), 1.5 μL of $MgCl_2$ (25mM; PerkinElmer, Waltham, MA), 0.25 μL of Platinum® *Taq* DNA polymerase (5U / μL; Invitrogen, Carlsbad, CA), and 0.5 μL each of 10 μM primers APOA4_Ex3dup:F and APOA4_Ex3dup:R or APOA4_Ex2_CDS:F and APOA4_Ex3c:R (Table 2-3; Figure 1-1). Amplifications were conducted in Applied Biosystems 9800 fast thermal cyclers (Applied Biosystems, Foster City, CA), starting with a denaturation step at 94°C for two minutes. The cDNA was amplified with thirty 3-step cycles that varied with each primer set (Table 2-3). After a final extension step at 72°C for ten minutes, samples were held at 15°C. The presence of PCR I products was assessed by running 5μL of each product mixed with 2.5 μL of Ficoll-based 10x loading buffer on a 1% (w/v) agarose/TBE gel at 80V or 100V for 1 hour and visualizing the gel by EtBr staining.

2.7.4) PCR II of RT Products

cDNA was further amplified in 25 μL reactions containing 1 μL of the PCR I product, 4 μL of dNTPs (4x 1.25mM; Invitrogen, Carlsbad, CA), 2.5 μL of 10x Platinum® *Taq* buffer (Invitrogen, Carlsbad, CA), 1.5 μL of $MgCl_2$ (25mM; PerkinElmer, Waltham, MA), 0.25 μL of Platinum® *Taq* DNA polymerase (Invitrogen, Carlsbad, CA), and 0.5 μL each of 6.25 μM primers APOA4_Ex3dup:F and APOA4_Ex3dup:R (Table 2-3; Figure 1-1). The initial denaturation step at 94°C for two minutes was followed by thirty 3-step cycles (Table 2-3). After the final extension step of 72°C for ten minutes, samples were held at 15°C. The

presence of PCR II products was assessed by running 5μL of each product mixed with 2.5 μL of Ficoll-based 10x loading buffer on a 1% (w/v) agarose/TBE gel at 80V for 1 hour and visualizing the gel by EtBr staining.

2.8) Protein Analysis

2.8.1) Protein Sample Preparation

Blood plasma from clinically well patients was isolated during DNA extractions and stored at -80°C. After thawing, each sample was centrifuged for 1 minute at approximately 10,000 RCF, and DNA was sheared by passing the plasma through a 25 gauge needle several times. The plasma was mixed with 2% β-mercaptoethanol and 1% saturated bromphenol blue in a 2x sample buffer (20% v/v glycerol; 4% w/v SDS; 0.13 M Tris; pH 6.8 with HCl) and boiled for 5 minutes prior to loading 5 μL on the SDS-PAGE gel.

2.8.2) Separation of Proteins

SDS-PAGE was carried out with a 4% stacking gel, followed by a 9% resolving gel in running buffer (0.025 M Sigma 7-9® (Sigma-Aldrich, St. Louis, MO); 0.192 M glycine; 0.1% w/v SDS). Proteins were separated alongside 7.5 μL of PageRuler™ Prestained Protein Ladder Plus (Fermentas, Hanover, MD) by applying a current of 30 to 80 mA until the 35 kDa protein-dye band reached the bottom of the gel. Electrophoresis was conducted in a Mini-PROTEAN® 3 Electrophoresis Module (Bio-Rad, Hercules, CA) with the corresponding PowerPac™ (Bio-Rad, Hercules, CA).

2.8.3) Transfer

Immobilon-P Membrane (Millipore, Billerica, MA) was immersed in methanol for 1 minute, and then soaked in transfer buffer (25 mM Tris base; 192 mM glycine; 20% v/v methanol) along with the filter paper, fiber pads, and gel. After assembling the Mini Trans-Blot® Electrophoretic Transfer Cell (Bio-Rad, Hercules, CA) according the the manufacturer's instructions, the size-fractioned proteins were transferred to the Immobilon-P Membrane (Millipore, Billerica, MA) using a constant voltage of 100 V for 1 hour.

2.8.4) Staining

While still wet from the transfer, the membrane was stained with amido black (0.1% w/v amido black dye; 25% v/v isopropanol; 10% v/v acetic acid) for two minutes on a rocking platform. After confirming protein presence, the stain was poured off and the membrane was destained with 25% v/v isopropanol and 10% v/v acetic acid. This was followed by two 5 minute washes in TBST.

2.8.5) Blocking

The membrane was immersed in Tris buffered saline-Tween (TBST: 20 mM Tris, pH 7.5; 137 mM NaCl; 0.1% v/v Tween-20; pH 7.6 with 1 N HCl) with 5% (w/v) non-fat dry milk powder (TBST-M) for 1 hour on a rocking platform (Orbital Shaker: VWR, Chester, PA). After blocking, the membrane was incubated with apoA-IV (C-20) antibody (Santa Cruz Biotechnology, Inc., Santa Cruz, CA) for 12 hours at 1/200 dilution in TBST-M on a rocking platform. The membrane was removed from the primary antibody and rinsed for three intervals of 10 minutes with TBST. A 1 hour incubation with donkey anti-goat IgG-HRP

(Immunoglobulin G – horse radish peroxidase) at 1/5000 dilution in TBSTM on a rocking platform, was followed by rinsing with TBST for three intervals of 10 minutes.

2.8.6) Detection System and Development

The secondary antibodies were detected using an enhanced chemiluminescence (ECL) system. The membrane was immersed in a 10 mL equal mixture of ECL solutions 1 and 2 (Millipore, Billerica, MA) for 1 minute. After removing the blot from the ECL reagents, it was digitally imaged on a Kodak Image Station 4000MM using Kodak MI software v4.0.5 (Carestream Health, Rochester, NY).

Table 2-1 Microsatellite markers for refining key recombinant positions. Intermediate PCR reaction conditions are indicated for each pair of microsatellite primers. All PCR reactions consisted of [94°C x 2 min], followed by the three-step cycle indicated in the table, then [72°C x 10 min], and finally held at 15°C until removed from the thermocycler.

#	Name	Primer sequence in 5'-3' orientation	PCR
1	MDL115.9MB:F	6-FAM/AACAGAAGAGAGAACCTAGCACTAAAACAT	[94°C x 30 sec, 55°C x 30 sec, 72°C x 30 sec] x 30
2	MDL115.9MB:R	CACACTAAGCAAAGCCTTTTCCTC	
3	MDL115.94MB:F	HEX/CCCCACAACCCCTGTCTTT	[94°C x 30 sec, 55°C x 30 sec, 72°C x 30 sec] x 30
4	MDL115.94MB:R	TGGTTCTAGCCTATTTCAGGTTGA	
5	MDL116.0MB:F	6-FAM/ACGTGGGATACAGCTAAAGCAAG	[94°C x 30 sec, 55°C x 30 sec, 72°C x 30 sec] x 30
6	MDL116.0MB:R	TTCCCCCATCTTTGTTGCC	
7	MDL116.03MB:F	HEX/CCTCATGCCTATCTCCCCACT	[94°C x 30 sec, 55°C x 30 sec, 72°C x 30 sec] x 30
8	MDL116.03MB:R	CTACCTGCCTGCTTTGCTGG	
9	MDL117.69MB:F	6-FAM/GGGAAATAGCCCCAAACTTTG	[94°C x 30 sec, 62.5°C x 30 sec, 72°C x 30 sec] x 30
10	MDL117.69MB:R	TTAACTCTTTGTTACCCCAACTCAAG	
11	MDL117.70MB:F	TET/GTGGAGGCAACCCAAATGC	[94°C x 30 sec, 65°C x 30 sec, 72°C x 30 sec] x 30
12	MDL117.70MB:R	CAATCTCATCTAGGTCGCTGTGA	
13	MDL117.76MB:F	HEX/CATTCATCTAACTTTCCCTGTCCTTT	[94°C x 30 sec, 62.5°C x 30 sec, 72°C x 30 sec] x 30
14	MDL117.76MB:R	TCTGTTACTCAGCATGATATGGCC	
15	MDL117.96MB:F	6-FAM/AATCTGCCGTTCTAGTTCTGACACT	[94°C x 30 sec, 62.5°C x 30 sec, 72°C x 30 sec] x 30
16	MDL117.96MB:R	CTACAGGCACATGCTACCGC	
17	D11S1341:F	TET/TGGCCTCTTGTCACTCCTA	[94°C x 30 sec, 57.5°C x 30 sec, 72°C x 30 sec] x 30
18	D11S1341:R	TGCTCTTCAAAGCAAAATG	
19	D11S1364:F	HEX/ACTCCAGCCTGGGCAA	[94°C x 30 sec, 57.5°C → 53.5°C x 30 sec, 72°C x 30 sec] x 5
20	D11S1364:R	GATAGATGGATCATGGATACAGG	[94°C x 30 sec, 52.5°C x 30 sec, 72°C x 30 sec] x 25
21	D11S1340:F	HEX/GCTGAATGAGTCCTGAGTAATAA	[94°C x 30 sec, 57.5°C x 30 sec, 72°C x 30 sec] x 30
22	D11S1340:R	GGCCTAGACGTTCTTTTGTG	
23	D11S4142:F	FAM/GAGATGGCTGCTTAATACCC	[94°C x 30 sec, 57.5°C x 30 sec, 72°C x 30 sec] x 30
24	D11S4142:R	TGATGTCCATGGCTGTTT	

"→" represents touchdown PCRs where there is a drop of 1°C after each of the 5 cycles.

Table 2-2 Amplification and sequencing primers for the exons of FEVE candidate genes. Intermediate PCR reaction conditions are indicated for each pair of primers. All PCR reactions consisted of [94°C x 2 min], followed by the three-step cycle indicated in the table, then [72°C x 10 min], and finally held at 15°C until removed from the thermocycler. Table continues onto next 4 pages.

#	Name	Primer sequence in 5'-3' orientation	PCR
1	EVA1_Ex1:F	GAAAGGAAGGAGGGCATTGG	[94°C x 30 sec, 55°C x 30 sec, 72°C x 30 sec] x 30
2	EVA1_Ex1:R	AACTGTATCTGTGGCTCAGGCTC	
3	EVA1_Ex2:F	TCTGGGTGAAGTAAGTTTGGGAG	[94°C x 30 sec, 55°C x 30 sec, 72°C x 30 sec] x 30
4	EVA1_Ex2:R	AACCTTGTGCTTGCTGCTAAGAA	
5	EVA1_Ex3:F	GACAGAGCTGCAGACAGGACAG	[94°C x 30 sec, 55°C x 30 sec, 72°C x 30 sec] x 30
6	EVA1_Ex3:R	CCTTAACAAAGATTGCCCCTTTC	
7	EVA1_Ex4:F	CTTCGAAGACCACACTTTGAGAAC	[94°C x 30 sec, 55°C x 30 sec, 72°C x 30 sec] x 30
8	EVA1_Ex4:R	GCAACTATTTAGCCCACTGCAA	
9	EVA1_Ex5:F	GGGAAAAATACCTTACCTGAAGCTT	[94°C x 30 sec, 55°C x 30 sec, 72°C x 30 sec] x 30
10	EVA1_Ex5:R	GATCTGGGAGTCCTCATTAGAGATG	
11	PAFAH1B2_Ex2:F	AGTGGTAACAAACCTTCCTG	[94°C x 30 sec, 60°C → 56°C x 30 sec, 72°C x 30 sec] x 5
12	PAFAH1B2_Ex2:R	GCTATATGGGAGGCTGAAGT	[94°C x 30 sec, 55°C x 30 sec, 72°C x 30 sec] x 25
13	PAFAH1B2_Ex3:F	CAGCCAGAAGTGCCAGT	[94°C x 30 sec, 55°C x 30 sec, 72°C x 30 sec] x 30
14	PAFAH1B2_Ex3:R	GAAAGTCTGTTAGTAATGAATGGA	
15	PAFAH1B2_Ex4:F	GATTAAACTTTCCCCTAGTTTT	[94°C x 30 sec, 55°C x 30 sec, 72°C x 30 sec] x 30
16	PAFAH1B2_Ex4:R	TTTACAGTTTCAGACAATTTAACTAT	
17	PAFAH1B2_Ex5:F	GACGTTCCTTTGTTCCTGGG	[94°C x 30 sec, 55°C x 30 sec, 72°C x 30 sec] x 30
18	PAFAH1B2_Ex5:R	GTATGATAAACTGCTTCCACCTCAAG	
19	PAFAH1B2_Ex6:F	TGTTTCACAACTCAAAGGTG	[94°C x 30 sec, 55°C x 30 sec, 72°C x 30 sec] x 30
20	PAFAH1B2_Ex6:R	CAATGCAAAGTGCCTTAAGA	
21	AMICA1_Ex1:F	CAGAATCAGCCAGCAAATGC	[94°C x 30 sec, 55°C x 30 sec, 72°C x 30 sec] x 30
22	AMICA1_Ex1:R	CCTATCCAGCCCCTTACACTTTT	
23	AMICA1_Ex2:F	GGAATTGATTTTTGTTGTTGA	[94°C x 30 sec, 55°C x 30 sec, 72°C x 30 sec] x 30
24	AMICA1_Ex2:R	TGCCTGACTCTTACACCACT	
25	AMICA1_Ex3:F	GCTCCTCGGTCTGGC	[94°C x 30 sec, 55°C x 30 sec, 72°C x 30 sec] x 30
26	AMICA1_Ex3:R	ATCAGTTTCCTTGCCTCTT	
27	AMICA1_Ex4:F	TTTGCTGCTGAGGGTCTTTG	[94°C x 30 sec, 55°C x 30 sec, 72°C x 30 sec] x 30
28	AMICA1_Ex4:R	AACACCTCCTCATGTGCCTG	
29	AMICA1_Ex5:F	GAGTCCTGAGATCTTCCCTC	[94°C x 30 sec, 55°C x 30 sec, 72°C x 30 sec] x 30
30	AMICA1_Ex5:R	CGGCCTCACTCTAGTCCT	

"→" represents touchdown PCRs where there is a drop of 1°C after each of the 5 cycles.

Table 2-2 Continued.

#	Name	Primer sequence in 5'-3' orientation	PCR
31	AMICA1_Ex6:F	GGCTCTCAGCTCTTTGCTAA	[94°C x 30 sec, 55°C x 30 sec, 72°C x 30 sec] x 30
32	AMICA1_Ex6:R	CCCTATCACCCTGTTCTACTTT	
33	AMICA1_Ex7:F	ATGTAGGGACCCTTGAATAA	[94°C x 30 sec, 55°C x 30 sec, 72°C x 30 sec] x 30
34	AMICA1_Ex7:R	GCGACATACAATGGGTAAGA	
35	AMICA1_Ex8:F	AGTGGGTGGCCTTTTCTCTG	[94°C x 30 sec, 55°C x 30 sec, 72°C x 30 sec] x 30
36	AMICA1_Ex8:R	CAGCCTCCCTTGGGCAA	
37	AMICA1_Ex9:F	GCTCAATGAACAGCAGCTG	[94°C x 30 sec, 55°C x 30 sec, 72°C x 30 sec] x 30
38	AMICA1_Ex9:R	ATCACTGGTAGAGTGGCCC	
39	SCN2B_Ex1:F	ATGCCCTCCCACCTGCTT	[94°C x 30 sec, 57.5°C x 30 sec, 72°C x 30 sec] x 30
40	SCN2B_Ex1:R	CACATTGCGGCTACACTTCTG	
41	SCN2B_Ex2:F	CAGCCAGACTCCTCACCAGC	[94°C x 30 sec, 65°C → 61°C x 30 sec, 72°C x 30 sec] x 5
42	SCN2B_Ex2:R	GGGCTTCATGCCATGGG	[94°C x 30 sec, 60°C x 30 sec, 72°C x 30 sec] x 25
43	SCN2B_Ex3:F	GGGCATCCTCACTGTCCTTGT	[94°C x 30 sec, 57.5°C x 30 sec, 72°C x 30 sec] x 30
44	SCN2B_Ex3:R	AGAGTAGGTGGGTGGGAAAGGT	
45	SCN2B_Ex4:F	ACGCATGCCACGGGTAGT	[94°C x 30 sec, 55°C x 30 sec, 72°C x 30 sec] x 30
46	SCN2B_Ex4:R	GAAGCACACCAAGAGCGAGC	
47	SCN4B_Ex2:F	GCCTAAGCATCCCCTTCCA	[94°C x 30 sec, 65°C → 61°C x 30 sec, 72°C x 30 sec] x 5
48	SCN4B_Ex2:R	CCAGAGCGTAGGAGGCGAG	[94°C x 30 sec, 60°C x 30 sec, 72°C x 30 sec] x 25
49	SCN4B_Ex3:F	CCCGATTCTTTCTCGGCTACT	[94°C x 30 sec, 57.5°C x 30 sec, 72°C x 30 sec] x 30
50	SCN4B_Ex3:R	TTCACTGTGATGCTGAGTTGGG	
51	SCN4B_Ex4:F	GTGGAGGCTACATGGCCCT	[94°C x 30 sec, 65°C → 61°C x 30 sec, 72°C x 30 sec] x 5
52	SCN4B_Ex4:R	AAGGCTGAAAGCTGGTGGG	[94°C x 30 sec, 60°C x 30 sec, 72°C x 30 sec] x 25
53	SCN4B_Ex5:F	CGGCTCCTGCCACAATTCT	[94°C x 30 sec, 55°C x 30 sec, 72°C x 30 sec] x 30
54	SCN4B_Ex5:R	GTTTGAGCCAAGCAGCAGATG	
55	TMPRSS4_Ex1:F	GGTGTTGTTCCAGCCCCTAA	[94°C x 30 sec, 55°C x 30 sec, 72°C x 30 sec] x 30
56	TMPRSS4_Ex1:R	TGGATGCTCAGGCTGCTTG	
57	TMPRSS4_Ex2:F	AAGACCCAAGAACCTCCCGT	[94°C x 30 sec, 55°C x 30 sec, 72°C x 30 sec] x 30
58	TMPRSS4_Ex2:R	GGCGCGAGTGGCTTAGG	
59	TMPRSS4_Ex3:F	GGAGGCTGTGGAGTTTGGC	[94°C x 30 sec, 65°C → 61°C x 30 sec, 72°C x 30 sec] x 5
60	TMPRSS4_Ex3:R	AGATCACCTGCCCCTGACTGT	[94°C x 30 sec, 60°C x 30 sec, 72°C x 30 sec] x 25
61	TMPRSS4_Ex4:F	TGAGCCTGGAACTCACACATG	[94°C x 30 sec, 57.5°C x 30 sec, 72°C x 30 sec] x 30
62	TMPRSS4_Ex4:R	GATACTATGCAGTGGGCCGTG	

"→" represents touchdown PCRs where there is a drop of 1°C after each of the 5 cycles.

Table 2-2 Continued.

#	Name	Primer sequence in 5'-3' orientation	PCR
63	TMPRSS4_Ex5:F	GCTGGTCTCATGATGAGTTCTGA	[94°C x 30 sec, 55°C x 30 sec, 72°C x 30 sec] x 30
64	TMPRSS4_Ex5:R	TGCCCGTAATTTTTAGGAAAGAGAG	
65	TMPRSS4_Ex6:F	CACCAAGCATTCTCTGCCACT	[94°C x 30 sec, 55°C x 30 sec, 72°C x 30 sec] x 30
66	TMPRSS4_Ex6:R	TGCTTACATTCCCCTGGCTG	
67	TMPRSS4_Ex7:F	TTAACAGCTTCGGGAGGCCT	[94°C x 30 sec, 57.5°C x 30 sec, 72°C x 30 sec] x 30
68	TMPRSS4_Ex7:R	GGAGTCCCAGAAATTTAGGAGTGA	
69	TMPRSS4_Ex8:F	CCCAGCCATAAGGGCCC	[94°C x 30 sec, 65°C → 61°C x 30 sec, 72°C x 30 sec] x 5
70	TMPRSS4_Ex8:R	GCCAGGAGACAGGACCCC	[94°C x 30 sec, 60°C x 30 sec, 72°C x 30 sec] x 25
71	TMPRSS4_Ex9:F	CCAGCACCCCGATCCC	[94°C x 30 sec, 62.5°C → 58.5°C x 30 sec, 72°C x 30 sec] x 5
72	TMPRSS4_Ex9:R	CAAGGGCGGTCAGTGAGCTA	[94°C x 30 sec, 57.5°C x 30 sec, 72°C x 30 sec] x 25
73	TMPRSS4_Ex10:F	GATCCCCATAATCATAAAGCATCAT	[94°C x 30 sec, 55°C x 30 sec, 72°C x 30 sec] x 30
74	TMPRSS4_Ex10:R	GCCTTGGTGCTTGGTCCTC	
75	TMPRSS4_Ex11:F	GCAGGAGATGCCCTTGTATGAG	[94°C x 30 sec, 55°C x 30 sec, 72°C x 30 sec] x 30
76	TMPRSS4_Ex11:R	TTCCTGTAGGGCATGCAGC	
77	TMPRSS4_Ex12:F	TCAGGGAGCAGAGAAGGAGAAG	[94°C x 30 sec, 55°C x 30 sec, 72°C x 30 sec] x 30
78	TMPRSS4_Ex12:R	AATAGTGCAATCTCAGGCTGTCC	
79	TMPRSS4_Ex13a:F	GACTCACGTTACACATGTCACCAC	[94°C x 30 sec, 57.5°C x 30 sec, 72°C x 30 sec] x 30
80	TMPRSS4_Ex13a:R	AAGACAGCCTGCTTCCATTCAG	
81	TMPRSS4_Ex13b:F	TTGGTGCTCCCAGCATCC	[94°C x 30 sec, 55°C x 30 sec, 72°C x 30 sec] x 30
82	TMPRSS4_Ex13b:R	TTTGAGACTCAATTGCTTCCCC	
83	PCSK7_Ex2:F	GTTTATCTAACCTCAGCTTGTTGCC	[94°C x 30 sec, 55°C x 30 sec, 72°C x 30 sec] x 30
84	PCSK7_Ex2:R	AATCTTTCCCTAGCTGACTCCTCA	
85	PCSK7_Ex3a:F	CATCTCCCTCTCAGATTCCTGC	[94°C x 30 sec, 55°C x 30 sec, 72°C x 30 sec] x 30
86	PCSK7_Ex3a:R	CGATGCGTCCAGCATTCA	
87	PCSK7_Ex3b:F	GGAAGAGACTCTGGAGCAGCA	[94°C x 30 sec, 55°C x 30 sec, 72°C x 30 sec] x 30
88	PCSK7_Ex3b:R	ACTGAAGAGTGATATAGTCAAAAGCCC	
89	PCSK7_Ex4:F	ATAACTTCATCTCCCTCTGGGCT	[94°C x 30 sec, 55°C x 30 sec, 72°C x 30 sec] x 30
90	PCSK7_Ex4:R	TTATTTGGCCCAAAGACCTCTAGA	
91	PCSK7_Ex5:F	CCCAGGACCTGATCCCCT	[94°C x 30 sec, 55°C x 30 sec, 72°C x 30 sec] x 30
92	PCSK7_Ex5:R	GCTATGGGATAAAGATGTTTCAGAGTAG	
93	PCSK7_Ex6:F	CCAGTTCCCCGGCTAGGA	[94°C x 30 sec, 55°C x 30 sec, 72°C x 30 sec] x 30
94	PCSK7_Ex6:R	CCCACTGGTTGGGATTTTGT	

"→" represents touchdown PCRs where there is a drop of 1°C after each of the 5 cycles.

Table 2-2 Continued.

#	Name	Primer sequence in 5'-3' orientation	PCR
95	PCSK7_Ex7:F	AGGCGCTGGGTGGGTAG	[94°C x 30 sec, 60°C → 56°C x 30 sec, 72°C x 30 sec] x 5
96	PCSK7_Ex7:R	GATGGGTCAACTTGCAGCAGT	[94°C x 30 sec, 55°C x 30 sec, 72°C x 30 sec] x 25
97	PCSK7_Ex8:F	TGATGTGGTAGGCGGAGGTC	[94°C x 30 sec, 55°C x 30 sec, 72°C x 30 sec] x 30
98	PCSK7_Ex8:R	TGAGCCCAAAGAGATTATTGTGC	
99	PCSK7_Ex9:F	TGACATTAGCAAGCCCCTGC	[94°C x 30 sec, 55°C x 30 sec, 72°C x 30 sec] x 30
100	PCSK7_Ex9:R	CTTAAGACATCCAGCTCTGTGGG	
101	PCSK7_Ex10:F	GCCGGGACTATAGGTGCACA	[94°C x 30 sec, 65°C → 61°C x 30 sec, 72°C x 30 sec] x 5
102	PCSK7_Ex10:R	ATTTGGGACATTGAGAATCTAAGGC	[94°C x 30 sec, 60°C x 30 sec, 72°C x 30 sec] x 25
103	PCSK7_Ex11:F	GGGAAACCAGAGTCAGATTGTTG	[94°C x 30 sec, 55°C x 30 sec, 72°C x 30 sec] x 30
104	PCSK7_Ex11:R	CTATGATATCCCAGGCAGTTTGG	
105	PCSK7_Ex12:F	TGTGAGAATGTGGGTGTGATCA	[94°C x 30 sec, 55°C x 30 sec, 72°C x 30 sec] x 30
106	PCSK7_Ex12:R	CAGGGAGGACGAGTTTAACTTCC	
107	PCSK7_Ex13:F	GGGTGAAGTGAAGGCGTGTT	[94°C x 30 sec, 55°C x 30 sec, 72°C x 30 sec] x 30
108	PCSK7_Ex13:R	CCAGGATCCACTTCTTCCATTTC	
109	PCSK7_Ex14:F	GGTTGTTTCCACGGCTACTACAG	[94°C x 30 sec, 55°C x 30 sec, 72°C x 30 sec] x 30
110	PCSK7_Ex14:R	ATATATTGCACACGGGACACTTTC	
111	PCSK7_Ex15:F	TGAGCCCCTTTGGGTGG	[94°C x 30 sec, 55°C x 30 sec, 72°C x 30 sec] x 30
112	PCSK7_Ex15:R	GAACTGGGAAGCACAGCTGG	
113	PCSK7_Ex16:F	CCTCTCCTTTTTGCTGTGGG	[94°C x 30 sec, 55°C x 30 sec, 72°C x 30 sec] x 30
114	PCSK7_Ex16:R	TCCTTCACCCCGCAGGT	
115	PCSK7_Ex17:F	CCTGGGCTGAGAAAGGCTG	[94°C x 30 sec, 60°C → 56°C x 30 sec, 72°C x 30 sec] x 5
116	PCSK7_Ex17:R	GAGTGGAGTCAGAGGATGCCTC	[94°C x 30 sec, 55°C x 30 sec, 72°C x 30 sec] x 25
117	APOA4_Ex1:F	GTCAGCTTCCACGTAGTCTCAGG	[94°C x 30 sec, 62.5°C→58.5°C x 30 sec, 72°C x 30sec] x 5
118	APOA4_Ex1:R	GAAGTGTCCTTTTGCTTTGGCT	[94°C x 30 sec, 57.5°C x 30 sec, 72°C x 30 sec] x 25
119	APOA4_Ex2:F	TGAGGCACCCCCACCA	[94°C x 30 sec, 62.5°C→58.5°C x 30 sec, 72°C x 30sec] x 5
120	APOA4_Ex2:R	AGCTCAGGGCTCCTGTCTCTAA	[94°C x 30 sec, 57.5°C x 30 sec, 72°C x 30 sec] x 25
121	APOA4_Ex3a:F	TGCATAAGGCGAGTGGTATACAA	[94°C x 30 sec, 62.5°C→58.5°C x 30 sec, 72°C x 30sec] x 5
122	APOA4_Ex3a:R	TTCTCCCGCAGCACTCTCTC	[94°C x 30 sec, 57.5°C x 30 sec, 72°C x 30 sec] x 25
123	APOA4_Ex3b:F	CTGCCCCATGCCAATGAG	[94°C x 30 sec, 62.5°C→58.5°C x 30 sec, 72°C x 30sec] x 5
124	APOA4_Ex3b:R	CATCTGGAAGGTCAGGCCC	[94°C x 30 sec, 57.5°C x 30 sec, 72°C x 30 sec] x 25
125	APOA4_Ex3c:F	GAGGAGCTCAAGGGACGCCT	[94°C x 30 sec, 62.5°C→58.5°C x 30 sec, 72°C x 30sec] x 5
126	APOA4_Ex3c:R	GGGCCCAGTTTCTGCCTGAG	[94°C x 30 sec, 57.5°C x 30 sec, 72°C x 30 sec] x 25

"→" represents touchdown PCRs where there is a drop of 1°C after each of the 5 cycles.

Table 2-2 Continued.

#	Name	Primer sequence in 5'-3' orientation	PCR
127	APOA4_Ex3d:F	GAGGACGTGCGTGGCAAC	[94°C x 30 sec, 62.5°C→58.5°C x 30 sec, 72°C x 30sec] x 5 [94°C x 30 sec, 57.5°C x 30 sec, 72°C x 30 sec] x 25
128	APOA4_Ex3d:R	CCAGAACTTCTTTGGGACAGACA	
129	APOA4_Ex3e:F	CAAGACTCTCTCCCTCCCTGAG	[94°C x 30 sec, 62.5°C→58.5°C x 30 sec, 72°C x 30sec] x 5 [94°C x 30 sec, 57.5°C x 30 sec, 72°C x 30 sec] x 25
130	APOA4_Ex3e:R	GCCGCTGCTAAGCTCTGC	
131	APOA4_Ex3dup:F	ACAGCGCATGGAGAGAGTGCT	[94°C x 30 sec, 65°C x 30 sec, 72°C x 1 min] x 30
132	APOA4_Ex3dup:R	TCTGCCGCAGCTCCTCG	

"→" represents touchdown PCRs where there is a drop of 1°C after each of the 5 cycles.

Table 2-3 Primers for amplification of cDNA. Intermediate PCR reaction conditions are indicated for each pair of primers. All PCR reactions consisted of [94°C x 2 min], followed by the three-step cycle indicated in the table, then [72°C x 10 min], and finally held at 15°C until removed from the thermocycler.

#	Name	Primer sequence in 5'-3' orientation	PCR
1	MLH1:16-2F	GTCCAGAGAGTGGCTGGA	PCR I: [94°C x 30 sec, 60°C→56°C x 30 sec, 72°C x 30sec] x 5 [94°C x 30 sec, 55°C x 30 sec, 72°C x 30 sec] x 25
2	MLH1:18-1R	CCGGGACTCCTCAGATATGTACTGCT	
3	APOA4_Ex3dup:F	ACAGCGCATGGAGAGAGTGCT	PCR I: [94°C x 30 sec, 65°C x 30 sec, 72°C x 30sec] x 30
4	APOA4_Ex3dup:R	TCTGCCGCAGCTCCTCG	
5	APOA4_Ex2_CDS:F	CAGAAATCTGAACTCACCCAGCAA	PCR I: [94°C x 30 sec, 55°C→51°C x 30 sec, 72°C x 30sec] x 5 [94°C x 30 sec, 50°C x 30 sec, 72°C x 30 sec] x 25 PCR II: [94°C x 30 sec, 67.5°C→63.5°C x 30 sec, 72°C x 30sec] x 5 [94°C x 30 sec, 62.5°C x 30 sec, 72°C x 30 sec] x 25 or PCR I: [94°C x 30 sec, 52.5°C→48.5°C x 30 sec, 72°C x 30sec] x 5 [94°C x 30 sec, 47.5°C x 30 sec, 72°C x 30 sec] x 25
6	APOA4_Ex3c:R	GGGCCCAGTTTCTGCCTGAG	

"→" represents touchdown PCRs where there is a drop of 1°C after each of the 5 cycles.

```
1     gatctgctgt cagcttccac gtagtctcag ggtcacaaaa gtccaagagg cctcttggga }Ex1:F
61    atgtgtcacc ttccagcgtg gagtcacact gaggaaggag gaggggaggg cagccagggg
121   ggtggcgata gggagagagt ttaaatgtct ggctggctct gagcttcagt cagttcccac
181   TGCAGCGCAG GTGAGCTCTC CTGAGGACCT CTCTGTCAGC TCCCCTGATT GTAGGGAGGA
241   TCCAGTGTGG CAAGAAACTC CTCCAGCCCA GCAAGCAGCT CAGGATGTTC CTGAAGGCCG
301   TGGTCCTGAC CCTGGCCCTG GTGGCTGTCG CCGgtgagta gaagctgtct ttggatggca
361   ctcctgggct gctgctctga gtagtgcagg atggaggctg agccaaagca aaaggacact }Ex1:R
421   tctgagtgcc catcagcccc cagctggaca tgaggtctgc ctggctgcca agtggctcac
481   aggagagctg gcccagtccc agtggtgggc ccattggcat tggtgctata ccagtttcac
541   atatccctgt ggcttccaaa aagctaagct cagacaggga aaatggcagg tgaggcacc }Ex2:F
601   ccccacatca tccagtctgc agctcagagc tggagcagag gggccacaca ggagacgggg
661   cctcatgaat tgctctctgt taccacccag GAGCCAGGGC TGAGGTCAGT GCTGACCAGG
721   TGGCCACGGT GATGTGGGAC TACTTCAGCC AGCTGAGCAA CAATGCCAAG GAGGCCGTGG
781   AACATCTCCA GAAATCTGAA CTCACCCAGC AACTCAAgta agagggacta cagtgtgcgg }Ex2_CDS:F
841   tggtgacggg gaattcttaa aggccatgca atgtactggc aagggttgag cgtagaacca }Ex2:R
901   ggagcctga gttaggata cccactgccc tgccactaac tggccgggcc tctgaaccta
961   ggatccacat atgtaaaccg gaagtttgga ccgaataatc cctgccatgt ccttttgctt
1021  tgacgttcta gagtttgaca aatggccaca tcctatcatt caggctcatg gaagagaggg
1081  agggaggaaa atgtcacgtg agctgatttc taatacgttt cagaaagaca ggccccagtg
1141  gaatcaaggg gagggaggtg ggaatatttg ggaggcccct gggcacaggc aaggaaagca
1201  gcaccttgtg ccactggaag accccagcag aggtcaagaa gacaacattg tgttacacaa
1261  tgtgatccta tggcccagaa cactccctct gggaaggacc tcaaagtccc accctctgca
1321  gacaaggagg ggaaagcaaa ctgctggagg tgacatggtg ggtagattct gagacaaact
1381  atgtgggaga tcctgagata gaaattcagc atcgtaactt agtctgtgac acccatcctc
1441  tccaatctgc accaccatag ggagggtgaa ctcggtacct ctgagcactc acctgtccta
1501  gcacgtgtgc ataagggcgag tggtatacaa gcagacaaag tcttgccgtg taaatgccaa }Ex3a:F
1561  atgtaacgtg gcctccttgt gcccttcccc acagTGCCCT CTTCCAGGAC AAACTTGGAG
1621  AAGTGAACAC TTACGCAGGT GACCTGCAGA AGAAGCTGGT GCCCTTTGCC ACCGAGCTGC
1681  ATGAACGCCT GGCCAAGGAC TCGGAGAAAC TGAAGGAGGA GATTGGGAAG GAGCTGGAGG
1741  AGCTGAGGGC CCGGCTGCTG CCCCATGCCA ATGAGGTGAG CCAGAAGATC GGGGACAACC }Ex3b:F
1801  TGCGAGAGCT TCAGCAGCGC CTGGAGCCCT ACGCGGACCA GCTGCGCACC CAGGTCAGCA
1861  CGCAGGCCGA GCAGCTGCGG CGCCAGCTGA CCCCCTACGC ACAGCGCATG                }Ex3dup:F
1921  TGCGGGAGAA CGCCGACAGC CTGCAGGCCT CGCTGAGGCC CCACGCCGAC GAGCTCAAGG }Ex3a:R
1981  CCAAGATCGA CCAGAACGTG                        TACGCCCTAC GCTGACGAAT }Ex3c:F
2041  TCAAAGTCAA GATTGACCAG ACCGTGGAGG AGCTGCGCCG CAGCCTGGCT CCCTATGCTC
2101  AGGACACGCA GGAGAAGCTC AACCACCAGC TTGA                    AAGAAGA }Ex3b:R
2161  ACGCCGAGGA GCTCAAGGCC AGGATCTCGG CCAGTGCCGA GGAGCTGCGG CAGAGGCTGG }Ex3dup:R
2221  CGCCCTTGGC CGAGGACGTG CGTGGCAACC TGAGGGGCAA CACCGAGGGG CTGCAGAAGT }Ex3d:F
2281  CACTGGCAGA GCTGGGTGGG CACCTGGACC AGCAGGTGGA GGAGTTCCGA CGCCGGGTGG
2341  AGCCCTACGG GGAAAACTTC AACAAAGCCC TGGTGCAGCA GATGGAACAG CTCAGGCAGA }Ex3c:R
2401  AACTGGGCCC CCATGCGGGG GACGTGGAAG GCCACTTGAG CTTCCTGGAG AAGGACCTGA
2461  GGGACAAGGT CAACTCCTTC TTCAGCACCT TCAAGGAGAA AGAGAGCCAG GACAAGACTC }Ex3e:F
2521  TCTCCCTCCC TGAGCTGGAG CAACAGCAGG AACAGCAGCA GGAGCAGCAG CAGGAGCAGG
2581  TGCAGATGCT GGCCCCTTTG GAGAGCTGAG CTGCCCCTGG TGCACTGGCC CCACCCTCGT
2641  GGACACCTGC CCTGCCCTGC CACCTGTCTG TCTGTCTGTC CCAAAGAACT TCTCCTATGA }Ex3d:R
2701  ACTTGAGGAC ACATGTCCAG TGGGAGGTGA GACCACCTCT CAATATTCAA TAAAGCTGCT
2761  GAGAATCTAG CCTCaactgg ttgccggatg aatcctcctt gcagctgggg aggtggggag
2821  gtaaccatga ctggcagag cttagcagcg gctggcagg agacacccag gattggggag }Ex3e:R
```

Figure 2-1 Genomic sequence for APOA4 with primer annealing positions indicated. The 3 exons of APOA4 are shown in capital letters and highlighted yellow. Coding sequence is bold and underlined. Primer annealing sequences are highlighted in black, and suffixes of primer names are indicated at right (prefix of primer names: "APOA4_"). Overlap between primer annealing positions for APOA4_Ex3dup:F and APOA4_Ex3a:R is indicated with green text. Coding sequence nucleotides 552 through to 749, inclusive, are shown in red.

CHAPTER 3: RESULTS

3.1) Linkage Analysis

Identification of the FEVE locus was based largely on linkage analysis done prior to starting the work for this thesis. A previously conducted genome-wide microsatellite screen and subsequent refinement defined the FEVE critical region as an approximately 2 Mb interval on chromosome 11q23.3 between markers D11S4142 and D11S1364 (see section 1.3.3.1). Two individuals were identified as having key recombinations, one in the interval D11S4142-D11S1340 and the other in the interval D11S1341-D11S1364. Four polymorphic markers, in the relevant interval, were analyzed in the respective key recombinant, their parents, and appropriate grandparents (Figure 3-1). This analysis refined the crossover positions to intervals D11S4142-MDL115.9 and MDL117.96-D11S1364 (Figure 3-1).

3.2) Selection of Positional Candidate Genes for Mutation Analysis

The positional candidate genes sequenced for this thesis were selected based on speculative insights as described in this section and related subsections. According to the NCBI Map Viewer (http://www.ncbi.nlm.nih.gov/mapview/), there are approximately 40 genes within the nearly 2 Mb FEVE critical region (Figure 3-1). The selection of candidate genes from this critical interval was based on gene functions and/or expression profiles that were consistent with the FEVE phenotype. Two of these positional candidate genes, *CD3D* and *IL10RA*, were previously sequenced and ruled out as candidates for FEVE based on the absence of mutations in affected individuals. Further investigations led to the selection of eight other positional candidate genes for mutation analysis: *EVA1*, *PAFAH1B2*, *AMICA1*, *SCN2B*, *SCN4B*, *TMPRSS4*, *PCSK7*, and

APOA4. The relevant functions and/or expression patterns of these genes are discussed in the chronological order in which each gene was investigated.

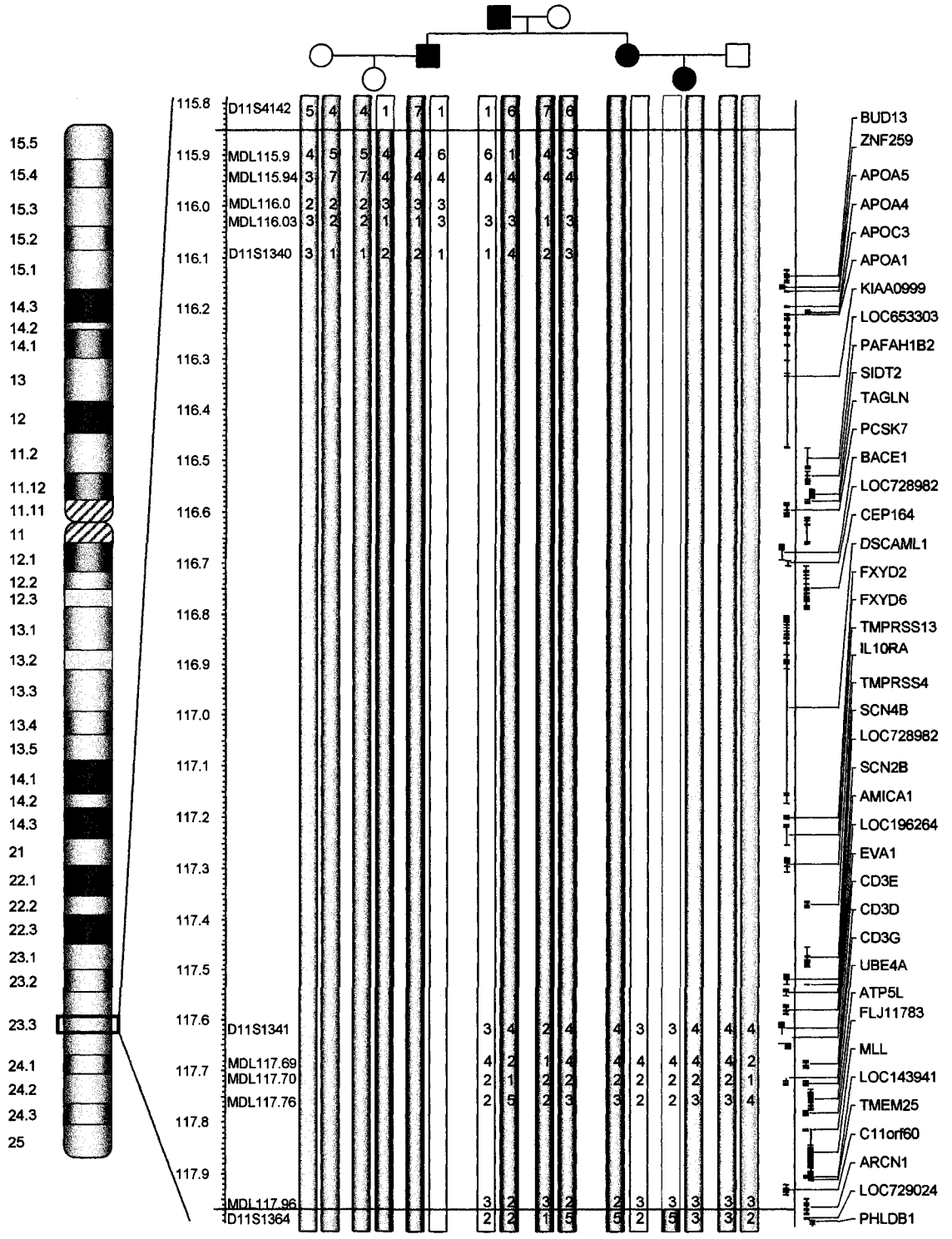

Figure 3-1 Linkage data showing key recombination events for FEVE at 11q23.3 between markers D11S4142 and D11S1364. Marker data is limited to the recombinant breakpoints in each branch of this family. Sample accession numbers of individuals from left to right are: 1238, 1242, 1240 (obligate affected), 1279, 1278, 1290, 1294, and 1288. Genes within the critical region are illustrated to scale at the right, with genes that were sequenced in this family highlighted in red (plotted from NCBI Map Viewer: http://www.ncbi.nlm.nih.gov/mapview/).

3.2.1) *EVA1*

Epithelial V-like Antigen 1 (*Eva1*) is a member of the immunoglobulin (Ig) superfamily that is highly expressed in adult mouse gut tissue (GUTTINGER *et al.* 1998). More specifically, the expression of *Eva1* has been documented in the small intestine of adult mice (SymAtlas; http://symatlas.gnf.org/SymAtlas; SU *et al.* 2002), as well as the epithelium of the gastrointestinal tract in mouse embryos (GUTTINGER *et al.* 1998). Furthermore, Eva1 is capable of mediating homophilic cell-cell adhesion, as illustrated by the cell clustering of *Eva1*-expressing CHO cells (GUTTINGER *et al.* 1998). Given its adhesive properties, Eva1 has the potential to join the list of other Ig superfamily adhesion molecules which play an important role in the inflammatory response (ALBELDA and BUCK 1990; DANESE *et al.* 2005; KUNKEL and BUTCHER 2003). In fact, the overexpression of Ig superfamily adhesion molecules in the intestinal mucosa of IBD patients (both CD and UC), as well as in the inflamed colonic microvasculature of animal models with experimental colitis, indicate a direct association between adhesion molecules and IBD (DANESE *et al.* 2005). Both the expression pattern and possible functional relevance of *EVA1* made it a worthwhile positional candidate to investigate in relation to FEVE.

3.2.2) *PAFAH1B2*

Platelet activating factor (PAF) is a potent proinflammatory mediator with PAF acetylhydrolase (PAFAH) acting as its functional antagonist (BLANK *et al.* 1981; ZIMMERMAN *et al.* 2002). PAFAH isoform 1B, beta subunit (PAFAH1B2) is a ubiquitously expressed catalytic component of the PAFAH enzyme (SymAtlas;

http://symatlas.gnf.org/SymAtlas; SU *et al.* 2002; ADACHI *et al.* 1997; MORO *et al.* 1998), thereby playing a critical role in the catabolism of PAF (BLANK *et al.* 1981; MORO *et al.* 1998). Intravenous administration of PAF can induce tissue damage in the small intestine of mice (SUN and HSUEH 1991). Furthermore, PAF is elevated in colonic biopsy specimens in both CD and UC patients (ELIAKIM *et al.* 1988; SOBHANI *et al.* 1992). In such instances, PAFAH could exert an anti-inflammatory effect by catalyzing PAF into two biologically inactive products (BLANK *et al.* 1981; CHEN 2004; TJOELKER *et al.* 1995). Other PAF antagonists have been considered for use in the treatment of human IBD cases, and have even been shown to attenuate the inflammatory response in the intestinal mucosa in an animal model of acute colitis (MEENAN *et al.* 1996; STACK *et al.* 1998). Acquired deficiencies in PAFAH activity have been observed in patients with other inflammatory diseases such as systemic lupus erythematosus and asthma (ITO *et al.* 2002; TETTA *et al.* 1990). The ability of PAFAH to inhibit the inflammatory effects of PAF suggested a functional relevance for positional candidate PAFAH1B2 in the pathology of FEVE.

3.2.3) *AMICA1*

Adhesion molecule, interacts with CXADR antigen 1 (AMICA1; also known as JAML) is a junction adhesion molecule (JAM) of the Ig superfamily (MOOG-LUTZ *et al.* 2003; ZEN *et al.* 2005). By binding to its counterreceptor, coxsackie and adenovirus receptor (CAR), AMICA1 modulates neutrophil transmigration across epithelial tight junctions (ZEN *et al.* 2005). This migration of neutrophils across the mucosal epithelia is characteristic of inflammatory conditions, including IBD (CHIN and PARKOS 2006).

Although AMICA1 is mainly expressed in hematopoietic tissues (MOOG-LUTZ *et al.* 2003), the high expression of CAR in epithelial cells (TOMKO *et al.* 2000) enables it to bind to tight junctions of the human intestinal epithelium (ZEN *et al.* 2005). Furthermore, various JAM family members are upregulated under inflammatory conditions (WEBER *et al.* 2007), and it has been suggested that future IBD treatments could inhibit neutrophil epithelial migration by targeting AMICA1 (CHIN and PARKOS 2006; KUCHARZIK *et al.* 2006). Altogether, this data indicated that *AMICA1* was a worthwhile positional candidate to investigate in relation to FEVE.

3.2.4) *SCN2B* and *SCN4B*

There was an interest in any positional candidate ion channel genes due to evidence that inflammatory diarrhea can be caused by impaired gastrointestinal ion transport (EISENHUT 2006; FIELD 2003). Sodium channel, voltage-gated, type II and IV, beta subunits (SCN2B and SCN4B, respectively) are positional candidates that modify the sodium channel kinetics of the alpha subunit ion conducting pore (ISOM *et al.* 1995; YU *et al.* 2003). These two beta subunits share a 35% amino acid identity (YU *et al.* 2003), and are each expressed slightly more in the small intestine than their own median expression across all tissues (SymAtlas; http://symatlas.gnf.org/SymAtlas; SU *et al.* 2002). However, unlike epithelial sodium channels which play a key role in intestinal sodium regulation (HUMMLER and HORISBERGER 1999), SCN2B and SCN4B are typically associated with neuronal sodium channels. Nevertheless, IBD-related intestinal dysmotility can result from neuronal ion channel abnormalities (OZAKI *et al.* 2005; YIANGOU *et al.* 2001a; YIANGOU *et al.* 2001b; YIANGOU *et al.* 2001c). Due to the slightly

elevated expression of both SCN2B and SCN4B in the small intestine, and the role of other ion channels in IBD, these genes were investigated as candidates for FEVE.

3.2.5) *TMPRSS4*

Transmembrane protease, serine 4 (*TMPRSS4*[2]) is a positional candidate that has relatively high expression in the small intestine compared to other normal tissues (SymAtlas; http://symatlas.gnf.org/SymAtlas; SU *et al.* 2002; WALLRAPP *et al.* 2000). As a member of the type II transmembrane serine protease (TTSP) family, TMPRSS4 is amidst a group of enzymes with greatly diverse roles (HOOPER *et al.* 2001; SZABO and BUGGE 2008). Another TTSP, which like TMPRSS4 has been associated with various cancers, has been implicated as an inflammatory regulator (LIST *et al.* 2005; MATHIAS *et al.* 2007; SZABO and BUGGE 2008). Various serine protease inhibitors have demonstrated the ability to attenuate the inflammatory response in some cases of IBD (SENDA *et al.* 1993). Since TMPRSS4 has not been extensively characterized, it may have an unidentified role in inflammation. Additionally, the proteolytic activity of the TMPRSS4 mouse ortholog (mCAP2) contributes to epithelial sodium channel (ENaC) activation (ANDREASEN *et al.* 2006; ROSSIER 2004; VUAGNIAUX *et al.* 2002). Impaired sodium absorption, which can be the result of reduced ENaC expression or activity, can contribute to diarrhea in both ulcerative and Crohn's colitis (HAWKER *et al.* 1980; SANDLE *et al.* 1990; ZEISSIG *et al.* 2008). Therefore, TMPRSS4 could contribute to the pathology of FEVE through its potential roles in inflammation and/or sodium transport.

---

[2] Originally designated TMPRSS3 (WALLRAPP *et al.* 2000). The Human Genome Nomenclature Committee approved symbol TMPRSS3 for another TTSP-encoding gene located on chromosome 21q22.3 (SCOTT *et al.* 2001).

3.2.6) *PCSK7*

Proprotein convertase, subtilisin/kexin-type 7 (PCSK7; also known as PC7 and PC8) is a ubiquitously expressed (SymAtlas; http://symatlas.gnf.org/SymAtlas; SU *et al.* 2002; BRUZZANITI *et al.* 1996) calcium dependent serine endoprotease that is responsible for cleaving various proproteins into their biologically active forms (BRUZZANITI *et al.* 1996; MUNZER *et al.* 1997; STAWOWY *et al.* 2005). One potential target of PCSK7 is the membrane type-1 matrix metalloproteinase (MT1-MMP; also known as MMP-14) zymogen (YANA and WEISS 2000), whose recognition sequence motif can be recognized by PCSK7 (MUNZER *et al.* 1997; STAWOWY *et al.* 2005; YANA and WEISS 2000). Once activated, MT1-MMP serves as the major activator of proMMP-2 (MCQUIBBAN *et al.* 2002). Activated MMP-2 (also known as gelatinase A) exerts an anti-inflammatory effect by cleaving and inactivating a macrophage chemoattractant protein (MCP-3) (MCQUIBBAN *et al.* 2000), and it is thought to be involved in proper intestinal barrier function (RAVI *et al.* 2007). Furthermore, both MT1-MMP and MMP-2 are thought to have anti-inflammatory roles in IBD (RAVI *et al.* 2007), suggesting that their decreased activation could exacerbate the inflammatory response. Also, given that hypoalbuminemia is observed during the clinical course of FEVE (SMITH *et al.* 1994), it should be noted that PCSK7 processes proalbumin into albumin (MORI *et al.* 1999). Altogether, this data indicated that *PCSK7* was a worthwhile positional candidate to investigate in relation to FEVE.

3.2.7) APOA4

Apolipoprotein A-IV (APOA4) expression is restricted to differentiated enterocytes of the villi in the proximal small intestine, where it is also implicated in the regulatory and signaling pathways that govern inflammation in enterocytes (PEIGNON *et al.* 2006). The mechanism of this anti-inflammatory activity is unknown, but has been attributed to suppression of endothelial cell expression of P-selectin, thereby inhibiting the recruitment of leukocytes to inflamed tissues (VOWINKEL *et al.* 2004). Human apoA-IV decreases the secretion of pro-inflammatory cytokines IL-4 and TNF-α in lymphocytes isolated from lipopolysaccharide-injected mice (RECALDE *et al.* 2004). These cytokines would otherwise induce the expression of P-selectin (WELLER *et al.* 1992). In addition, apoA-IV is downregulated in IBD mucosal tissues, even in non-inflamed regions where yeast-two-hybrid screening has revealed interactions between apoA-IV and α-catenin as well as α_1-antichymotrypsin (ORSÓ *et al.* 2007). Alpha-catenin is a junctional anchor protein that contributes to intercellular integrity and α_1-antichymotrypsin is an acute phase inflammatory responsive protein that is up-regulated in IBD patients (GRZYMISŁAWSKI *et al.* 2006).

APOA4 knockout mice have no clinical signs of intestinal inflammation under normal conditions, but they exhibit acute colitis when given dextran sodium sulfate (DSS) as an experimental IBD-inducing toxin (VOWINKEL *et al.* 2004). Treated mice exhibit inflammation of the colonic mucosa with crypt damage, mucosal ulceration, and accompanying submucosal edema that has a marked histological resemblance to the pathology in individuals with FEVE (SMITH *et al.* 1994). Furthermore, the inflammatory

effects of DSS in these APOA4 knockout mice were attenuated with intraperitoneal administration of recombinant human apoA-IV (VOWINKEL *et al.* 2004).

More recently, an inverse association was found between apoA-IV plasma levels and disease activity in patients with Crohn's disease (BROEDL *et al.* 2007), and reduced expression of apoA-IV has been observed in IBD mucosa (KIM *et al.* 2006; ORSÓ *et al.* 2007). All of the aforementioned findings made APOA4 a worthwhile positional candidate to investigate in relation to FEVE.

3.3) Mutation Analysis

Following PCR and gel electrophoresis, samples from one affected individual, who had a child die due to FEVE, and one obligate carrier (hereafter referred to as affected for simplicity) were bi-directionally sequenced for mutations in the open reading frames of the 8 selected candidate genes. Heterozygous sequence variants in either affected individual were examined through comparison with the sequence from the other affected individual as well as the sequences from one biopsy-confirmed FEVE-unaffected relative, one ethnicity-matched control, two unrelated anonymous controls, and the corresponding GenBank® reference sequence (NC_000011.8). Several sequence variants were identified (Table 3-1), including some that were previously documented in the human Single Nucleotide Polymorphism database (dbSNP; http://ncbi.nih.gov/SNP).

3.3.1) *EVA1*

Five amplicons, each of which flanked an entire *EVA1* exon including the exon/intron boundaries, were sequenced. Exon 6, which is within the 3'-UTR, was not sequenced.

A novel variant was identified in the first intron of *EVA1* in an affected individual. The variant was a four base duplication, starting 13 nucleotides downstream of coding nucleotide 58 (c.58+13_16dup; GenBank® NC_000011.8; Figure 3-2a). This duplication was also present in the biopsy-confirmed FEVE-unaffected control.

3.3.2) *PAFAH1B2*

Five amplicons, which covered the entire coding region of *PAFAH1B2*, were sequenced. Exon 1 and the 3'-end of exon 6 are within the untranslated regions and therefore were not sequenced. All other exons were sequenced in their entirety, including exon/intron boundaries.

One of 11 T nucleotides was deleted in a mononucleotide repeat stretch in the second intron of *PAFAH1B2* in an affected individual. This deletion was 25 nucleotides upstream of coding nucleotide 82 (c.82-25delT; GenBank® NC_000011.8; Figure 3-2b). The biopsy-confirmed unaffected relative and the ethnicity-matched control were also heterozygous for this deletion. Both unrelated controls were homozygous for 10 T nucleotides, whereas the other affected individual was homozygous for 11 T nucleotides at this position. This mononucleotide repeat variation is a previously reported SNP (dbSNP: rs35139041).

Another previously documented SNP (dbSNP: rs7122944) was identified in the fifth intron of *PAFAH1B2* in both affected individuals. This SNP is a G to T transversion located 11 base pairs downstream of coding nucleotide 411 (c.411+11G>T; GenBank® NC_000011.8; Figure 3-2c). The four other individuals were homozygous for T at this position.

3.3.3) *AMICA1*

Nine amplicons, which covered the entire coding region of *AMICA1*, were sequenced. The 5'-end of exon 1 and the 3'-end of exon 9 are within untranslated regions and therefore were not sequenced. All other exons were sequenced in their entirety, including exon/intron boundaries. No variants or mutations were identified in *AMICA1* of the affected individuals.

3.3.4) *SCN2B*

Four amplicons, which covered the entire coding region of *SCN2B*, were sequenced. The 3'-end of exon 4 is within an untranslated region and therefore was not sequenced. The other 3 exons were sequenced in their entirety, including exon/intron boundaries.

An A to C transversion was identified in the third intron of an affected individual, 12 nucleotides upstream of coding nucleotide 449 in *SCN2B* (c.449-12A>C; GenBank® NC_000011.8; Figure 3-2d). This variant was also present in the biopsy-confirmed unaffected relative, and one of the unrelated controls. The remaining affected individual and the ethnicity-matched control were each homozygous for A, whereas the other unrelated control was homozygous for C at this position. This transversion is a previously documented SNP (dbSNP: rs8192613).

3.3.5) *SCN4B*

Exon 1 of *SCN4B*, which contains the first 61 coding nucleotides, was not sequenced due to repeat failed attempts at designing primers that would exclusively amplify the region

of interest. The remainder of the coding region was sequenced with four amplicons. Exons 2, 3, and 4 were sequenced in their entirety, including exon/intron boundaries. The 3'-end of exon 5 is within an untranslated region and therefore was not sequenced. No variants or mutations were identified in *SCN4B* in the affected individuals.

3.3.6) *TMPRSS4*

The coding sequence for isoform 1 of TMPRSS4 (GenBank® NP_063947.1) was investigated. All 13 exons were sequenced in their entirety, including exon/intron boundaries. Exon 13 was sequenced with two overlapping primer sets.

An A to G transition was identified in the 3'-UTR of an affected individual, 156 nucleotides downstream of coding nucleotide 1,314 in *TMPRSS4* (c.1314+156A>G; GenBank® NC_000011.8; Figure 3-2e). One unrelated control was homozygous for A, while all other individuals were homozygous for G at this position. This transition is a previously documented SNP (rs8924).

3.3.7) *PCSK7*

Seventeen amplicons, which covered the entire coding region of *PCSK7*, were sequenced. Exons 2 through 16 were sequenced in their entirety, including exon/intron boundaries. Exon 3 was sequenced with two overlapping primer sets. The 3'-end of exon 17 is within an untranslated region, and therefore was not sequenced. Exons 1 and 2 are within the 5'-UTR and therefore did not require sequencing.

A G to A transition was identified in exon 5 of *PCSK7*, at coding nucleotide 711 (c.711G>A; GenBank® NC_000011.8; Figure 3-2f) in an affected individual. This silent

substitution was not found in any of the other 5 individuals, but it is a previously documented SNP (dbSNP: rs45528535).

A novel silent variant was identified in exon 14 of *PCSK7* in both affected individuals. The variant is a T to G transversion at coding nucleotide 1770 (c.1770T>G; GenBank® NC_000011.8; Figure 3-2g). This substitution was also found in the biopsy-confirmed unaffected relative and the ethnicity matched control. Both unrelated controls were homozygous for T at this position.

A novel variant was also identified in intron 14 of *PCSK7* in both affected individuals. This variant is a C to T transition 7 nucleotides downstream of coding nucleotide 1786 (c.1786+7C>T; GenBank® NC_000011.8; Figure 3-2h). The biopsy-confirmed unaffected relative and the ethnicity-matched control were also heterozygous for this substitution. Both unrelated controls were homozygous for C at this position.

Another novel variant was identified in intron 14 of *PCSK7* in one affected individual. This variant is an A to G transition 30 nucleotides downstream of coding nucleotide 1786 (c.1786+30A>G; GenBank® NC_000011.8; Figure 3-2i). The biopsy-confirmed unaffected relative and the ethnicity-matched control were also heterozygous for this substitution. Both of the unrelated controls and the other affected individual were homozygous for A at this position.

3.3.8) APOA4

Seven amplicons, which covered the entire coding region of APOA4, were sequenced. All 3 exons were sequenced in their entirety, including exon/intron boundaries. Exon 3

was initially sequenced with five overlapping primer sets. Another pair of sequencing primers were introduced later to flank a duplication in exon 3 (Figure 2-1).

A G to A transition was identified 98 nucleotides upstream of the first coding nucleotide of APOA4 (c.1-98G>A; GenBank® NC_000011.8; Figure 3-2j) in an affected individual. None of the other 5 individuals had this SNP, but it was previously documented (dbSNP: rs5091).

An A to G transition was identified at coding nucleotide 87 of APOA4 (c.87A>G; GenBank® NC_000011.8; Figure 3-2k) in both affected individuals. This silent substitution was not detected in any of the other 4 individuals, however it is a previously documented SNP (dbSNP: rs5092).

Two alleles of different sizes were detected in both of the affected individuals after PCR and gel electrophoresis with primer sets APOA4_Ex3b:F / APOA4_Ex3b:R and APOA4_Ex3c:F / APOA4_Ex3c:R (Figure 3-3a). The larger allele, which was exclusive to the affected individuals, was more clearly visualized by PCR and gel electrophoresis using primers APOA4_Ex3c:F and APOA4_Ex3b:R (Figure 3-3b). After excising this higher molecular weight band from the gel, sequencing analysis determined that a tandem duplication was present, but the aforementioned primers did not completely flank the relevant sequence (Figure 2-1). Primers APOA4_Ex3dup:F and APOA4_Ex3dup:R were designed to flank the entire duplication, thus providing an easy to interpret sequence (Figure 3-4). The subsequent sequencing analysis revealed a novel 198 bp in-frame duplication within exon 3, from coding nucleotide 552 to 749 (c.552_749dup; GenBank® NC_000011.8; Figure 3-2l). Further sequence analysis

showed a 24 out of 26 (>92%) base pair homology at the duplication junction sites (Figure 3-4). This 198 bp duplication was not present in any of the other 4 indiviudals.

A novel A to G transition was identified in an affected individual at coding nucleotide 1099 of APOA4 (c.1099A>G; GenBank® NC_000011.8; Figure 3-2m), which results in a threonine to alanine substitution at amino acid position 367 (p.367Thr>Ala; GenBank® NP_000473.2). A previously reported A to T transversion at the same position, which causes a threonine to serine substitution, was identified in one of the unrelated controls (dbSNP: rs45474794, rs675). The four remaining individuals were homozygous for A at this position, including the other affected individual.

A four base deletion was identified in a tetranucleotide repeat (CTGT) stretch in the 3'-UTR of APOA4 in an affected individual. This deletion was 55 nucleotides downstream of the last coding nucleotide of APOA4 (c.1191+55_58del; GenBank® NC_000011.8; Figure 3-2n). One unrelated control was homozygous, and the three other controls were heterozygous, for this deletion. The other affected individual was homozygous normal. This tetranucleotide repeat variation is a previously reported polymorphism (dbSNP: rs9282602).

3.3.9) Summary

Mutation analysis of the coding regions of 8 positional candidate genes revealed 14 previously reported polymorphisms or novel variants in 6 different genes: 1 in-frame duplication, 1 missense variant, 3 silent variants, 3 UTR variants, and 6 intronic variants (Table 3-1; Figure 3-2). The only variant unique to both affected individuals that wasn't a previously documented SNP was the 198 bp duplication identified in the third exon of

APOA4 (c.552_749dup; GenBank® NC_000011.8). Also, as would be expected, the inheritance patterns of the identified variants and SNPs were consistent with the previously established haplotype data.

Table 3-1 Sequence variants identified in positional candidate genes for FEVE. The only novel variant unique to FEVE affected individuals is shaded grey.

Gene	Location	Sequence Variant Nomenclature*	dbSNP
EVA1	Intron 1	c.58+13_16dup	-
PAFAH1B2	Intron 2	c.82-25delT	rs35139041
PAFAH1B2	Intron 5	c.411+G>T	rs7122944
AMICA1	-	-	-
SCN2B	Intron 3	c.449-12A>C	rs8192613
SCN4B†	-	-	-
TMPRSS4	Exon 13, 3'-UTR	c.1314+156A>G	rs8924
PCSK7	Exon 5	c.711G>A	rs45528535
PCSK7	Exon 14	c.1770T>G	-
PCSK7	Intron 14	c.1786+7C>T	-
PCSK7	Intron 14	c.1786+30A>G	-
APOA4	Exon 1, 5'-UTR	c.1-98G>A	rs5091
APOA4	Exon 2	c.87A>G	rs5092
APOA4	Exon 3	c.552_749dup	-
APOA4	Exon 3	c.1099A>G	-
APOA4	Exon 3, 3'-UTR	c.1191+55_58del	rs9282602

* Based on GenBank® genomic reference sequence NC_000011.8

† CDS from exon 1 was not sequenced

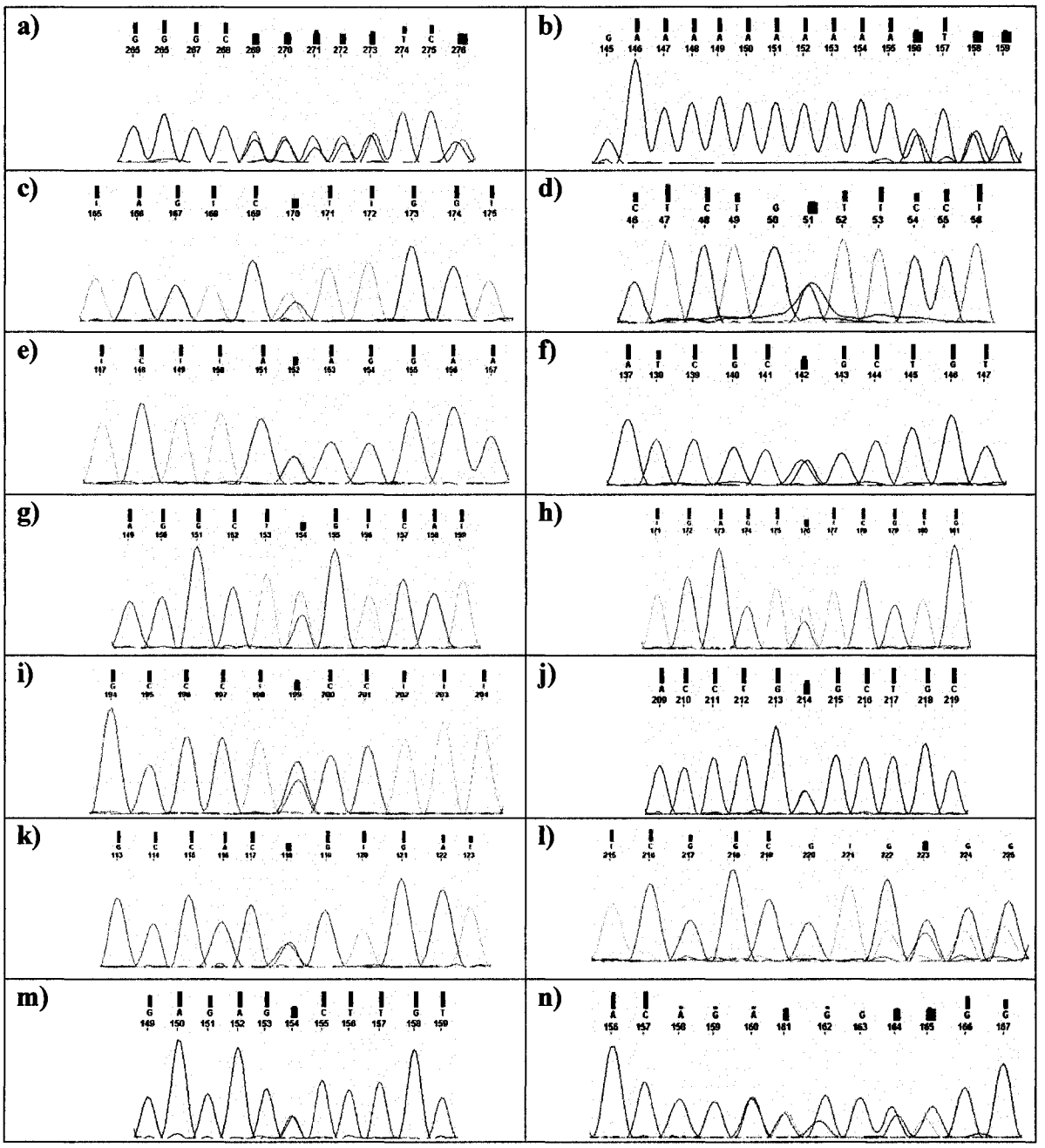

Figure 3-2 Electropherograms of sequence variants in various FEVE candidate genes. Forward strand sequencing results shown for: a, c, d, f, g, h, i, & k. Reverse strand sequencing results shown for: b, e, j, l, m, & n. **a)** *EVA1* c.58+13_16dup. **b)** *PAFAH1B2* c.82-25delT. **c)** *PAFAH1B2* c.411+11T>G. **d)** *SCN2B* c.499-12A>C. **e)** *TMPRSS4* c.1314+156A>G. **f)** *PCSK7* c.711G>A. **g)** *PCSK7* c.1770T>G. **h)** *PCSK7* c.1786+7C>T. **i)** *PCSK7* c.1786+30A>G. **j)** APOA4 c.1-98G>A. **k)** APOA4 c.87A>G. **l)** 3'-end of APOA4 c.552_749dup. **m)** APOA4 c.1099A>G. **n)** APOA4 c.1191+55_58del.

a)

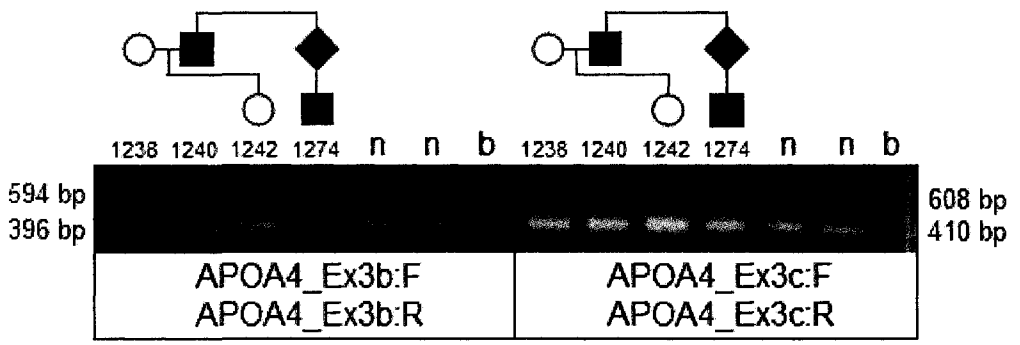

b)

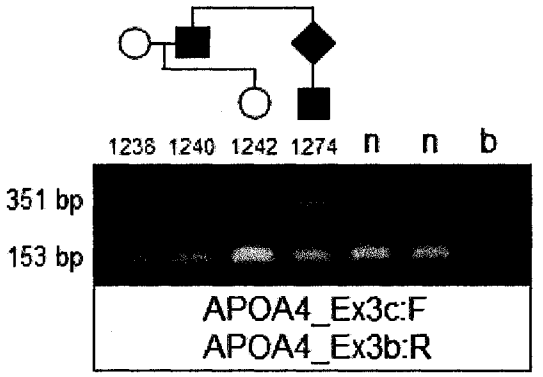

Figure 3-3 Amplified DNA products showing the expanded APOA4 fragment in addition to the wildtype fragment. Primers are listed under their respective agarose gels. The corresponding pedigree section is shown above, including an uncle who is an obligate carrier and his affected nephew. Sample accession numbers are indicated. Normal population controls (n) and a blank (b) are in the right lanes. **a)** The products from which the duplication was initially identified. **b)** A more distinct visualization of the duplicated fragment.

a)

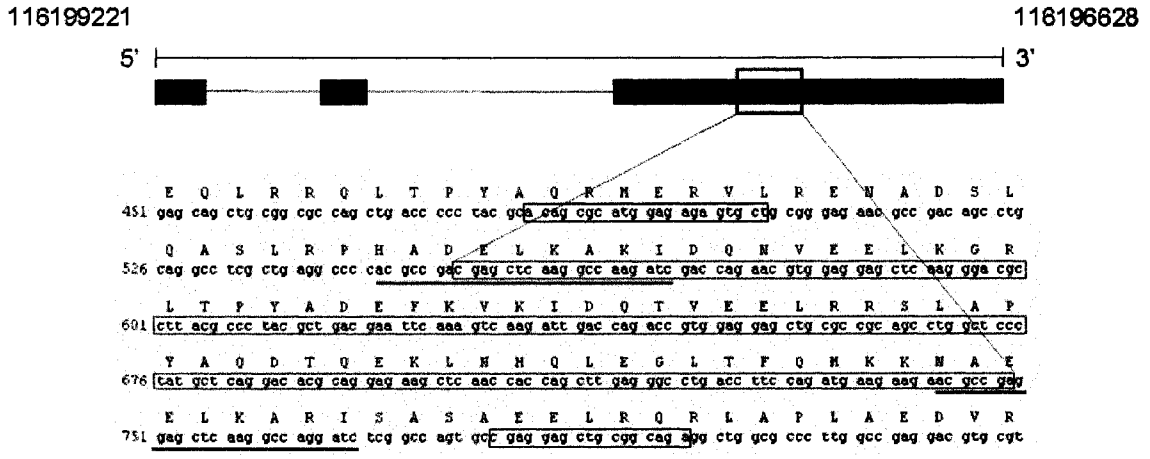

b)

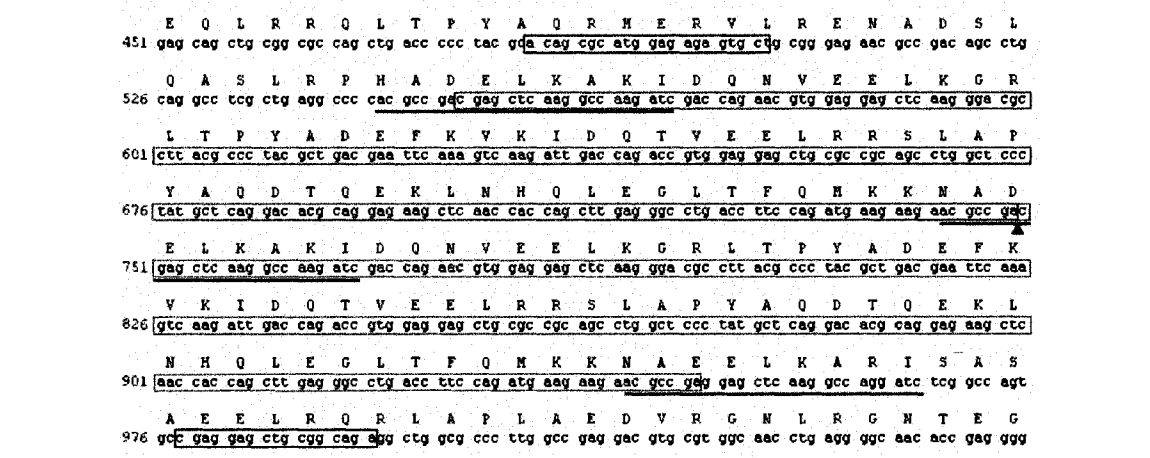

Figure 3-4 Sequence homology at APOA4 duplication breakpoints. a) Schematic of the wildtype APOA4 genomic sequence showing untranslated regions (blue) and open reading frame (brown). **b)** The duplicated APOA4 genomic sequence, as seen in FEVE affected individuals, with an arrowhead indicating the duplication junction. The location of the duplicated sequence is outlined in red, with the purple outline, in part 'b', indicating the actual duplication. The highly homologous sequences spanning the breakpoints are underlined in blue, and the primers designed to flank and detect the duplication (APOA4_Ex3dup:F/APOA4_Ex3dup:R) are outlined in green.

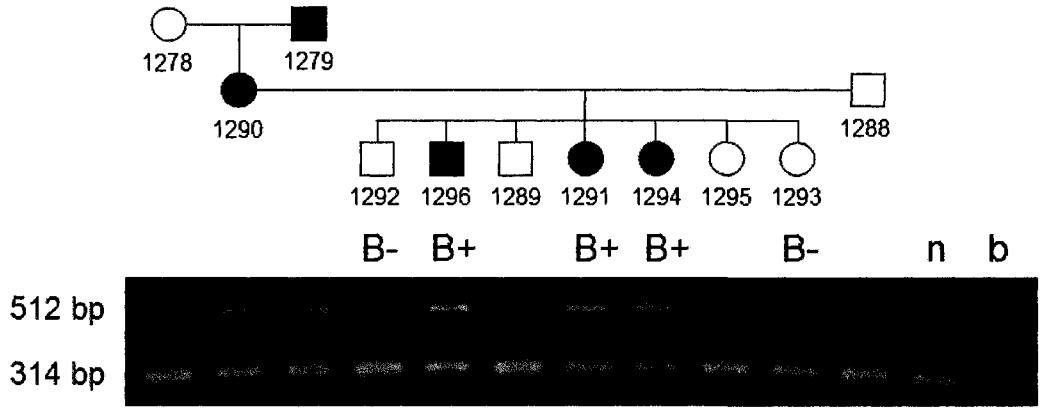

Figure 3-5 Amplified DNA products showing segregation of APOA4 duplication with FEVE affected individuals. A branch of the family pedigree is shown with affected (biopsy-confirmed positive: B+) and unaffected individuals (biopsy-confirmed negative: B-) above corresponding agarose gel analysis of PCR products derived from the duplicated region in APOA4. Primers used to produce this image were APOA4_Ex3dup:F and APOA4_Ex3dup:R. Sample accession numbers are indicated.

3.4) Segregation of APOA4 c.552_749dup

Individuals were tested for the APOA4 c.552_749dup by conducting PCR and electrophoresis with primers APOA4_Ex3c:F and APOA4_Ex3b:R (Figure 3-3b). The duplication was observed in all 14 biopsy-confirmed FEVE affected individuals, but not in any of the 6 biopsy-confirmed FEVE unaffected individuals (Figure 3-5). Furthermore, the mutation was not found in 32 ethnicity-matched control chromosomes or in 400 normal chromosomes from the general population. Of the 60 family members who had not been biopsied, 19 tested positive for the duplication. These results indicate a penetrance of 0.79 based on phenotype reported by family history, and 1.00 based on biopsy-confirmed pathology (Figure 3-6).

3.5) RNA Expression Analysis of APOA4

Following RT-PCR of both blood- and dermal epithelial cell-derived RNA from clinically well individuals, the presence of cDNA was confirmed (results not shown). However, several attempts at amplifying APOA4 cDNA from both FEVE affected and unaffected individuals proved unsuccessful, as indicated by the absence of PCR products (results not shown).

3.6) Protein Analysis of apoA-IV

The intragenic c. 552_749dup in APOA4 is predicted to add 66 amino acids within a helicoidal domain of the 396 aa 46 kDa apoA-IV protein (p.184_249dup; GenBank® NP_000473.2; Figures 3-7 & 3-8), increasing the mutant protein's molecular weight by 7.7 kDa (calculated using the Protein Calculator available at

http://www.scripps.edu/~cdputnam/protcalc.html). This 54 kDa mutant protein was the predominant form of apoA-IV detected in the plasma of clinically well FEVE affected individuals (Figure 3-9). Investigation into the evolutionary conservation of human apoA-IV revealed that of the 66 aa's in the duplication, only 4 (6%) differed from a consensus sequence based on the apoA-IV of humans and 6 other species (Figure 3-10). Of an additional 10 amino acids on each side of the duplication breakpoints, only 1 varied from the consensus sequence (Figure 3-10).

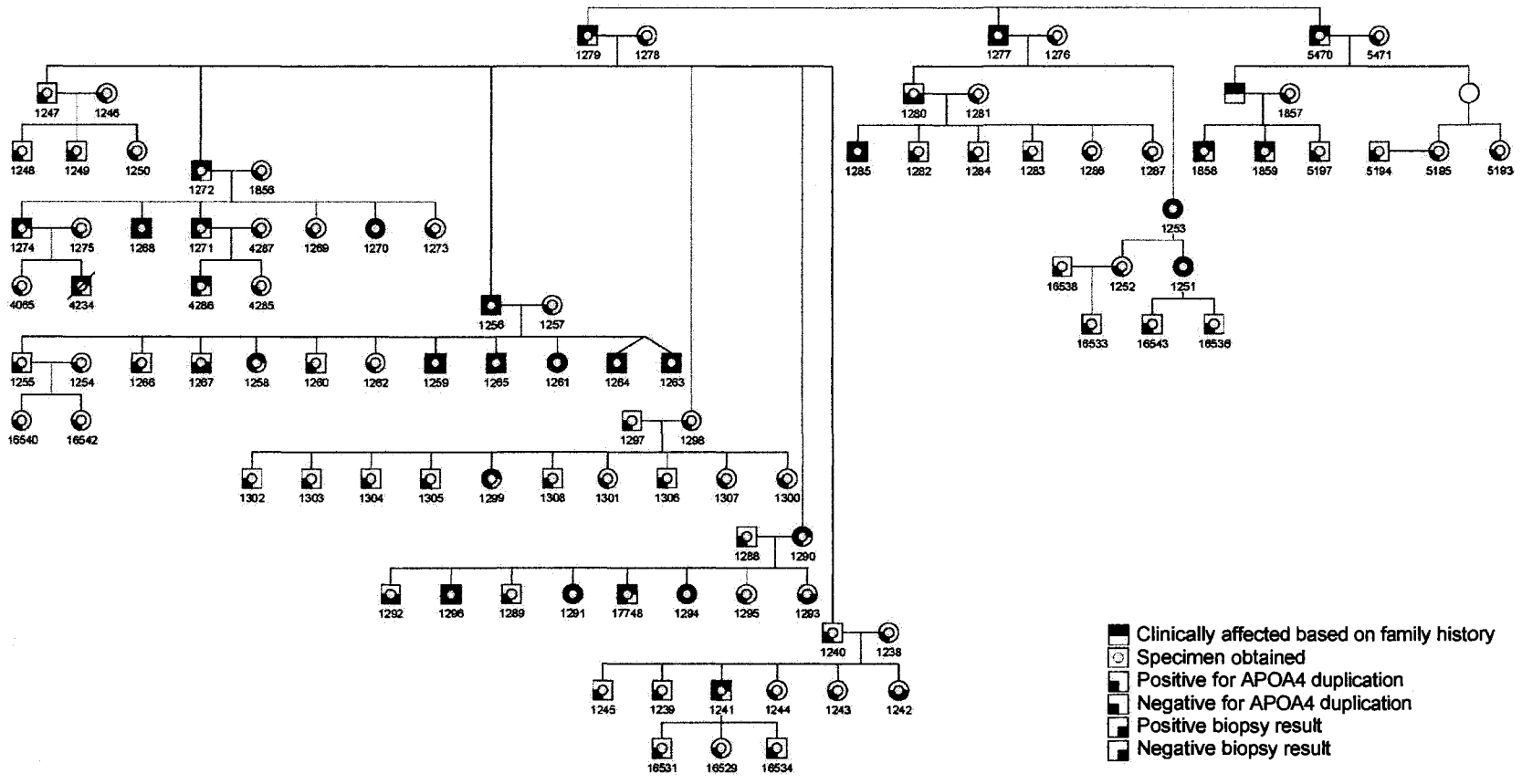

Figure 3-6 Pedigree of FEVE-affected kindred showing clinically affected status, APOA4 duplication and biopsy results. Ninety-eight members from the Mennonite kindred are shown, including the 96 individuals who were tested for the APOA4 duplication. Penetrance of the disorder is 0.79, based on 33 people testing positive for the APOA4 duplication, 26 of which were clinically affected. Sample accession numbers are included where applicable. The legend is shown at bottom right.

Wildtype

1-32	mflkavvltl alvavagara evsadqvatv mw
33-59	dyfsqlsnna keavehlqks eltqqln
60-81	alfqdklgevn tyagdlqkklv
82-103	pfatelherla kdseklkeeig
104-114	keleelrarll
115-136	phanevsqkig dnlrelqqrle
137-158	pyadqlrtqvs tqaeqlrrqlt
159-180	pyaqrmervlr enadslqaslr
181-202	phadelkakid qnveelkqrlt
203-224	pyadefkvkid qtveelrrsla
225-246	pyaqdtqekln hqleqltfqmk
247-268	knaeelkaris asaeelrqrla
269-290	plaedvrgnlr gnteglqksla
291-308	elgghldqqve efrrrve
309-330	pygenfnkalv qqmeqlrqklg
331-352	phagdveghls flekdlrdkvn
353-396	sffstfkekes qdktlslpele qqqeqqqeqqq eqvqmlaples

p.184_249dup

mflkavvltl alvavagara evsadqvatv mw	1-32
dyfsqlsnna keavehlqks eltqqln	33-59
alfqdklgevn tyagdlqkklv	60-81
pfatelherla kdseklkeeig	82-103
keleelrarll	104-114
phanevsqkig dnlrelqqrle	115-136
pyadqlrtqvs tqaeqlrrqlt	137-158
pyaqrmervlr enadslqaslr	159-180
phadelkakid qnveelkqrlt	181-202
pyadefkvkid qtveelrrsla	203-224
pyaqdtqekln hqleqltfqmk	225-246
knadelkakid qnveelkqrlt	247-268
pyadefkvkid qtveelrrsla	269-290
pyaqdtqekln hqleqltfqmk	291-312
knaeelkaris asaeelrqrla	313-334
plaedvrgnlr gnteglqksla	335-356
elgghldqqve efrrrve	357-374
pygenfnkalv qqmeqlrqklg	375-396
phagdveghls flekdlrdkvn	397-418
sffstfkekes qdktlslpele qqqeqqqeqqq eqvqmlaples	419-462

Figure 3-7 Apolipoprotein A-IV amino acid alignment sequences. Helicoidal domains (blue letters), non-helicoidal domains (black letters), and non-degenerated helices (red letters). The portion of the helicoidal domain duplicated is underlined, with black arrow showing the duplication breakpoint in the p.184_249dup sequence. Adapted from Figure 1 in (EMMANUEL *et al.* 1994).

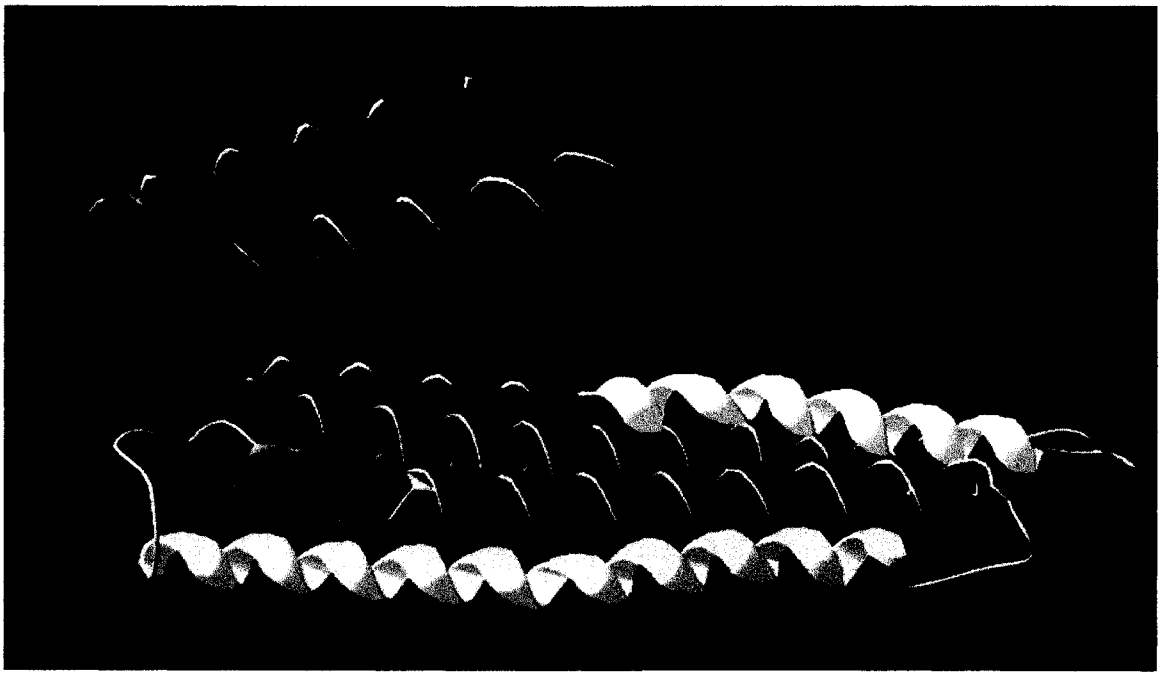

Figure 3-8 The predicted protein conformation of the 376 aa wildtype apoA-IV from amino acid 25 to 259. The segment duplicated in FEVE affected individuals is shown in red. This 3-D model was created by 3D-JIGSAW (http://www.bmm.icnet.uk/~3djigsaw) using the human apoA-IV sequence from Ensembl (http://www.ensembl.org), and visualized with Swiss-Pdb viewer v3.7 (http://expasy.org/spdbv).

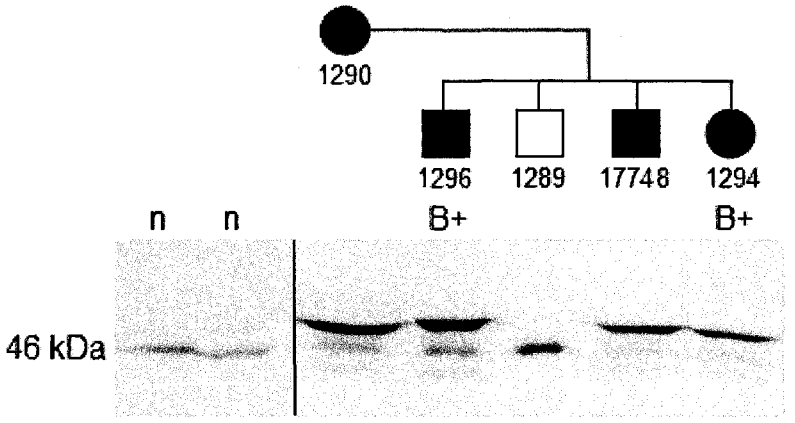

Figure 3-9 Western blot of apoA-IV in FEVE family members. Comparison of wildtype and mutant protein by immunoblot analysis. A branch of the family that includes two biopsy-confirmed affected individuals (B+) is shown with two normal control samples (n). Wildtype apoA-IV is visible as a 46 kDa band, and the mutant protein is visible as a 54 kDa band in all affected individuals. Sample accession numbers are indicated.

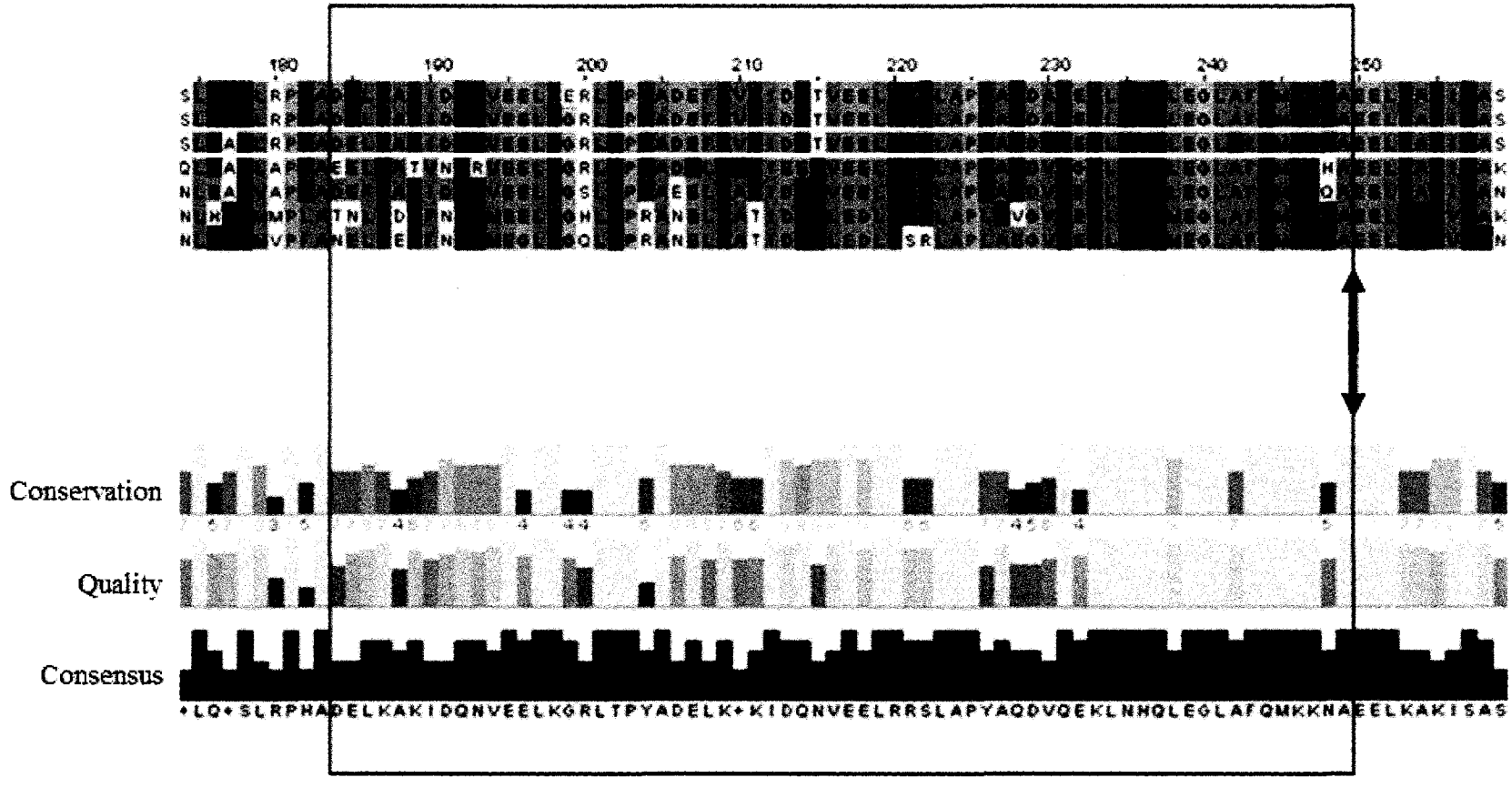

Figure 3-10 Conservation of apoA-IV amino acid sequence across species. 86 amino acids of the 396 amino acid apoA-IV protein are shown. The amino acids duplicated in FEVE affected individuals are enclosed in the black box, with the double-sided arrow indicating the duplication junction. From top to bottom, the species represented in the upper block of amino acid sequences are: *Macaca fascicularis* (cynomologus monkey), *Papio anubis* (olive baboon), *Homo sapiens* (human; outlined in yellow), *Bos Taurus* (bovine), *Sus scrofa* (pig), *Mus musculus* (mouse), and *Rattus norvegicus* (rat). Image developed with ClustalW2 (http://www.ebi.ac.uk/Tools/clustalw2) using protein sequences from Ensembl (http://www.ensembl.org).

CHAPTER 4: DISCUSSION

4.1) Importance of Identifying the Genetic Basis of FEVE

Despite many advances in understanding the pathophysiology of IBD, its precise causes remain largely unknown (GOYETTE *et al.* 2007). This thesis describes a large Mennonite kindred in which a severe autosomal dominant inflammatory intestinal disorder (FEVE) is observed. A positional candidate approach was used to identify the gene responsible for the characteristic inflammatory pathology in FEVE, with the expectation that this might also give insight into other intestinal disorders, such as IBD.

4.2) FEVE Critical Region and Candidate Genes

The refinement of informative crossover positions to intervals D11S4142-MDL11S115.9 and MDL11S117.96-D11S1364 confirmed a minimum candidate interval for FEVE between markers D11S4142 and D11S1364 (Figure 3-1). The identification of this critical region established a basis for the positional candidate approach to pinpoint the FEVE disease gene. Approximately 40 genes exist within that defined FEVE critical region, 2 of which (*CD3D* and *IL10RA*) were previously sequenced and ruled out as candidates for FEVE based on the absence of mutations in affected individuals. Direct sequencing of an additional 8 positional candidate genes revealed various novel variants and previously reported SNPs in the affected individuals (Table 3-1; Figure 3-2). These sequencing results were consistent with the previously established haplotypes, and the heterozygous variants confirmed that both alleles were successfully amplified. Most importantly, this mutation screening uncovered a FEVE-specific mutation in positional candidate APOA4.

4.3) APOA4 Mutation and its Segregation with FEVE

The only novel variant unique to the FEVE affected individuals was a 198 bp (66 aa) tandem duplication in exon 3 of APOA4 (c.552_749dup; GenBank® NC_000011.8). The amino acid sequence of the duplicated region is highly conserved across several species, reflecting the functional biological importance of the affected region (Figure 3-10). Of the 80 family members tested from 4 generations, 33 (41%) were found to have this APOA4 duplication (Figure 3-6). The segregation of this mutation displayed 100% concordance with all biopsy-confirmed FEVE affected (n = 14) and unaffected (n = 6) individuals (Figure 3-6). Furthermore, the absence of this mutation in 36 ethnicity-matched chromosomes and 400 chromosomes from the general population indicates that it is unlikely to be an innocuous variant.

The sequence homology observed at this duplication's junctions suggests a duplication mechanism involving misalignment followed by homologous recombination during meiosis (Figure 3-4; Figure 4-1). This sequence homology also identifies this as a likely site for reciprocal deletion events (Figure 4-1). Therefore, due to the sequence similarity, it is plausible that similar sporadic mutations may exist at this site outside of the identified FEVE Mennonite kindred.

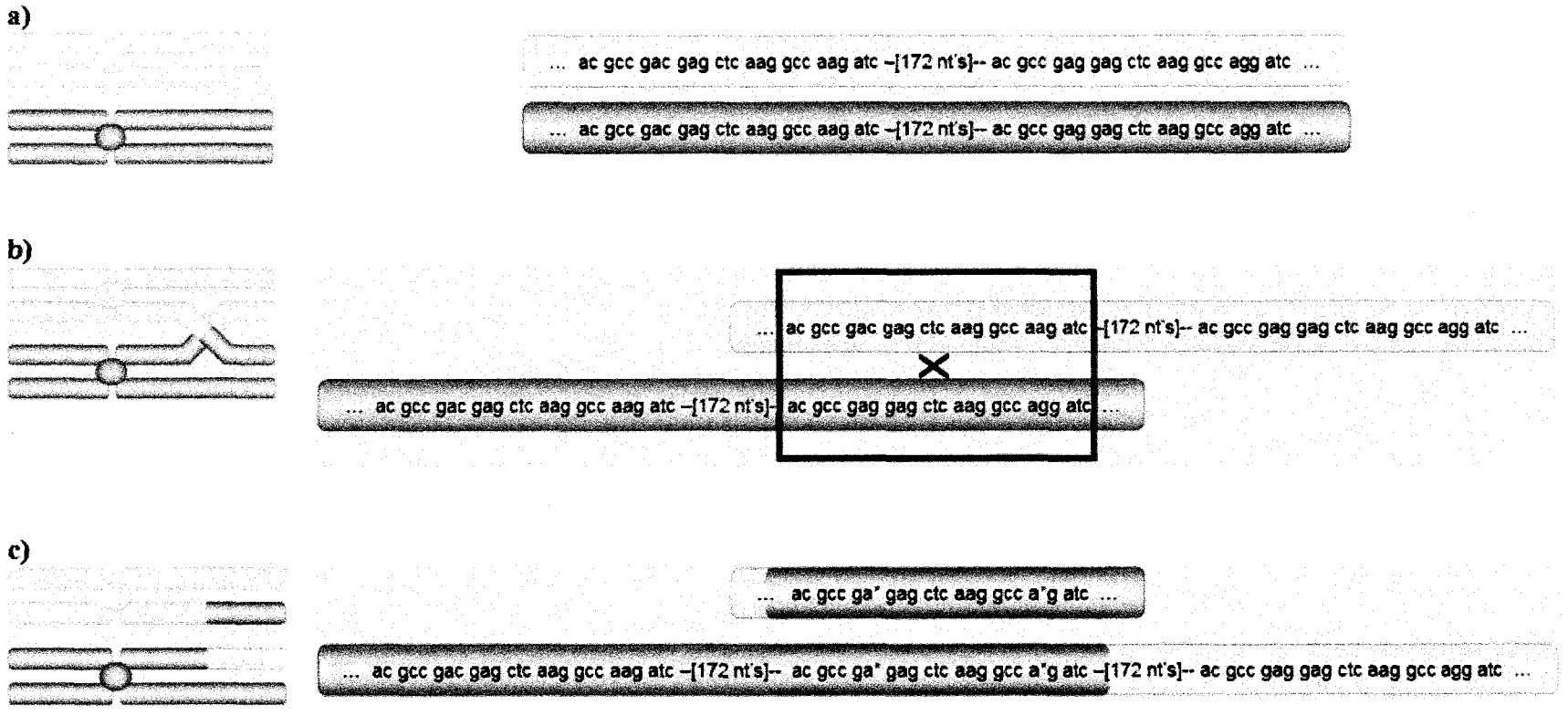

Figure 4-1 Misalignment followed by homologous recombination resulting in APOA4 duplications and deletions. Full chromosomes shown at left. Magnified images of the chromosomes' 26 bp homologous APOA4 sequences shown at right. The homologous sequences flank 172 nucleotides as indicated. **a)** Chromosomes in proper alignment. **b)** Cross-over event in misaligned chromosomes (Note: misalignment is not visible at full chromosome level). Black box indicates region where 24 out of 26 bp homology facilitates misaligned homologous recombination. Mismatched nucleotides are shown in red. **c)** Recombinant chromosomes resulting from misalignment followed by homologous recombination. Grey area indicates crossover region. Asterisks are shown in place of mismatched nucleotides due to various potential cross-over locations. The top chromosome has a deletion, whereas the bottom chromosome has a tandem duplication (Note: deletion and duplication are not visible at full chromosome level).

4.4) Population Genetics of FEVE Mutation

The founding members of the FEVE kindred adopted the Mennonite denomination when they arrived in Alberta in the 1920s. It is thought that one or more of these first settlers introduced the autosomal dominant APOA4 mutation, which is now overrepresented in their descendents. The perpetuation of this mutation was facilitated in part by the variable penetrance and variable expressivity of the disorder, whereby some individuals with the APOA4 duplication exhibited either no symptoms or only minor symptoms. Additionally, those who experienced and survived the life-threatening FEVE episodes went on to lead normal lives. Therefore, numerous individuals with the APOA4 mutation survived into adulthood and could successfully reproduce. The perpetuation of the APOA4 mutation was also aided by their tendency, as Mennonites, to have large families. So despite having the mutation for a potentially life-threatening disorder, FEVE survivors have exhibited a level of biological fitness comparable to their unaffected counterparts (i.e. the average number of offspring is >7 for both affected and unaffected individuals in this family[3]). Therefore, the overrepresentation of the APOA4 mutation in this kindred was initiated by a founder effect, and perpetuated within this kindred due to the relatively high fitness of the affected individuals.

[3] Based on the individuals in generations I & II who were tested for the APOA4 duplication. Individuals in subsequent generations were excluded from this calculation because they have not necessarily started/completed their production of offspring. Note: not all offspring were tested for the APOA4 duplication, therefore not all of them appear on the pedigree presented in this thesis.

4.5) Role of apoA-IV in FEVE

Failure to amplify APOA4 from blood- and dermal epithelial cell-derived RNA corresponds with the literature which indicates that APOA4 is exclusively expressed in differentiated enterocytes of the villi in the proximal small intestine (PEIGNON *et al.* 2006). This exclusive intestinal expression of APOA4 fits with the pathological effect of FEVE which is restricted to the small intestine (SMITH *et al.* 1994). In addition, apoA-IV is implicated in the regulatory and signaling pathways that govern inflammation in enterocytes (PEIGNON *et al.* 2006). The anti-inflammatory mechanism of apoA-IV is unknown, but has been attributed to the suppression of endothelial cell expression of P-selectin, thereby inhibiting the recruitment of leukocytes to inflamed tissues (VOWINKEL *et al.* 2004). ApoA-IV also decreases the secretion of IL-4 and TNF-α, which are pro-inflammatory cytokines that would otherwise induce the expression of P-selectin (RECALDE *et al.* 2004; WELLER *et al.* 1992). The interactions between apoA-IV and α-catenin, a junctional anchor protein, and α_1-antichymotrypsin, an acute phase inflammatory responsive protein, indicate additional pathways by which apoA-IV may exert its anti-inflammatory effect (DREES *et al.* 2005; GRZYMISŁAWSKI *et al.* 2006; ORSÓ *et al.* 2007).

The similar pathology between individuals with FEVE and DSS-induced colitis in APOA4 knockout mice suggests that both inflammatory responses may be the result of a related mechanism (SMITH *et al.* 1994; VOWINKEL *et al.* 2004). If this were the case, then it implies that the heterozygous APOA4 duplication in humans is functionally related to the homozygous null alleles in mice, and therefore is not a gain of function mutation. Investigation of people heterozygous for a genomic deletion encompassing APOA1,

APOC3, and APOA4, revealed that apoA-IV levels were only 35% ($p<0.05$) lower than those of their relatives not carrying the deletion (ORDOVAS *et al.* 1989). Since no significant gastrointestinal problems were reported by the 15 heterozygous individuals, haploinsufficiency of apoA-IV is unlikely to be responsible for the disease observed in FEVE (SCHAEFER *et al.* 1985). In a generation of 11 siblings produced by parents who were both heterozygous for the genomic deletion encompassing APOA4, 2 non-genotyped children died from gastroenteritis at one year of age (SCHAEFER *et al.* 1982). The possibility that their deaths resulted from homozygous loss of APOA4 should be considered. If a homozygous knockout of APOA4 is required for intestinal inflammation, then it is most likely that the APOA4 duplication in our family acts through a dominant negative mechanism, either by suppression of wildtype apoA-IV expression or function, or an increase in its turn-over by the mutant apoA-IV protein. Immunoblot analysis of clinically well FEVE affected individuals detected mutant apoA-IV as the predominant form of the protein in their plasma, as well as a third lower molecular weight band which could indicate degradation of the wildtype protein (Figure 3-9). These results provide evidence of reduced expression, increased turn-over, or degradation of wildtype apoA-IV. Further analyses are required to determine which of these possibilities applies, as for example, an increased half-life for a non-active mutant protein may be sufficient to cause reduced levels of wildtype protein. It is also worth considering that the wildtype and mutant apoA-IV levels may be different during acute FEVE episodes.

4.6) APOA4 as a Susceptibility Gene for IBD

Previous genome-wide association studies for IBD have not implicated the 11q23 locus (CHO and ABRAHAM 2007; RIOUX *et al.* 2007), but there are direct lines of evidence implicating APOA4 itself. First, APOA4 expression is significantly downregulated in IBD mucosal tissues, even in non-inflamed regions (KIM *et al.* 2006; ORSÓ *et al.* 2007). Second, an inverse association was found between apoA-IV plasma levels and disease activity in patients with Crohn's disease (BROEDL *et al.* 2007). Additionally, the penetrance of the heterozygous APOA4 mutation is 79.0% (Figure 3-6), which is much greater than the penetrance of 4.9% reported for homozygotes/compound heterozygotes of the strongest associated IBD gene variants (see section 1.3.1.3) (BRANT *et al.* 2007). This indicates that APOA4 has a lower dependence on environmental factors and a greater direct effect on intestinal inflammation than any of the genes associated with IBD to date. The findings of this thesis combined with those from the literature suggest that APOA4, which confers susceptibility to a rare monogenic form of IBD (FEVE), may be associated with more common complex and multifactorial forms of IBD (UC and CD).

4.7) Future Directions

With respect to the affected Mennonite kindred, an investigation is warranted into the possible treatment of acute FEVE episodes via administration of exogenous apoA-IV. Furthermore, future intestinal biopsies from affected family members may be examined for aberrant expression of wildtype APOA4 or atypical localization of wildtype apoA-IV.

Proof that the APOA4 duplication is indeed causing FEVE can be ascertained by introduction of an equivalent apoA4 duplication in an animal model, and subsequent

observation of the characteristic FEVE pathology within that animal model. Elucidation of the trigger(s) of acute FEVE episodes may be achieved through exposure of the animal model to various possible inflammatory triggers (i.e. dietary factors or pathogens). The potential involvement of the intestinal flora in FEVE can also be determined by comparing the inflammatory response of the conventional animal model with that of its germ-free counterpart.

In a more general context, future research should address the anti-inflammatory function of wildtype apoA-IV in the gastrointestinal tract. Such studies could compare basal APOA4 expression levels with those elicited in response to various inflammatory triggers, and analyze protein interactions to gain insight into the apoA-IV anti-inflammatory pathways. Additionally, the potential role of apoA-IV in other gastrointestinal disorders, such as the common forms of IBD, can be evaluated. For instance, samples from CD and UC patients could be sequenced for mutations and/or susceptibility SNPs in APOA4.

4.8) Summary and Conclusions

A total of 10 positional candidate genes at 11q23.3 were investigated for mutations in individuals affected by FEVE. Sequencing analysis identified a 198 bp tandem duplication in exon 3 of APOA4 (c.552_749dup; GenBank® NC_000011.8) that was present in all biopsy confirmed FEVE affected individuals, and absent in all biopsy confirmed FEVE unaffected individuals. This mutation was also absent in all ethnicity-matched and normal population controls, aiding in the confirmation of APOA4 as the disease locus for FEVE. Production of a mouse model of the disease and restoration of

the normal phenotype via introduction of a normal allele/protein are 2 additional means of demonstrating that a candidate gene is likely to be a disease locus (STRACHAN and READ 1999). An APOA4 knockout mouse model previously demonstrated an intestinal inflammatory phenotype similar to FEVE (VOWINKEL *et al.* 2004). Administration of recombinant human apoA-IV attenuated the inflammatory process in these mice, thereby achieving restoration of a normal phenotype (VOWINKEL *et al.* 2004). Therefore there is substantial evidence supporting the role of APOA4 in the pathology of FEVE. Also, given the hypothesis that the APOA4 mutation is functionally equivalent to a homozygous knockout, there may be recessive forms of the disorder which result in less severe manifestations.

In conclusion, this research has identified a mutation in APOA4 that confers susceptibility to FEVE. It is hypothesized that the APOA4 in-frame duplication acts as a dominant negative mutation that reduces wildtype apoA-IV synthesis or half-life. This mutant form of apoA-IV may be unable to suppress the endothelial expression of P-selectin, thereby allowing venular leukocyte adhesion and its resultant inflammation. This initial event could be exacerbated by a deficiency in promoting α-catenin mediated integrity of the enterocytic barrier to infiltration by inflammatory cells. It is hypothesized that treatment of affected individuals with exogenous apoA-IV during an acute FEVE episode may attenuate the inflammatory effects. Furthermore, various findings suggest that APOA4 may be a susceptibility gene for other inflammatory gastrointestinal disorders. Future investigations are warranted into the potential role of apoA-IV in other gastrointestinal disorders, such as IBD, as well as its anti-inflammatory function in the gastrointestinal system.

BIBLIOGRAPHY

ACHESON, D. W. K., and S. LUCCIOLI, 2004 Mucosal immune responses. Best Pract Res Clin Gastroenterol **18:** 387-404.

ADACHI, H., M. TSUJIMOTO, M. HATTORI, H. ARAI and K. INOUE, 1997 Differential tissue distribution of the β- and γ-subunits of human cytosolic platelet-activating factor acetylhydrolase (isoform I). Biochem Biophys Res Commun **233:** 10-13.

AHMAD, T., A. ARMUZZI, M. BUNCE, K. MULCAHY-HAWES, S. E. MARSHALL *et al.*, 2002 The molecular classification of the clinical manifestations of Crohn's disease. Gastroenterology **122:** 854-866.

ALBELDA, S. M., and C. A. BUCK, 1990 Integrins and other cell adhesion molecules. FASEB J **4:** 2868-2880.

ALTSCHUL, S. F., W. GISH, W. MILLER, E. W. MYERS and D. J. LIPMAN, 1990 Basic local alignment search tool. J Mol Biol **215:** 403-410.

ANDREASEN, D., G. VUAGNIAUX, N. FOWLER-JAEGER, E. HUMMLER and B. C. ROSSIER, 2006 Activation of epithelial sodium channels by mouse channel activating proteases (mCAP) expressed in *Xenopus* oocytes requires catalytic activity of mCAP3 and mCAP2 but not mCAP1. J Am Soc Nephrol **17:** 968-976.

ANTONARAKIS, S. E., and J. S. BECKMANN, 2006 Mendelian disorders deserve more attention. Nat Rev Genet **7:** 277-282.

AYABE, T., D. P. SATCHELL, C. L. WILSON, W. C. PARKS, M. E. SELSTED *et al.*, 2000 Secretion of microbial α-defensins by intestinal Paneth cells in response to bacteria. Nature Immunol **1:** 113-118.

BEATTIE, R. M., N. M. CROFT, J. M. FELL, N. A. AFZAL and R. B. HEUSCHKEL, 2006 Inflammatory bowel disease. Arch Dis Child **91:** 426-432.

BEIL, W. J., P. F. WELLER, M. A. PEPPERCORN, S. J. GALLI and A. M. DVORAK, 1995 Ultrastructural immunogold localization of subcellular sites of TNF-α in colonic Crohn's disease. J Leukoc Biol **58:** 284-298.

BERNSTEIN, C. N., A. WAJDA, L. W. SVENSON, A. MACKENZIE, M. KOEHOORN *et al.*, 2006 The epidemiology of inflammatory bowel disease in Canada: A population-based study. Am J Gastroenterol **101:** 1559-1568.

BLANK, M. L., T. LEE, V. FITZGERALD and F. SNYDER, 1981 A specific acetylhydrolase for 1-alkyl-2-acetyl-sn-glycero-3- phosphocholine (a hypotensive and platelet-activating lipid). J Biol Chem **256:** 175-178.

BONEN, D. K., Y. OGURA, D. L. NICOLAE, N. INOHARA, L. SAAB *et al.*, 2003 Crohn's disease-associated NOD2 variants share a signaling defect in response to lipopolysaccharide and peptidoglycan. Gastroenterology **124:** 140-146.

BOUMA, G., and W. STROBER, 2003 The immunological and genetic basis of inflammatory bowel disease. Nat Rev Immunol **3:** 521-533.

BRANT, S. R., M.-H. WANG, P. RAWSTHORNE, M. SARGENT, L. W. DATTA *et al.*, 2007 A population-based case-control study of CARD15 and other risk factors in Crohn's disease and ulcerative colitis. Am J Gastroenterol **102:** 313-323.

BRIDGE, P. J., 1997 The calculation of genetic risks: worked examples in DNA diagnositics, pp. 97. The Johns Hopkins University Press, Baltimore, MD.

BROEDL, U. C., V. SCHACHINGER, A. LINGENHEL, M. LEHRKE, R. STARK *et al.*, 2007 Apolipoprotein A-IV is an independent predictor of disease activity in patients with inflammatory bowel disease. Inflamm Bowel Dis **13:** 391-397.

BROOK, I., 1999 Bacterial interference. Crit Rev Microbiol **25:** 155-172.

BRUZZANITI, A., K. GOODGE, P. JAY, S. A. TAVIAUX, M. H. LAM *et al.*, 1996 PC8 [corrected], a new member of the convertase family. Biochem J **314:** 727-731.

CHEN, C.-H., 2004 Platelet-activating factor acetylhydrolase: Is it good or bad for you? Curr Opin Lipidol **15:** 337-341.

CHERTOV, O., D. F. MICHIEL, L. XU, J. M. WANG, K. TANI *et al.*, 1996 Identification of defensin-1, defensin-2, and CAP37/azurocidin as T-cell chemoattractant proteins released from interleukin-8-stimulated neutrophils. J Biol Chem **271:** 2935-2940.

CHIN, A. C., and C. A. PARKOS, 2006 Neutrophil transepithelial migration and epithelial barrier function in IBD: Potential targets for inhibiting neutrophil trafficking. Ann N Y Acad Sci **1072:** 276-287.

CHO, J. H., and C. ABRAHAM, 2007 Inflammatory bowel disease genetics: Nod2. Annu Rev Med **58:** 401.

CUMMINGS, J. R. F., R. COONEY, S. PATHAN, C. A. ANDERSON, J. C. BARRETT *et al.*, 2007 Confirmation of the role of *ATG16l1* as a Crohn's disease susceptibility gene. Inflamm Bowel Dis **13:** 941-946.

CUTHBERT, A. P., S. A. FISHER, M. M. MIRZA, K. KING, J. HAMPE *et al.*, 2002 The contribution of *NOD2* gene mutations to the risk and site of disease in inflammatory bowel disease. Gastroenterology **122:** 867-874.

DANESE, S., S. SEMERARO, M. MARINI, I. ROBERTO, A. ARMUZZI *et al.*, 2005 Adhesion molecules in inflammatory bowel disease: Therapeutic implications for gut inflammation. Dig Liver Dis **37:** 811-818.

DEN DUNNEN, J. T., and S. E. ANTONARAKIS, 2000 Mutation nomenclature extensions and suggestions to describe complex mutations: A discussion. Hum Mutat **15:** 7-12.

DREES, F., S. POKUTTA, S. YAMADA, W. J. NELSON and W. I. WEIS, 2005 α-catenin is a molecular switch that binds E-cadherin-β-catenin and regulates actin-filament assembly. Cell **123:** 903-915.

DUERR, R. H., K. D. TAYLOR, S. R. BRANT, J. D. RIOUX, M. S. SILVERBERG *et al.*, 2006 A genome-wide association study identifies *IL23R* as an inflammatory bowel disease gene. Science **314:** 1461-1463.

ECKMANN, L., M. F. KAGNOFF and J. FIERER, 1995 Intestinal epithelial cells as watchdogs for the natural immune system. Trends Microbiol **3:** 118-120.

ECONOMOU, M., T. A. TRIKALINOS, K. T. LOIZOU, E. V. TSIANOS and J. P. A. IOANNIDIS, 2004 Differential effects of NOD2 variants on Crohn's disease risk and phenotype in diverse populations: A metaanalysis. Am J Gastroenterol **99:** 2393-2404.

EISENHUT, M., 2006 Changes in ion transport in inflammatory disease. J Inflamm **3:** 5.

ELIAKIM, R., F. KARMELI, E. RASIN and D. RACHMILEWITZ, 1988 Role of platelet-activating factor in ulcerative colitis: Enhanced production during active disease and inhibition by sulfasalazine and prednisolone. Gastroenterology **95:** 1167.

EMMANUEL, F., A. STEINMETZ, M. ROSSENEU, R. BRASSEUR, N. GOSSELET *et al.*, 1994 Identification of specific amphipathic alpha-helical sequence of human apolipoprotein A-IV involved in lecithin:cholesterol acyltransferase activation. J Biol Chem **269:** 29883-29890.

FAGARASAN, S., and T. HONJO, 2003 Intestinal IgA synthesis: Regulation of front-line body defences. Nat Rev Immunol **3:** 63-72.

FASANO, A., B. BAUDRY, D. W. PUMPLIN, S. S. WASSERMAN, B. D. TALL *et al.*, 1991 *Vibrio cholerae* produces a second enterotoxin, which affects intestinal tight junctions. Proc Natl Acad Sci U S A **88:** 5242-5246.

FIELD, M., 2003 Intestinal ion transport and the pathophysiology of diarrhea. J Clin Invest **111:** 931-943.

FIOCCHI, C., 1998 Inflammatory bowel disease: Etiology and pathogenesis. Gastroenterology **115:** 182-205.

FRANCHIMONT, D., S. VERMEIRE, H. EL HOUSNI, M. PIERIK, K. VAN STEEN *et al.*, 2004 Deficient host-bacteria interactions in inflammatory bowel disease? The toll-like receptor (TLR)-4 Asp299gly polymorphism is associated with Crohn's disease and ulcerative colitis. Gut **53:** 987-992.

GANZ, T., 2003 Defensins: Antimicrobial peptides of innate immunity. Nat Rev Immunol **3:** 710-720.

GIRARDIN, S. E., I. G. BONECA, J. VIALA, M. CHAMAILLARD, A. LABIGNE *et al.*, 2003 Nod2 is a general sensor of peptidoglycan through muramyl dipeptide (MDP) detection. J Biol Chem **278:** 8869-8872.

GLAS, J., J. SEIDERER, M. WETZKE, A. KONRAD, H.-P. TÖRÖK *et al.*, 2007 rs1004819 is the main disease-associated *IL23R* variant in German Crohn's disease patients: combined analysis of *IL23R*, *CARD15*, and *OCTN1/2* variants. PLoS ONE **2:** e819.

GOYETTE, P., C. LABBE, T. T. TRINH, R. J. XAVIER and J. D. RIOUX, 2007 Molecular pathogenesis of inflammatory bowel disease: Genotypes, phenotypes and personalized medicine. Ann Med **39:** 177 - 199.

GRZYMISŁAWSKI, M., K. DERC, M. SOBIESKA and K. WIKTOROWICZ, 2006 Microheterogeneity of acute phase proteins in patients with ulcerative colitis. World J Gastroenterol **12:** 5191-5195.

GUTTINGER, M., F. SUTTI, M. PANIGADA, S. PORCELLINI, B. MERATI *et al.*, 1998 Epithelial V-like antigen (EVA), a novel member of the immunoglobulin superfamily, expressed in embryonic epithelia with a potential role as homotypic adhesion molecule in thymus histogenesis. J Cell Biol **141:** 1061-1071.

HAMADA, H., T. HIROI, Y. NISHIYAMA, H. TAKAHASHI, Y. MASUNAGA *et al.*, 2002 Identification of multiple isolated lymphoid follicles on the antimesenteric wall of the mouse small intestine. J Immunol **168:** 57-64.

HAMPE, J., A. CUTHBERT, P. J. P. CROUCHER, M. M. MIRZA, S. MASCHERETTI *et al.*, 2001 Association between insertion mutation in *NOD2* gene and Crohn's disease in German and British populations. Lancet **357:** 1925-1928.

HAMPE, J., A. FRANKE, P. ROSENSTIEL, A. TILL, M. TEUBER *et al.*, 2007 A genome-wide association scan of nonsynonymous SNPs identifies a susceptibility variant for Crohn disease in *ATG16L1*. Nat Genet **39:** 207-211.

HAMPE, J., K. HEYMANN, W. KRUIS, A. RAEDLER, U. R. FÖLSCH *et al.*, 2000 Anticipation in inflammatory bowel disease: A phenomenon caused by an accumulation of confounders. Am J Med Genet **92:** 178-183.

HARWIG, S. S., L. TAN, X. D. QU, Y. CHO, P. B. EISENHAUER *et al.*, 1995 Bactericidal properties of murine intestinal phospholipase A_2. J Clin Invest **95:** 603-610.

HAWKER, P. C., J. S. MCKAY and L. A. TURNBER, 1980 Electrolyte transport across colonic mucosa from patients with inflammatory bowel disease. Gastroenterology **79:** 508-511.

HERESBACH, D., B. GULWANI-AKOLKAR, M. LESSER, P. N. AKOLKAR, X.-Y. LIN *et al.*, 1998 Anticipation in Crohn's disease may be influenced by gender and ethnicity of the transmitting parent. Am J Gastroenterol **93:** 2368-2372.

HERSHBERG, R. M., P. E. FRAMSON, D. H. CHO, L. Y. LEE, S. KOVATS *et al.*, 1997 Intestinal epithelial cells use two distinct pathways for HLA class II antigen processing. J Clin Invest **100:** 204-215.

HOOPER, J. D., J. A. CLEMENTS, J. P. QUIGLEY and T. M. ANTALIS, 2001 Type II transmembrane serine proteases: Insights into an emerging class of cell surface proteolytic enzymes. J Biol Chem **276:** 857-860.

HUGOT, J.-P., M. CHAMAILLARD, H. ZOUALI, S. LESAGE, J.-P. CEZARD *et al.*, 2001 Association of NOD2 leucine-rich repeat variants with susceptibility to Crohn's disease. Nature **411:** 599-603.

HUMMLER, E., and J.-D. HORISBERGER, 1999 Genetic disorders of membrane transport: V. The epithelial sodium channel and its implication in human diseases. Am J Physiol Gastrointest Liver Physiol **276:** G567-G571.

IIJIMA, H., I. TAKAHASHI and H. KIYONO, 2001 Mucosal immune network in the gut for the control of infectious diseases. Rev Med Virol **11:** 117-133.

ILIEV, I. D., G. MATTEOLI and M. RESCIGNO, 2007 The yin and yang of intestinal epithelial cells in controlling dendritic cell function. J Exp Med **204:** 2253-2257.

INOHARA, N., Y. OGURA, A. FONTALBA, O. GUTIERREZ, F. PONS *et al.*, 2003 Host recognition of bacterial muramyl dipeptide mediated through NOD2: Implications for Crohn's disease. J Biol Chem **278:** 5509-5512.

INTERNATIONAL HUMAN GENOME CONSORTIUM, 2004 Finishing the euchromatic sequence of the human genome. Nature **431:** 931-945.

ISOM, L. L., D. S. RAGSDALE, K. S. DE JONGH, R. E. WESTENBROEK, B. F. X. REBER *et al.*, 1995 Structure and function of the β2 subunit of brain sodium channels, a transmembrane glycoprotein with a CAM motif. Cell **83:** 433-442.

ITO, S., E. NOGUCHI, M. SHIBASAKI, K. YAMAKAWA-KOBAYASHI, H. WATANABE *et al.*, 2002 Evidence for an association between plasma platelet-activating factor

acetylhydrolase deficiency and increased risk of childhood atopic asthma. J Hum Genet **47:** 99-101.

JAYE, D. L., and C. A. PARKOS, 2000 Neutrophil migration across intestinal epithelium. Ann N Y Acad Sci **915:** 151-161.

KIM, M., S. LEE, S. K. YANG, K. SONG and I. LEE, 2006 Differential expression in histologically normal crypts of ulcerative colitis suggests primary crypt disorder. Oncol Rep **16:** 663-670.

KOBAYASHI, K. S., M. CHAMAILLARD, Y. OGURA, O. HENEGARIU, N. INOHARA *et al.*, 2005 Nod2-dependent regulation of innate and adaptive immunity in the intestinal tract. Science **307:** 731-734.

KUCHARZIK, T., C. MAASER, A. LÜGERING, M. KAGNOFF, L. MAYER *et al.*, 2006 Recent understanding of IBD pathogenesis: Implications for future therapies. Inflamm Bowel Dis **12:** 1068-1083.

KUMAR, V., R. S. COTRAN and S. L. ROBBINS, 2003a, pp. 572-577 in *Robbins Basic Pathology*. Saunders, Philadelphia, PA.

KUMAR, V., R. S. COTRAN and S. L. ROBBINS, 2003b Chapter 2 in *Robbins Basic Pathology*. Saunders, Philadelphia, PA.

KUMAR, V., R. S. COTRAN and S. L. ROBBINS, 2003c Chapter 7 in *Robbins Basic Pathology*. Saunders, Philadelphia, PA.

KUNKEL, E. J., and E. C. BUTCHER, 2002 Chemokines and the tissue-specific migration of lymphocytes. Immunity **16:** 1-4.

KUNKEL, E. J., and E. C. BUTCHER, 2003 Plasma-cell homing. Nat Rev Immunol **3:** 822-829.

LAI, Y., and F. SUN, 2003 The relationship between microsatellite slippage mutation rate and the number of repeat units. Mol Biol Evol **20:** 2123-2131.

LALA, S., Y. OGURA, C. OSBORNE, S. Y. HOR, A. BROMFIELD *et al.*, 2003 Crohn's disease and the NOD2 gene: A role for paneth cells. Gastroenterology **125:** 47-57.

LAMONT, J. T., 1992 Mucus: The front line of intestinal mucosal defense. Ann N Y Acad Sci **664:** 190-201.

LEUNG, E., H. JIWON, A. G. FRASER, T. R. MERRIMAN, P. VISHNU *et al.*, 2006 Polymorphisms in the organic cation transporter genes *SLC22A4* and *SLC22A5* and Crohn's disease in a New Zealand Caucasian cohort. Immunol Cell Biol **84:** 233-236.

LIST, K., R. SZABO, A. MOLINOLO, V. SRIURANPONG, V. REDEYE *et al.*, 2005 Deregulated matriptase causes *ras*-independent multistage carcinogenesis and promotes *ras*-mediated malignant transformation. Genes Dev **19:** 1934-1950.

LOFTUS, E. V., and W. J. SANDBORN, 2002 Epidemiology of inflammatory bowel disease. Gastroenterol Clin N Am **31:** 1-20.

LYNCH, H. T., R. E. BRAND and G. Y. LOCKER, 2004 Inflammatory bowel disease in Ashkenazi Jews: implications for familial colorectal cancer. Fam Cancer **3:** 229-232.

MACDONALD, T. T., 2003 The mucosal immune system. Parasite Immunol **25:** 235-246.

MACDONALD, T. T., and G. MONTELEONE, 2005 Immunity, inflammation, and allergy in the gut. Science **307:** 1920-1925.

MADARA, J. L., 1998 Regulation of the movement of solutes across tight junctions. Annu Rev Physiol **60:** 143-159.

MALLOW, E. B., A. HARRIS, N. SALZMAN, J. P. RUSSELL, R. J. DEBERARDINIS *et al.*, 1996 Human enteric defensins: Gene structure and developmental expression. J Biol Chem **271:** 4038-4045.

MASSCHALCK, B., and C. W. MICHIELS, 2003 Antimicrobial properties of lysozyme in relation to foodborne vegetative bacteria. Crit Rev Microbiol **29:** 191 - 214.

MATHIAS, J. R., M. E. DODD, K. B. WALTERS, J. RHODES, J. P. KANKI *et al.*, 2007 Live imaging of chronic inflammation caused by mutation of zebrafish Hai1. J Cell Sci **120:** 3372-3383.

MCQUIBBAN, G. A., J.-H. GONG, E. M. TAM, C. A. G. MCCULLOCH, I. CLARK-LEWIS *et al.*, 2000 Inflammation dampened by gelatinase A cleavage of monocyte chemoattractant protein-3. Science **289:** 1202-1206.

MCQUIBBAN, G. A., J.-H. GONG, J. P. WONG, J. L. WALLACE, I. CLARK-LEWIS *et al.*, 2002 Matrix metalloproteinase processing of monocyte chemoattractant proteins generates CC chemokine receptor antagonists with anti-inflammatory properties in vivo. Blood **100:** 1160-1167.

MEENAN, J., T. A. GROOL, D. W. HOMMES, S. DIJKHUIZEN, F. J. TEN KATE *et al.*, 1996 Lexipafant (BB-882), a platelet activating factor receptor antagonist, ameliorates mucosal inflammation in an animal model of colitis. Eur J Gastroenterol Hepatol **8:** 569-573.

MICHAIL, S., E. MEZOFF and F. ABERNATHY, 2005 Role of selectins in the intestinal epithelial migration of eosinophils. Pediatr Res **58:** 644-647.

MOE, H., 1953 Mucus-producing goblet cells of the small intestine. Nature **172:** 309-309.

MOOG-LUTZ, C., F. CAVE-RIANT, F. C. GUIBAL, M. A. BREAU, Y. DI GIOIA *et al.*, 2003 JAML, a novel protein with characteristics of a junctional adhesion molecule, is induced during differentiation of myeloid leukemia cells. Blood **102:** 3371-3378.

MORA, J. R., M. IWATA, B. EKSTEEN, S.-Y. SONG, T. JUNT *et al.*, 2006 Generation of gut-homing IgA-secreting B cells by intestinal dendritic cells. Science **314:** 1157-1160.

MORI, K., A. IMAMAKI, K. NAGATA, Y. YONETOMI, R. KIYOKAGE-YOSHIMOTO *et al.*, 1999 Subtilisin-like proprotein convertases, PACE4 and PC8, as well as furin, are endogenous proalbumin convertases in HepG2 cells. J Biochem **125:** 627-633.

MORO, F., G. ARRIGO, A. FOGLI, L. BERNARD and R. CARROZZO, 1998 The β and γ subunits of the human platelet-activating factor acetyl hydrolase isoform Ib (PAFAH1B2 and PAFAH1B3) map to chromosome 11q23 and 19q13.1, respectively. Genomics **51:** 157-159.

MÜLLER, C. A., I. B. AUTENRIETH and A. PESCHEL, 2005 Intestinal epithelial barrier and mucosal immunity. Cell Mol Life Sci **62:** 1297-1307.

MUNZER, J. S., A. BASAK, M. ZHONG, A. MAMARBACHI, J. HAMELIN *et al.*, 1997 *In vitro* characterization of the novel proprotein convertase PC7. J Biol Chem **272:** 19672-19681.

NAGLER-ANDERSON, C., 2001 Man the barrier! Strategic defences in the intestinal mucosa. Nat Rev Immunol **1:** 59-67.

NGUYEN, G. C., E. A. TORRES, M. REGUEIRO, G. BROMFIELD, A. BITTON *et al.*, 2006 Inflammatory bowel disease characteristics among African Americans, Hispanics, and non-Hispanic whites: Characterization of a large North American cohort. Am J Gastroenterol **101:** 1012-1023.

NIYONSABA, F., K. IWABUCHI, H. MATSUDA, H. OGAWA and I. NAGAOKA, 2002 Epithelial cell-derived human β-defensin-2 acts as a chemotaxin for mast cells through a pertussis toxin-sensitive and phospholipase C-dependent pathway. Int Immunol **14:** 421-426.

OGURA, Y., D. K. BONEN, N. INOHARA, D. L. NICOLAE, F. F. CHEN *et al.*, 2001 A frameshift mutation in *NOD2* associated with susceptibility to Crohn's disease. Nature **411:** 603-606.

OGURA, Y., S. LALA, W. XIN, E. SMITH, T. A. DOWDS *et al.*, 2003 Expression of NOD2 in Paneth cells: A possible link to Crohn's ileitis. Gut **52:** 1591-1597.

OOSTENBRUG, L. E., J. P. H. DRENTH, D. J. DE JONG, I. M. NOLTE, E. OOSTEROM *et al.*, 2005 Association between toll-like receptor 4 and inflammatory bowel disease. Inflamm Bowel Dis **11:** 567-575.

OOSTENBRUG, L. E., I. M. NOLTE, E. OOSTEROM, G. VAN DER STEEGE, G. J. TE MEERMAN *et al.*, 2006 CARD15 in inflammatory bowel disease and Crohn's disease phenotypes: An association study and pooled analysis. Dig Liver Dis **38:** 834-845.

OPPENHEIM, J. J., C. O. C. ZACHARIAE, N. MUKAIDA and K. MATSUSHIMA, 1991 Properties of the novel proinflammatory supergene "intercrine" cytokine family. Annu Rev Immunol **9:** 617.

ORDOVAS, J. M., D. K. CASSIDY, F. CIVEIRA, C. L. BISGAIER and E. J. SCHAEFER, 1989 Familial apolipoprotein A-I, C-III, and A-IV deficiency and premature atherosclerosis due to deletion of a gene complex on chromosome 11. J Biol Chem **264:** 16339-16342.

ORHOLM, M., V. BINDER, T. I. A. SØRENSEN, L. P. RASMUSSEN and K. O. KYVIK, 2000 Concordance of inflammatory bowel disease among Danish twins: Results of a nationwide study. Scand J Gastroenterol **35:** 1075-1081.

ORHOLM, M., P. MUNKHOLM, E. LANGHOLZ, O. H. NIELSEN, I. A. SORENSEN *et al.*, 1991 Familial occurrence of inflammatory bowel disease. N Engl J Med **324:** 84-88.

ORSÓ, E., C. MOEHLE, A. BOETTCHER, K. SZAKSZON, T. WERNER *et al.*, 2007 The satiety factor apolipoprotein A-IV modulates intestinal epithelial permeability through its interaction with alpha-catenin: Implications for inflammatory bowel diseases. Horm Metab Res **39:** 601-611.

OZAKI, H., M. HORI, K. KINOSHITA and T. OHAMA, 2005 Intestinal dysmotility in inflammatory bowel disease: Mechanisms of the reduced activity of smooth muscle contraction. Inflammopharmacology **13:** 103-111.

PEETERS, M., H. NEVENS, F. BAERT, M. HIELE, A. M. DE MEYER *et al.*, 1996 Familial aggregation in Crohn's disease: Increased age-adjusted risk and concordance in clinical characteristics. Gastroenterology **111:** 597-603.

PEETERS, T., and G. VANTRAPPEN, 1975 The Paneth cell: A source of intestinal lysozyme. Gut **16:** 553-558.

PEIGNON, G., S. THENET, C. SCHREIDER, S. FOUQUET, A. RIBEIRO *et al.*, 2006 E-cadherin-dependent transcriptional control of apolipoprotein A-IV gene expression in

intestinal epithelial cells: A role for the hepatic nuclear factor 4. J Biol Chem **281:** 3560-3568.

PELTEKOVA, V. D., R. F. WINTLE, L. A. RUBIN, C. I. AMOS, Q. HUANG *et al.*, 2004 Functional variants of OCTN cation transporter genes are associated with Crohn disease. Nat Genet **36:** 471-475.

PELTONEN, L., M. PEROLA, J. NAUKKARINEN and A. PALOTIE, 2006 Lessons from studying monogenic disease for common disease. Hum Molec Genet **15:** R67-R74.

PURVES, W. K., D. SADAVA, G. H. ORIANS and C. HELLER, 2001, pp. 84-85 in *Life: the science of biology*. Sinauer Associates, Ltd., Sunderland, MA.

QU, X. D., K. C. LLOYD, J. H. WALSH and R. I. LEHRER, 1996 Secretion of type II phospholipase A_2 and cryptdin by rat small intestinal Paneth cells. Infect Immunity **64:** 5161-5165.

RAVI, A., P. GARG and S. V. SITARAMAN, 2007 Matrix metalloproteinases in inflammatory bowel disease: Boon or a bane? Inflamm Bowel Dis **13:** 97-107.

RECALDE, D., M. A. OSTOS, E. BADELL, A.-L. GARCIA-OTIN, J. PIDOUX *et al.*, 2004 Human apolipoprotein A-IV reduces secretion of proinflammatory cytokines and atherosclerotic effects of a chronic infection mimicked by lipopolysaccharide. Arterioscler Thromb Vasc Biol **24:** 756-761.

REID, G., J. HOWARD and B. S. GAN, 2001 Can bacterial interference prevent infection? Trends Microbiol **9:** 424-428.

RESCIGNO, M., M. URBANO, B. VALZASINA, M. FRANCOLINI, G. ROTTA *et al.*, 2001 Dendritic cells express tight junction proteins and penetrate gut epithelial monolayers to sample bacteria. Nat Immunol **2:** 361-367.

RIOUX, J. D., R. J. XAVIER, K. D. TAYLOR, M. S. SILVERBERG, P. GOYETTE *et al.*, 2007 Genome-wide association study identifies new susceptibility loci for Crohn disease and implicates autophagy in disease pathogenesis. Nat Genet **39:** 596-604.

ROSSIER, B. C., 2004 The epithelial sodium channel: Activation by membrane-bound serine proteases. Proc Am Thorac Soc **1:** 4-9.

RUSSELL, R. K., and J. SATSANGI, 2004 IBD: A family affair. Best Pract Res Clin Gastroenterol **18:** 525-539.

SALAZAR-GONZALEZ, R. M., J. H. NIESS, D. J. ZAMMIT, R. RAVINDRAN, A. SRINIVASAN *et al.*, 2006 CCR6-mediated dendritic cell activation of pathogen-specific T cells in Peyer's patches. Immunity **24:** 623-632.

SÁNCHEZ, J., and J. HOLMGREN, 2008 Cholera toxin structure, gene regulation and pathophysiological and immunological aspects. Cell Mol Life Sci **65:** 1347-1360.

SANDLE, G. I., N. HIGGS, P. CROWE, M. N. MARSH, S. VENKATESAN *et al.*, 1990 Cellular basis for defective electrolyte transport in inflamed human colon. Gastroenterology **99:** 97-105.

SATO, A., M. HASHIGUCHI, E. TODA, A. IWASAKI, S. HACHIMURA *et al.*, 2003 CD11b+ Peyer's patch dendritic cells secrete IL-6 and induce IgA secretion from naïve B Cells. J Immunol **171:** 3684-3690.

SATSANGI, J., C. GROOTSCHOLTEN, H. HOLT and D. P. JEWELL, 1996 Clinical patterns of familial inflammatory bowel disease. Gut **38:** 738-741.

SCHAEFER, E. J., W. H. HEATON, M. G. WETZEL and H. B. BREWER, JR., 1982 Plasma apolipoprotein A-1 absence associated with a marked reduction of high density lipoproteins and premature coronary artery disease. Arteriosclerosis **2:** 16-26.

SCHAEFER, E. J., J. M. ORDOVAS, S. W. LAW, G. GHISELLI, M. L. KASHYAP *et al.*, 1985 Familial apolipoprotein A-I and C-III deficiency, variant II. J Lipid Res **26:** 1089-1101.

SCOTT, H. S., J. KUDOH, M. WATTENHOFER, K. SHIBUYA, A. BERRY *et al.*, 2001 Insertion of β-satellite repeats identifies a transmembrane protease causing both congenital and childhood onset autosomal recessive deafness. Nat Genet **27:** 59-63.

SENDA, S., Y. FUJIYAMA, T. BAMBA and S. HOSODA, 1993 Treatment of ulcerative colitis with camostat mesilate, a serine protease inhibitor. Intern Med **32:** 350-354.

SHIBAHARA, T., J. N. WILCOX, T. COUSE and J. L. MADARA, 2001 Characterization of epithelial chemoattractants for human intestinal intraepithelial lymphocytes. Gastroenterology **120:** 60-70.

SMITH, L. J., W. SZYMANSKI, C. FOULSTON, L. D. JEWELL and H. F. PABST, 1994 Familial enteropathy with villous edema and immunoglobulin G2 subclass deficiency. J Pediatr **125:** 541-548.

SOBHANI, I., S. HOCHLAF, Y. DENIZOT, C. VISSUZAINE, E. RENE *et al.*, 1992 Raised concentrations of platelet activating factor in colonic mucosa of Crohn's disease patients. Gut **33:** 1220-1225.

SPAHN, T. W., and T. KUCHARZIK, 2004 Modulating the intestinal immune system: The role of lymphotoxin and GALT organs. Gut **53:** 456-465.

STACK, W. A., D. JENKINS, P. VIVET and C. J. HAWKEY, 1998 Lack of effectiveness of the platelet-activating factor antagonist SR27417A in patients with active ulcerative colitis: A randomized controlled trial. Gastroenterology **115:** 1340-1345.

STAWOWY, P., H. MEYBORG, D. STIBENZ, N. B. P. STAWOWY, M. ROSER *et al.*, 2005 Furin-like proprotein convertases are central regulators of the membrane type matrix metalloproteinase-pro-matrix metalloproteinase-2 proteolytic cascade in atherosclerosis. Circulation **111:** 2820-2827.

STOLL, M., B. CORNELIUSSEN, C. M. COSTELLO, G. H. WAETZIG, B. MELLGARD *et al.*, 2004 Genetic variation in *DLG5* is associated with inflammatory bowel disease. Nat Genet **36:** 476-480.

STRACHAN, T., and A. P. READ, 1999 Chapter 15 in *Human Molecular Genetics*. John Wiley and Sons, Ltd., Rexdale, ON.

SU, A. I., M. P. COOKE, K. A. CHING, Y. HAKAK, J. R. WALKER *et al.*, 2002 Large-scale analysis of the human and mouse transcriptomes. Proceedings of the National Academy of Sciences **99:** 4465-4470.

SUN, X., and W. HSUEH, 1991 Platelet-activating factor produces shock, in vivo complement activation, and tissue injury in mice. J Immunol **147:** 509-514.

SZABO, R., and T. H. BUGGE, 2008 Type II transmembrane serine proteases in development and disease. Int J Biochem Cell Biol **40:** 1297-1316.

TERWILLIGER, J. D., and J. OTT, 1994, pp. 40-42 in *Handbook of human genetic linkage*. The John Hopkins University Press, Baltimore, MD.

TETTA, C., F. BUSSOLINO, V. MODENA, G. MONTRUCCHIO, G. SEGOLONI *et al.*, 1990 Release of platelet-activating factor in systemic lupus erythematosus. Int Arch Allergy Immunol **91:** 244-256.

THOMPSON, N. P., R. DRISCOLL, R. E. POUNDER and A. J. WAKEFIELD, 1996 Genetics versus environment in inflammatory bowel disease: Results of a British twin study. BMJ **312:** 95-96.

TJOELKER, L. W., C. WILDER, C. EBERHARDT, D. M. STAFFORINIT, G. DIETSCH *et al.*, 1995 Anti-inflammatory properties of a platelet-activating factor acetylhydrolase. Nature **374:** 549-553.

TOMKO, R. P., C. B. JOHANSSON, M. TOTROV, R. ABAGYAN, J. FRISÉN *et al.*, 2000 Expression of the adenovirus receptor and its interaction with the fiber knob. Exp Cell Res **255:** 47-55.

TURNER, J. R., B. K. RILL, S. L. CARLSON, D. CARNES, R. KERNER *et al.*, 1997 Physiological regulation of epithelial tight junctions is associated with myosin light-chain phosphorylation. Am J Physiol Cell Physiol **273:** C1378-C1385.

TYSK, C., E. LINDBERG, G. JARNEROT and B. FLODERUS-MYRHED, 1988 Ulcerative colitis and Crohn's disease in an unselected population of monozygotic and dizygotic twins. A study of heritability and the influence of smoking. Gut **29:** 990-996.

VAN KRUININGEN, H. J., A. B. WEST, B. J. FREDA and K. A. HOLMES, 2002 Distribution of Peyer's patches in the distal ileum. Inflamm Bowel Dis **8:** 180-185.

VASSALLI, P., 1992 The pathophysiology of tumor necrosis factors. Annu Rev Immunol **10:** 411.

VOWINKEL, T., M. MORI, C. F. KRIEGLSTEIN, J. RUSSELL, F. SAIJO *et al.*, 2004 Apolipoprotein A-IV inhibits experimental colitis. J Clin Invest **114:** 260-269.

VUAGNIAUX, G., V. VALLET, N. F. JAEGER, E. HUMMLER and B. C. ROSSIER, 2002 Synergistic Activation of ENaC by three membrane-bound channel-activating serine proteases (mCAP1, mCAP2, and mCAP3) and serum- and glucocorticoid-regulated kinase (Sgk1) in *Xenopus* oocytes. J Gen Physiol **120:** 191-201.

WALLRAPP, C., S. HAHNEL, F. MULLER-PILLASCH, B. BURGHARDT, T. IWAMURA *et al.*, 2000 A novel transmembrane serine protease (TMPRSS3) overexpressed in pancreatic cancer. Cancer Res **60:** 2602-2606.

WEBER, C., L. FRAEMOHS and E. DEJANA, 2007 The role of junctional adhesion molecules in vascular inflammation. Nat Rev Immunol **7:** 467-477.

WEERSMA, R. K., H. M. VAN DULLEMEN, G. VAN DER STEEGE, I. M. NOLTE, J. H. KLEIBEUKER *et al.*, 2007 Review article: Inflammatory bowel disease and genetics. Aliment Pharmacol Ther **26:** 57-65.

WEHKAMP, J., J. HARDER, M. WEICHENTHAL, M. SCHWAB, E. SCHAFFELER *et al.*, 2004 NOD2 (CARD15) mutations in Crohn's disease are associated with diminished mucosal α-defensin expression. Gut **53:** 1658-1664.

WEHKAMP, J., N. H. SALZMAN, E. PORTER, S. NUDING, M. WEICHENTHAL *et al.*, 2005 Reduced Paneth cell α-defensins in ileal Crohn's disease. Proc Natl Acad Sci U S A **102:** 18129-18134.

WELLER, A., S. ISENMANN and D. VESTWEBER, 1992 Cloning of the mouse endothelial selectins. Expression of both E- and P- selectin is inducible by tumor necrosis factor alpha. J Biol Chem **267:** 15176-15183.

WORLD HEALTH ORGANIZATION, 2007 Fact Sheet N° 107: Cholera, http://www.who.int/mediacentre/factsheets/fs107.

XAVIER, R. J., and D. K. PODOLSKY, 2007 Unravelling the pathogenesis of inflammatory bowel disease. Nature **448:** 427-434.

YAMAZAKI, K., D. MCGOVERN, J. RAGOUSSIS, M. PAOLUCCI, H. BUTLER *et al.*, 2005 Single nucleotide polymorphisms in *TNFSF15* confer susceptibility to Crohn's disease. Hum Molec Genet **14:** 3499-3506.

YANA, I., and S. J. WEISS, 2000 Regulation of membrane type-1 matrix metalloproteinase activation by proprotein convertases. Mol Biol Cell **11:** 2387-2401.

YANG, D., A. BIRAGYN, L. W. KWAK and J. J. OPPENHEIM, 2002 Mammalian defensins in immunity: More than just microbicidal. Trends Immunol **23:** 291-296.

YANG, D., O. CHERTOV, S. N. BYKOVSKAIA, Q. CHEN, M. J. BUFFO *et al.*, 1999 β-Defensins: Linking innate and adaptive immunity through dendritic and T cell CCR6. Science **286:** 525-528.

YIANGOU, Y., P. FACER, P. A. BAECKER, A. P. FORD, C. H. KNOWLES *et al.*, 2001a ATP-gated ion channel $P2X_3$ is increased in human inflammatory bowel disease. Neurogastroenterol Motil **13:** 365-369.

YIANGOU, Y., P. FACER, N. H. C. DYER, C. L. H. CHAN, C. KNOWLES *et al.*, 2001b Vanilloid receptor 1 immunoreactivity in inflamed human bowel. Lancet **357:** 1338-1339.

YIANGOU, Y., P. FACER, J. A. SMITH, L. SANGAMESWARAN, R. EGLEN *et al.*, 2001c Increased acid-sensing ion channel ASIC-3 in inflamed human intestine. Eur J Gastroenterol Hepatol **13:** 891-896.

YU, F. H., R. E. WESTENBROEK, I. SILOS-SANTIAGO, K. A. MCCORMICK, D. LAWSON *et al.*, 2003 Sodium Channel β4, a New Disulfide-Linked Auxiliary Subunit with Similarity to β2. J Neurosci **23:** 7577-7585.

ZEISSIG, S., T. BERGANN, A. FROMM, C. BOJARSKI, F. HELLER *et al.*, 2008 Altered ENaC expression leads to impaired sodium absorption in the noninflamed intestine in Crohn's disease. Gastroenterology **134:** 1436-1447.

ZEN, K., Y. LIU, I. C. MCCALL, T. WU, W. LEE *et al.*, 2005 Neutrophil migration across tight junctions is mediated by adhesive interactions between epithelial coxsackie and adenovirus receptor and a junctional adhesion molecule-like protein on neutrophils. Mol Biol Cell **16:** 2694-2703.

ZHENG, C.-Q., G.-Z. HU, Z.-S. ZENG, L.-J. LIN and G.-G. GU, 2003 Progress in searching for susceptibility gene for inflammatory bowel disease by positional cloning. World J Gastroenterol **9:** 1646-1656.

ZIMMERMAN, G. A., T. MCINTYRE, S. PRESCOTT and D. STAFFORINIT, 2002 The platelet-activating factor signaling system and its regulators in syndromes of inflammation and thrombosis. Crit Care Med **30:** S294-S301.